A Study of the Vibrational Reliability Performance of Different Doped Low-Creep Lead-Free Solder Paste and Solder BGA Packages

by

Derrick Stone

A thesis submitted to the Graduate Faculty of
Auburn University
in partial fulfillment of the
requirements for the Degree of
Master of Science

Auburn, Alabama
August 01, 2015

Keywords: Lead-Free Solder, BGA, Reliability Performance, Vibration, Doping

Approved by

George T. Flowers, Chair, Professor of Mechanical Engineering
John Evans, Professor of Industrial and Systems Engineering
Dan Marghitu, Professor of Mechanical Engineering

Abstract

The growing use of smaller and more powerful electronic components in more varied and adverse environments, especially in regards to mobile consumer electronics, has created the need to better understand how recent lead-free solder replacements for the toxic eutectic tin-lead alloy are impacted by manufacturing variations and solder doping, especially in terms of their general reliability performance under vibration and thermal shock environments. This thesis focuses on the fatigue life characteristics of 15 mm CABGA packages with 208 perimeter solder balls on a 0.8 mm pitch which have been mounted on a vertically-oriented printed circuit board using various formulations and manufacturing parameters of lead-free solder balls and solder paste before being subjected to 4.6 G_{rms} of random vibration using an LDS LV217 electro-dynamic shaker machine over the course of about 20-hour testing spans and with electrical tests being performed once every hour. The test vehicles were built to withstand JEDEC JESD22-B103B standards of high stress while the test alloy formulations involved 12 different lead-free pastes, including a SAC305 equivalent paste, and seven solder ball alloys that were manufactured using three reflow profiles (Low, Best, & High) and two stencil sizes (4 mil & 6 mil). Half of the formulations were tested immediately after they were manufactured, and the other half were placed inside a thermal aging chamber that maintained an internal temperature of 125^{o}C for 6 months before being removed and

subjected to vibration testing. A 2-parameter Weibull analysis was primarily used to characterize the ATTIF and MTTF of the samples in an attempt to discover any general trends affecting the vibrational reliability performance of the samples inherent to the variation of certain experimental parameters. In-depth analysis of the data revealed that two of the specific formulations, J6BN and J6L, achieved improvements in ATTIF of 1900% and 900%, respectively, over the performance of the equivalent test samples from the control group which used SAC105 and SAC305 solder balls with SAC305 paste. Even though the long-term performance of these two formulations was disappointing, their outstanding initial performance still earns them the greatest overall recommendation for short-term reliability. In terms of long-term reliability, however, the K6H test group emerged as the overall frontrunner. This test group was calculated to have an average 20% greater initial ATTIF than the equivalent control test group and was predicted to have a general failure rate that was either the same or better than the control group over the course of its life. This formulation could provide manufacturers with the ability to only employ a single SAC305 paste substitute and a slightly higher reflow temperature in order to dramatically increase the long-term reliability performance of the products constructed in their single or mixed-SAC BGA production facility as well as boosting the initial reliability performance for their SAC305 BGA components. If used as such, the K6H formulation would be most appropriate for use in less reliability-critical applications, namely consumer mobile electronics.

Acknowledgements

The author would like to thank his committee, chaired by Dr. George T. Flowers and comprising Dr. John Evans and Dr. Daniel Marghitu, for their constant guidance and support throughout his graduate coursework and research.

The author sincerely thanks Dr. George T. Flowers and Dr. John Evans for providing him with such a great opportunity to further his education and granting him the privilege to work under their leadership. The author would also like to thank his undergraduate and graduate academic advisors Dr. Sushil H. Bhavnani and Dr. Hareesh Tippur for their moral support and assistance in navigating the intricacies of Auburn University paperwork. The author would like to also extend appreciation towards his colleagues Thomas Sanders, Robin Muthukumar, Sivasubramanian Thirugnanasambandam, Anto Jeson Robert Raj, and Akash Nayyar for all of their contributions in performing testing and analyzing data as well as for their valuable inputs throughout his research and coursework. A debt of gratitude is owed to Haoyue Yang for his assistance in the operation, calibration, and maintenance of the vibration equipment. Much gratitude is also owed to Linda Pitchford and Ramona Shierling-Nelson for providing the author with their personal endorsements of his character and overall moral support throughout this entire process.

The author would like to thank his girlfriend Robyn Windsor, his parents Neal and Sandy, his grandparents John and Carolyn Kristy, his relatives Dave and Kristi Kristy, his future in-laws Clark and Ann Windsor, and all of his younger brothers Drew, Forrest, Skyler, Ashton, and Kieran for their constant love and confidence in him throughout his career and everything they have done to ensure he is successful in his educational endeavors. The author also wants to truly thank his friends Grant Kirkland, Jonathan Nguyen, Cory Garfunkel, Brianna Sanguily, Tyco Stone, and everyone else in the OAC for their unbridled friendship and moral support during some of the most challenging points in his life at Auburn and for providing him with countless treasured memories during these past seven years. Finally, the author would like to sincerely thank his grandfather, Dean Stone, to whom he is dedicating this work, for all the support he provided during the author's college career and without whom this work would not have been possible.

Table of Contents

List of Tables

List of Figures

List of Abbreviations

ATTIF	Approximate Time To Initial Failure (at 99% reliability)
BGA	Ball Grid Array
BPAFN	Best Performing Alloy Formulation for No-Aging
CABGA	Chip Array Ball Grid Array
DIP	Dual Inline Package
I/O	Input/Output
IC	Integrated Circuit
J6BN	J-Series Paste with 6mil Stencil, Best Reflow Profile, & N-type solder balls
J6L	J-Series Paste with 6mil Stencil, Low Reflow Profile
JEDEC	Joint Electron Device Engineering Council
K6H	K-Series Paste with 6mil Stencil, High Reflow Profile
MTTF	Mean Time To Failure
PCB	Printed Circuit Board
QFP	Quad Flatpack

QFN	Quad Flatpack No-Lead
SAC	Tin-Silver-Copper
SAC105	99.4% Tin, 0.1% Silver, and 0.5% Copper Alloy
SAC305	99.2% Tin, 0.3% Silver, and 0.5% Copper Alloy
SEM	Scanning Electron Microscope
SMR	Surface Mount Resistor
SMT	Surface Mounting Technology
SOP	Small Outline Package
THMT	Through-Hole Mounting Technology

Chapter 1

INTRODUCTION

Ever since the first integrated circuit was developed in 1959 by Jack Kilby and Robert Noyce, engineers have been thinking of new and innovative ways to further improve and refine their circuit design, making it smaller and more powerful [1]. This miniaturization of electronics is responsible for the rapid development of computer technology over the last few decades, and the rise in popularity of BGAs due to their compactness and high I/O density has made them one of the most successful and prevalent component packages in the industry today. Achieving the greatest possible reliability performance with BGAs and other electronic components requires the use of the strongest, most reliable solder for mechanically and electrically joining the integrated circuits to the printed circuit board. For much of its history, eutectic tin-lead solder has dominated this role in the electronics industry. However, its recent ban from use in electronics in the mid-2000's by Japan and the European Union due to its toxicity caused manufacturers to scramble to find lead-free replacements that could perform just as reliably as lead-based solder. Many lead-free alloys such as SAC105 and SAC305 have become popular alternatives but much of their characteristic behavior involving variations in manufacturing methods or doping compositions is still relatively unknown and requires additional research on the part of scientists and engineers.

Chapter 2

LITERATURE REVIEW

Integrated Circuits

Before current electronics packaging technology can be understood, it is first necessary to understand a brief account of its history, beginning with the evolution of integrated circuitry. Originally, vacuum tubes and transistors were individually mounted and wired to each other on top of a metal chassis or printed circuit board, similar to a breadbox circuit system [1]. Vacuum based computers were very expensive, so they were eventually replaced by transistors, which were significantly better in many ways including cost, performance, reliability, and power consumption. These transistors were then integrated onto a single silicon chip, called an integrated circuit, in 1958. Since all of their active and passive components were interconnected during the fabrication process without the need for thick wires, they were more reliable and monumentally smaller in size than their transistor counterparts (sometimes as much as 1000x smaller) and therefore represented a significant improvement over the traditional individualized transistors [2]. These integrated circuits can be classified into three different types depending on the manufacturing process used to create them, namely monolithic, film,

and hybrid. Monolithic circuits are the most basic type of integrated circuit, as all of the necessary active and passive components of the chip are overlaid

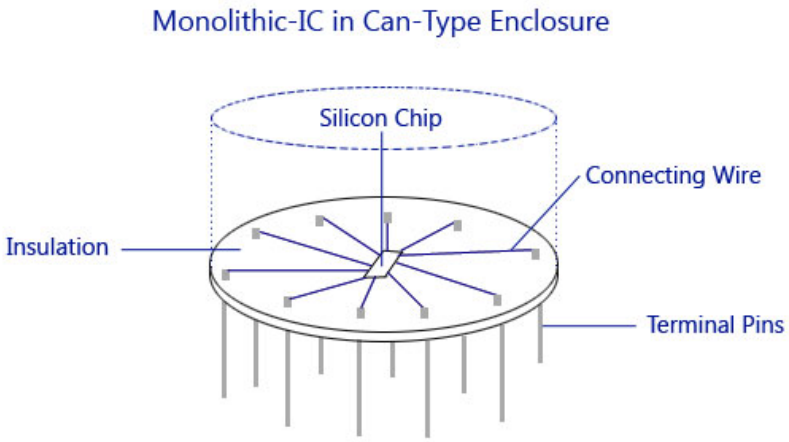

Figure 1: Diagram of a basic monolithic circuit [2]

and connected using a single chip of silicon. The basic layout and construction of a monolithic integrated circuit is pictured in Figure 1 and Figure 2. This is one of the most popular types of IC since they can be cheaply mass-produced and are highly reliable. Their chief drawback is their low power rating which prevents them from being used in high power applications. They also have fairly poor component insulation and are unable to integrate inductors into their design [2].

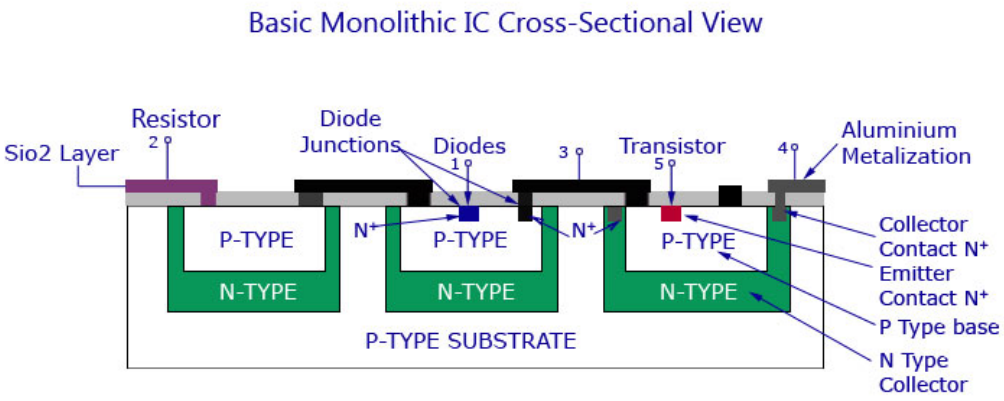

Figure 2: Cross-section view of monolithic IC [2]

Film integrated circuits are slightly larger and more costly than monolithic integrated circuits, but they are also able to handle much higher power requirements and have better isolation between components than monolithic ICs. Hybrid ICs are essentially the result of interconnecting multiple types of monolithic and film integrated circuits. This results in boosts in circuit performance by capitalizing on the advantages offered by each type of IC but is usually too costly for mass production. These are the three primary types of integrated circuits in use today.

Printed Circuit Boards

However, the processes and technologies used to manufacture the chip are only one part of the overall electronics packaging technology in use in industry. The structure that provides the physical mounting structure and electrical interconnect between integrated circuit chips and other components is known as a printed circuit board or PCB. Before PCBs were developed in 1925 by Charles Ducas, point to point construction

was used. This resulted in extremely bulky and unreliable circuits which required large sockets and continuous replacement. These issues were subsequently solved with the inception of the printed circuit board, as the electrical paths necessary to connect various components were already fabricated into an insulated surface [3]. Over time, these circuit boards slowly became more complex due to advancements in manufacturing technology that allowed for the inclusion of electrical connection points on both sides of the board substrate and the creation of multiple layers of interconnected copper traces, thus allowing more and more complex and computationally powerful chips to be attached to them. Figure 3 reveals the typical inner structure found in modern PCBs. As packaging technology evolved, the PCBs were transformed with them, slowly transitioning from devices dominated by the use of through-hole mounted components to ones that catered to surface mounted components during the 1980's. This transition allowed for further size reductions to be achieved while simultaneously increasing performance [3].

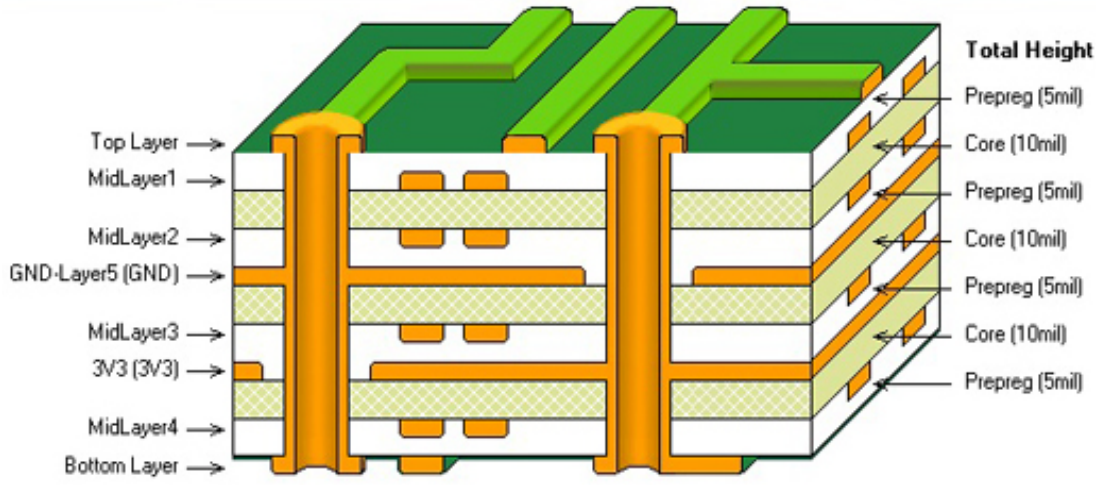

Figure 3: Inner structure of typical PCB [4]

Today, the manufacturing process for printed circuit boards has become fairly standardized, with only slight variations needed in the manufacturing process to accommodate the specific performance, cost, reliability, and thermal requirements required by the consumer. The process begins by gluing a sheet of a glass epoxy polymer to a relatively thick sheet of copper. This copper layer is then covered in a photo-sensitive material that acts like a stencil, only allowing portions of the copper that are to be used as an internal circuit wire to be exposed to the ultraviolet light and creating a hardened, protective crust along their top. The unhardened portion of photo-sensitive material is then removed using a chemical bath, leaving only the unwanted copper exposed and the desired copper circuitry protected by the hardened photo-resist material. The entire board is then dipped into an alkali solution, where the acid dissolves or “etches” away any exposed copper, leaving behind a plexi-board with copper circuits that are covered by a hardened photoresist. The photoresist is then stripped using pressure washers, leaving only the desired copper wiring on top of the plexi-board. This portion of the final product is known as the inner board. This inner layer is then sandwiched between two thin copper films which are bonded to the inner board using two layers of pre-impregnated epoxy on each side of the film and subjecting them to intense heat and pressure. This assembly is then aligned and precisely drilled using automatic computer controlled drilling machines. This is when the holes for leaded/through-hole components as well as soon-to-be-vias are drilled. Vias are the three-dimensional wiring that connect the top and bottom copper layers to the copper wiring on the internal board. Once the drilling is complete, the process is not quite over.

The via holes are not conductive, because they are still lined with the plexi-board material and pre-impregnated epoxy resin. To correct this, a multi-stage process is used to first chemically deposit a thin layer of copper in the vias. However, this layer is very uneven and must be reinforced for the PCB to function reliably. So, similarly to what was done to the inner board, a photo-sensitive material and stencil is used on the outer copper layers to harden and protect only the portions of copper material that need to be removed. Since the entire board is now electrically conductive, including the shabbily plated copper vias, the substrate is dipped into a chemical bath. This is done so that a thick, smooth layer of copper can be electrodeposited onto any exposed coppers areas, which are coincidentally the only areas where circuits are intended to be placed. Once the copper circuitry is solid and smooth and the vias adequately copper plated, those same areas are coated with a thin layer of tin using a process very similar to the one from before. This thin layer of tin is used to protect the finished copper circuits from a copper-eating acid bath after the photo-resistive material has been washed off, which etches away all the remaining unnecessary copper material from the boards. Once finished, the tin is then removed, leaving nothing but thick copper traces on the top and bottom layers of the PCB as well as copper vias running throughout its inner structure. Next, photosensitive solder mask ink, typically green in color, is overlaid to completely cover both the front and back layers of the board. This serves to protect the copper traces on the outer portions of the substrate from oxidation and to help prevent short-circuits due to slipshod soldering from occurring. Using a light stencil like before, the entire solder mask, except for the small areas on and around future soldering points, is

exposed to light to harden and permanently bond the mask to the board. The remaining exposed areas, such as the vias and outer solder points, are then coated in a gold-nickel alloy to protect the copper from oxidation. A silk screen containing the printed information about specific components and their placement is then overlaid onto the board and UV light is used to bond it to the top layer of the solder mask. Each individual board is then carefully cut out from the panel using special drilling techniques to prevent cracking and damage to the board before being sent off for a final inspection [5]. This is the fairly well-established manufacturing process used in the current production of most printed circuit boards.

Chip Packaging

The integrated circuit chips and the printed circuit board they use as their electrical and mechanical support are two out of the three major portions of electronics packaging technology. The final portion of the subject serves as the conduit with which to electrically and mechanically connect these two different electronic constituents, and it is known as a package. In addition to protecting the IC die from physical damage, the package is also responsible for redistributing the I/O to a more manageable pitch for assembly [6]. Like the printed circuit board, package technology evolved to keep up with the ever-changing standards required by new integrated circuit chips. The first packages were developed in the 1970's and were called dual in-line packages or DIP.

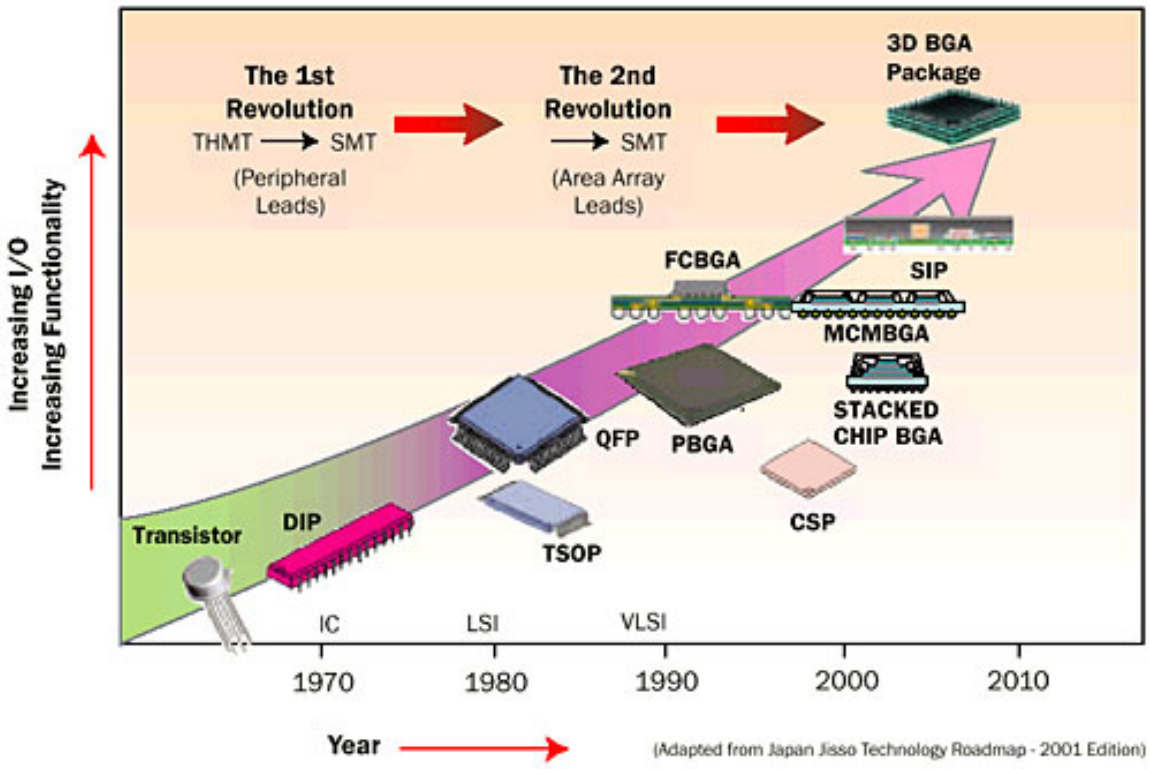

Figure 4: Visual representation of evolution of electronics packaging [4]

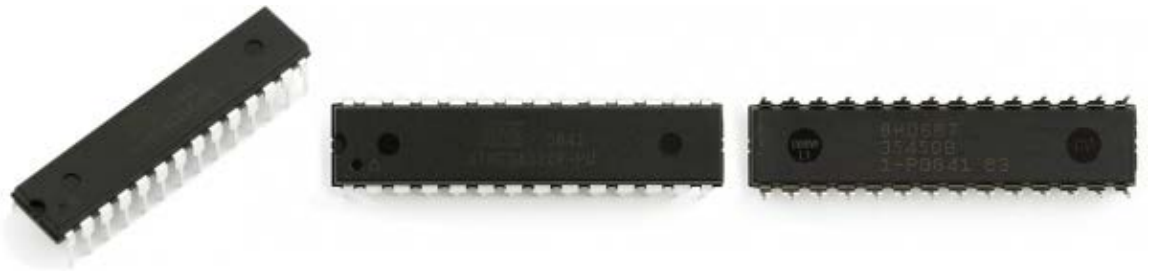

Figure 5: Picture of a typical DIP [7]

These packages used through-hole packaging techniques, in which two parallel rows of lead pins spaced a tenth of an inch apart were inserted through holes drilled into the PCB and then welded on the bottom layer using wave soldering. This type of package worked well for fitting into breadboards and their soldered joints were extremely tough and reliable. However, they were only capable of supporting between 4 to 64 pin leads.

As demand for packages capable of supporting higher input/output operations in a smaller and smaller space began to increase, engineers developed a new way of attaching chip packages that did not require the holes to be drilled in the PCB. Instead, packages using this new type of attachment method, known as surface-mount technology, had leads or connection points that were soldered or wire-bonded directly to the surface of the printed circuit board, usually using a solder reflow process. Instead of running a wave of molten solder over exposed metal leads to bond components to the PCB, reflow soldering melts solder paste that has already been printed directly onto the PCBs using a form of stencil, as shown in Figure 6.

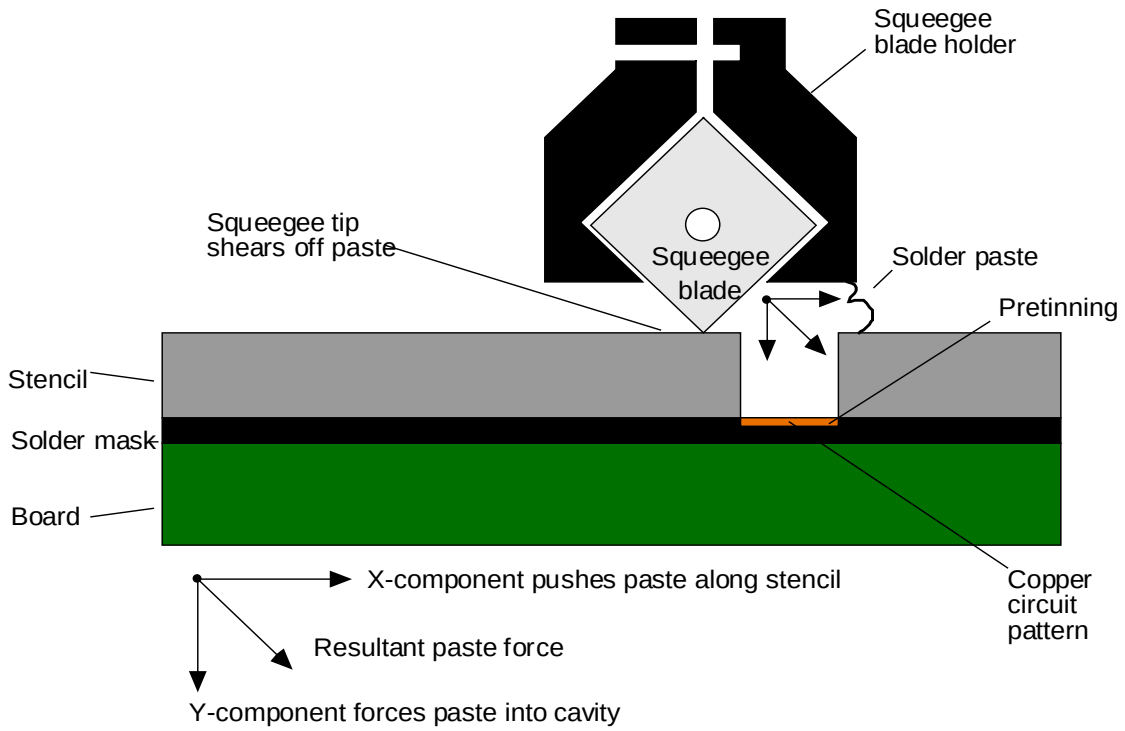

Figure 6: Schematic of paste printing using stencil for reflow soldering [4]

These type of packages can often save electronics manufacturers money due to the lower costs generally involved during their production. This is because surface mount components can be positioned onto PCBs using automated pick and place machines, which increases the product yield while also requiring less drilling to be done on the PCBs. As a general rule, surface mounted components can typically be made about two to five times smaller than conventional leaded components since the diameter of their leads is not dependent on the sizing constraints inherent to drilled PCB holes. In fact, if the long leads on a dual in-line package are bent outward and shrunk, the resulting surface-mount package is called a small-outline package or SOP [7]. The pins on this type of package are usually spaced out by about 0.05 inches. Although it offers a considerable improvement in packaging size over DIPs, this type of package still has somewhat limited I/O capabilities. As a result, a new type of package had to be developed that could meet the increasing computational capabilities of the current generation IC chips. Thus, quad flat packages were developed. Instead of only having leads on two sides of the package like SOPs, quad flat packages or QFPs had leads on all four sides. Utilizing four instead of two sides of a component for lead placement essentially doubled the total number of leads and, thus, I/O that was achievable within a specified surface area of the PCB. These packages usually had anywhere between 32 to 300 in leads, sporting an even finer pin pitch of between 0.4 mm to 1 mm [7].

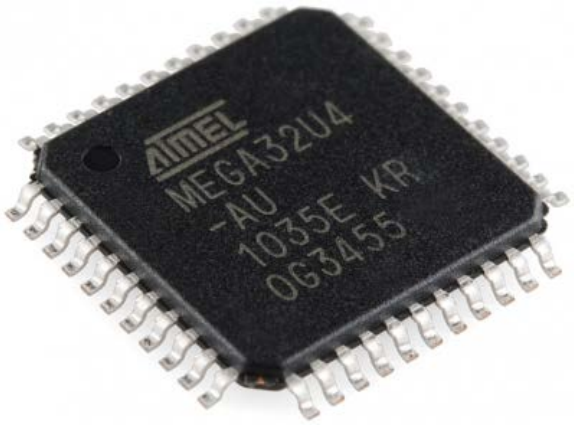

Figure 7: Picture of a standard QFP [7]

This type of package was refined even further by removing the protruding wire leads in favor of using tiny, exposed pads on the bottom corner edges of the chip. These chips were named quad flat no-leads, or QFNs, as a result.

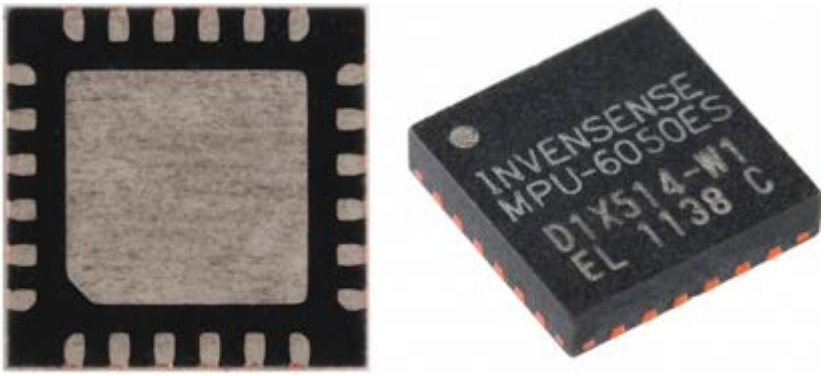

Figure 8: Picture of a standard QFN [7]

These helped to reduce the chip size even further without sacrificing performance. As chips continued to become more and more powerful while remaining small and compact into the early 2000's, engineers were once again in need of a package that could handle higher capacity chips that would be compact enough to fit inside

smartphones and desktop computers. The solution was to exploit the unused area under traditional QFNs for use as additional leads, but instead of pads, this package would employ solder balls attached to the die itself and arranged in a grid to form the necessary electrical connections. As such, this new revolutionary package came to be known as a BGA, or ball grid array package. Utilizing the area under the component dramatically increased the total number of leads and, thus, I/O that was possible within a certain area of PCB real estate, as the relationship between the length of a package and its maximum I/O was polynomial in nature for BGAs instead of linear like for SOPs or QFPs as shown in Figure 9. Their ability to handle high I/O without sacrificing precious PCB space, among other traits, has made them one of the most popular electronic packages used in commercial applications today.

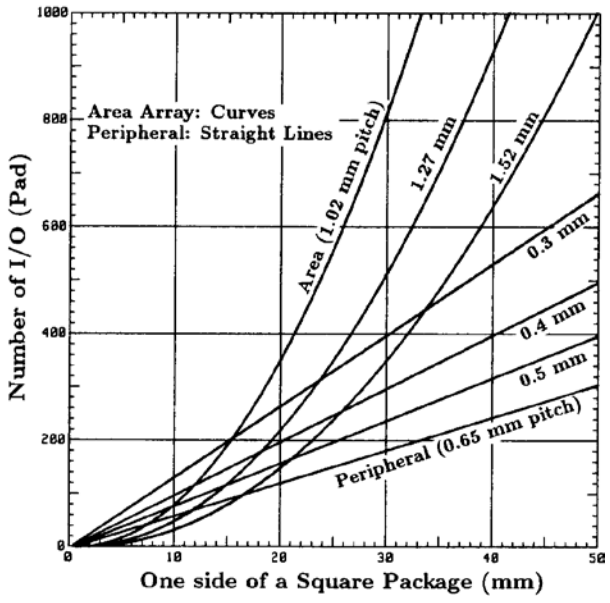

Figure 9: Plot of length of peripheral and area packages vs. number of I/O [4]

Definition of Soldering

Over the course of human history, the ability to mechanically join separate metal work pieces together became an ever-growing need, whether it was to create extravagant pieces of gold jewelry as was done by the Egyptians or for much more utilitarian purposes such as building elaborate lead-based aqueduct plumbing systems as was the case with the Romans [4]. There are three different processes available to accomplish this type of mechanical fusion, namely soldering, brazing, and welding. Soldering is a process in which the two metal surfaces to be joined are subjected to a high temperature but remain solid and do not melt. Instead, an intermediary metal with a lower melting temperature than the two surface metals, known as solder, is melted in between the two surfaces and then cooled in order to join the metals together. Any process which follows this formula for joining metals and takes place below 450°C, i.e. when the liquidus of the filler material is lower than 450°C and the solidus of the base metals, is considered to be soldering. However, if this process is performed at a temperature above 450°C, then it is arbitrarily considered to be brazing. This process is very similar to soldering, in that it produces a coalescence of materials through heat, with the only exception being that the filler metal has a liquidus above 450°C while still being below the solidus of the base materials [8]. If this process is carried out at even higher temperatures where not only the filler solder material melts but the actual surface metals melt as well, then that process is considered to be welding [9]. Although brazing and welding certainly have their place in industry, soldering is the most apropos process for use in electronics manufacturing as it occurs at the lowest possible

temperatures. This is a valuable trait since high temperature fluctuations have been known to damage electronic components. In order to keep the soldering process to as low an operating temperature as possible, the solder material used to join the two surfaces together is usually selected to be a solid solution of two or more metals, known as an alloy. This is because alloys are generally stronger than pure metals while also having much lower melting points.

Crucial Solder Properties

However, there are an almost infinite number of possible solder alloy combinations in the universe, so it is important to know what material properties are necessary in order to have an effective solder joint. As was mentioned earlier, metal alloys generally have lower melting temperatures than their pure metal counterparts. The exact point at which they begin to melt is a direct function of their metallic composition, as raising or lowering the percentage by mass of a certain metal may increase or decrease the alloy's overall melting temperature.

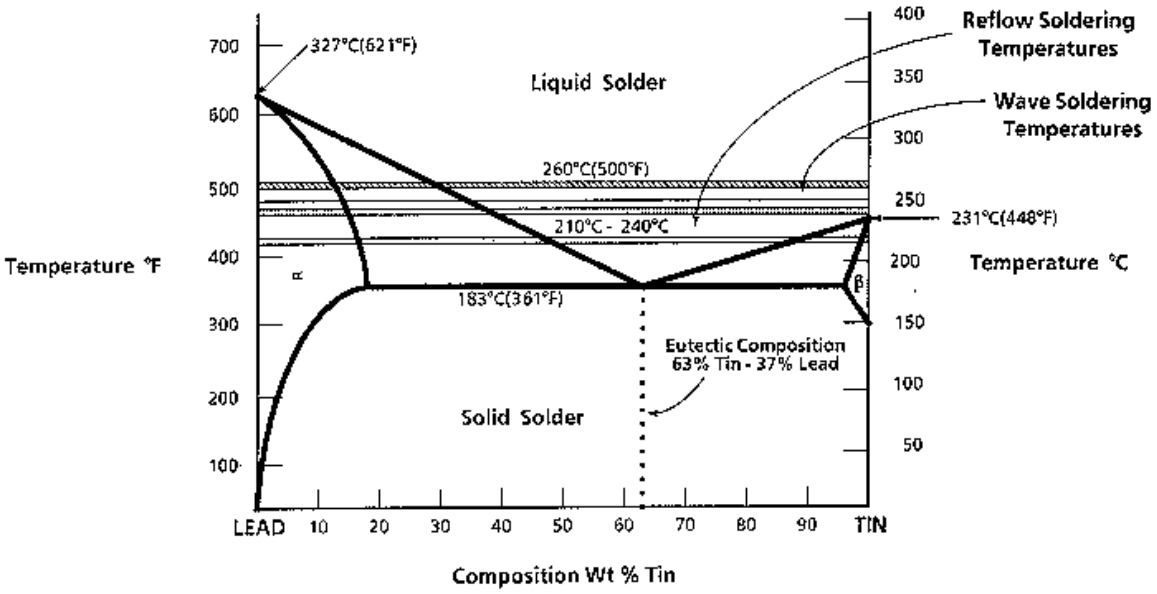

Figure 10: Phase diagram of eutectic tin-lead solder [4]

These relationships are often linear, and so the specific combination and ratio of metals which will produce the alloy with the lowest possible melting temperature can be mathematically determined. This point in the alloy mixture ratio that produces the lowest possible melting temperature is known as the alloy's eutectic point [4]. Since it is better to create electrical connections using the lowest temperature change possible so as to avoid unwanted damage from occurring to the components being attached, a solder mixture based on or very close to the alloy's eutectic point is usually preferred. In addition, since reflow soldering is typically possible between 210°C and 240°C and wave soldering occurs around 260°C, it is obviously imperative that the solder alloy's melting temperature be below the operating temperature of the respective soldering activity being used. Another important aspect in determining the viability of an alloy as a successful solder is the relative cost and availability of its component metals. This is

especially important in fields heavily influenced by market forces, such as consumer electronics, where pricing points of a product's materials can determine the product's overall feasibility. In other words, if an alloy employs a high quantity of an extremely rare, precious metal that is difficult to gather and is magnitudes more expensive than all other metals, then it is usually renders the alloy's use as a solder a moot point. Because even if that alloy performs better than every other alloy, it is not financially feasible to use in industry. As such, a preferred quality of alloys is that all of their components are readily available and extremely cheap. Another beneficial and key characteristic of all solder alloys are their high wettability. Wettability is the measure of the degree to which "a liquid is able to maintain contact with a solid surface, resulting from intermolecular interactions when the two are brought together… [and] is determined by a force balance between adhesive and cohesive forces" [10]. Essentially, a liquid, including liquid solder, has two properties which influence how it "sticks". Its adhesive properties determine how much it is attracted and sticks to other materials, while its cohesive properties determines how much it is attracted and sticks to itself. In order for a solder alloy to form a strong solder bond, i.e. one where the contact angle between the liquid solder and the solder surface is equal to or less than 90 degrees, its adhesive forces must be stronger than its cohesive forces. This allows the solder to prefer to adhere to the solder surface more than itself and form a strong solder fillet. Therefore, a solder alloy with a high wettability to a wide range of surfaces is definitely a preferred trait in the electronics manufacturing industry. Another characteristic of the solder alloy that needs to be considered is its inherent risk or resistance to leaching. "Leaching is a kinetic

metallurgical phenomenon in which one element dissolves into another at soldering temperatures" [4]. This is typically a problem for surface mount components, because they usually employ an adhesion layer made of palladium, gold, or silver. These elements have an extremely high dissolution rate during soldering, especially compared to elements like copper, nickel, or platinum [4]. Depending on the type of components being soldered, a specific solder alloy may be chosen for use on the basis that it contains similar metals as the components' adhesion layers, which helps to mitigate the effects of leaching. Other preferable solder alloy attributes include high mechanical joint strength (both in tension and in shear), resistance to oxidation, resistance to fatigue, and high solderability.

Tin-Lead Eutectic Solder: Rise to Stardom

Tin/lead solder alloys have been satisfying most of these technical requirements of electronics manufacturers ever since they were first discovered by the Celts and Gauls in 1900 B.C. [11]. However, through the optimization of all of these aforementioned factors, the electronics industry was able to develop a tin/lead solder alloy so well-suited for soldering that it became the industry standard for decades and has only recently started to be replaced by other alternative solder alloys. That industry standard was the tin-lead eutectic alloy. This alloy is comprised of 63% tin and 37% lead by weight. It is a true eutectic solder, meaning that it has the lowest melting point of all tin/lead alloys and that melting point is actually a point and not a range. This is a highly

preferable trait, because it means electronic components do not have to experience very high temperatures during the soldering process. It also means that the components will not have a chance to move during cooling as the alloy does not have a pasty range during reflow. Both of these traits result in less failures and higher reliability of the electronics manufactured using tin-lead eutectic solder. The fact that this solder alloy also contains slightly more than half its weight in tin means that it has relatively high tensile and shear strength. Its high tin content also makes this alloy very resistant to oxidation and provides good wettability on a wide variety of surfaces. In terms of cost, nearly 40% of the alloy is composed of lead, one of the cheapest minerals on earth. Tin is only about 7x more expensive than lead, making this alloy very cost effective, especially considering its excellent performance characteristics [4]. With all of these factors in mind, it is no wonder why the tin-lead eutectic alloy emerged as the standard solder in various industries for so many years.

Tin-Lead Eutectic Solder: Fall from Grace

However, tin-lead eutectic solder's reign as the standard alloy for soldering is finally coming to a close. The cause of its downfall: lead toxicity. Despite its many advantages, one of its major components, lead, presents a significant toxicity concern to humans. Lead toxicity occurs when a person is exposed to lead, even low levels, over an extended period of time. This is because the lead slowly accumulates over time in the bones and blood of the exposed individual. This accumulation of lead within the human

body can have a number of negative effects, including but not limited to, anemia, ADHD, autism, epilepsy, impaired mental or cognitive function, depression, antisocial behavior, gout, hypertension, decreased kidney function, cardiovascular disease, and learning disabilities [12]. The health hazards associated with lead exposure were already so well-known that by the late 1970s, the United States had already banned its use within gasoline and most paints. However, it was not until the mid-2000s that the electronics industry realized that the lead used in obsolete electronics could slowly leach out of the landfills into which they were dumped, leak into the soil, and find its way into ground water. This realization sparked reforms in Japan and the European Union concerning which materials were considered acceptable for use in future electronic devices and resulted in an outright ban of lead-based solder [4]. This was the nail in the coffin for tin-lead eutectic solder and ignited the search for a new drop-in solder alloy alternative that could take its place.

Near-Eutectic Ternary SAC Solders: The Future of Solder

In order to quickly meet the newly instituted regulations requiring lead-free solder while minimizing negative impacts on other portions of the manufacturing process, scientists and engineers began searching for a “drop-in” replacement, i.e. a solder that could be substituted for tin-lead and essentially have no other effects on the current system. However, in order for this to be possible, the replacement solder needed to have chemical and mechanical properties similar to the eutectic lead solder.

Also due to tin's high availability, relatively low cost, high strength, and natural resistance to oxidation, it would be preferable if the next generation solder alloy was a mixture containing tin. Researchers from across the globe, including Japan, Europe, and the United States, strived to find the next generation tin-based lead-free solder. By the early 2000s, they eventually converged onto a small series of near-eutectic Tin-Silver-Copper (Sn-Ag-Cu), or SAC, solder alloys [4]. They found that not only did various mixtures of SAC have a low melting point, lying somewhere between that of pure tin, 232°C, and the tin-lead eutectic, 183°C, but that they also provided adequate wettability to a wide variety of surfaces as well as offered similar or sometimes even superior mechanical properties compared to that of tin-lead solder. As a result of various optimization techniques, four main SAC formulations emerged to compete for the title of the new industry standard. The first SAC mixture is known as SAC396, because it contains tin with 3.9% silver and 0.6% copper. This mixture was developed based on research conducted by the National Electronics Manufacturing Initiative of the United States. It is very similar to a formulation created by the European IDEALS Consortium known as SAC387, due to it containing 3.8% silver and 0.7% copper with the remainder being tin. Although SAC396 and SAC387 both have excellent mechanical and chemical properties, they also have the second and third highest concentration of silver, respectively, of any industry standard lead-free solder [13]. As was mentioned before, the cost of the materials required to manufacturer a solder alloy plays a huge role in its success for use in consumer electronics. In terms of cost, silver is one of the most expensive elements to use in a solder alloy, averaging more than 200x more expensive

than lead [4]. In addition, once the industry began using these two alloys, a new type of defect known as “tombstoning” began to occur. This is a defect that can occur during reflow soldering in which the surface tension at one end of a component forces it to stand up vertically, like a tombstone, and result in only one end of the component being soldered. This is because, unlike the popular tin-lead solder, SAC396 and SAC387 are only *near*-eutectic solders, meaning not all of their phases melt at once. Due to this inherent flaw in both reflow soldering and cost, these two solder alloys are not commonly used in industry. Instead, a new solder alloy, SAC305, was created using tin spliced with 3% silver and 0.5% copper. This different composition helped diminish the difference in wetting forces during reflow and allowed more components to stay in their designated locations, decreasing the incidence of defects compared to the SAC396 and SAC387 solder alloys. The 0.8% decrease in silver content also helped make SAC305 solder more cost effective. SAC305 was positioned to become the next overall industry standard, until escalating shock requirements from the consumer electronics industry and a sharp price increase in silver in 2010-2012 caused a new formulation of 1% silver and 0.5% copper, or SAC105, to take the mobile phone industry by storm [14]. Although SAC105 has an inferior thermal shock resistance compared to SAC305, it has a much higher drop and shock resistance. This and its 2% smaller silver requirement, and therefore lowered cost premium, made SAC105 the prime choice for solder for use in consumer electronics, especially the cell phone industry. SAC305 and SAC105 are still battling it out for the position of best lead-free solder today, with each having its own advantages and weaknesses in specific situations.

Current Research

Even after being used in electronics products for nearly a decade, there is still much that is not understood regarding the aged performance behaviors of lead-free solders used in BGA components. This can be attributed to the fact that the industry has only recently begun to realize their limitations in terms of long-term performance. Much of the most accurate data regarding their behavior comes from the reports of research conducted within the last 5 years, with most of those sources of information still performing on-going research. For instance, a team at Wuhan Textile University in China performed a study investigating the relationship between the intensity of a vibrational environment and the locations and modes by which failure occurred in the solder joints of lead-free BGA packages. They found that as the intensity of the vibration increased, the failure modes began to switch from fatigue cracks to brittle cracks, causing the location of the failure in the joints to change. They also noted that once the amplitude of the vibration attained a certain magnitude, the failure mechanism began to resemble ones present during drop impact loading. Some SEM photos that illustrate the most common modes of failure that were experienced by the BGA solder joints subjected to a vibrational stress test at 60 $(m/s^2)^2/Hz$ are shown in Figure 11 [15].

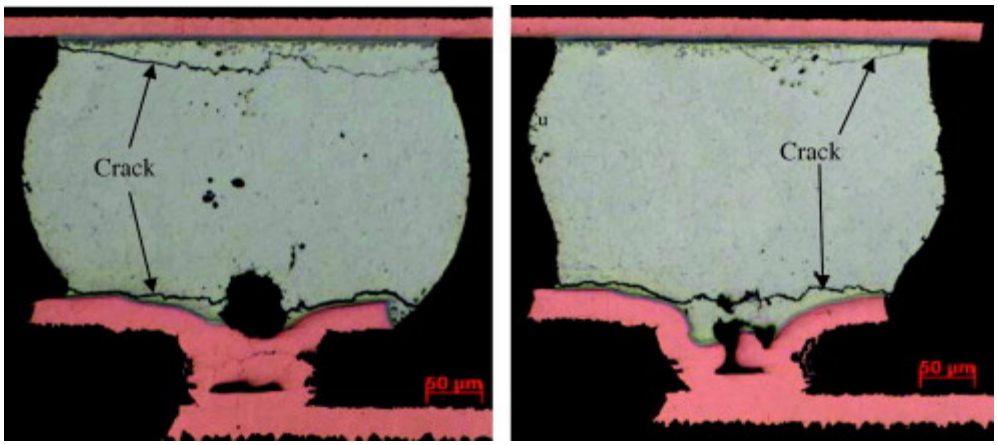

Figure 11: SEM photos of solder ball joint cracking [15]

Most of the cutting-edge research around this topic is being performed at the Center for Advanced Vehicle and Extreme Environment Electronics at Auburn University. One study published there by Jiawei Zhang focused on quantifying the effects of isothermal aging on the thermal-cycling reliability of BGA components ranging in size from a 19 mm body with 0.8 mm lead pitch to a 5 mm body with 0.4 mm lead pitch. The components had one of three possible board finishes and were aged at 25°C, 55°C, 85°C, or 125°C for six months before being thermally cycled from –40°C to 125°C with 15 min dwell times at each end of the temperature spectrum. Zhang found that BGAs using SAC105 and SAC305 lead-free solder that had been aged at 125°C experienced roughly a 50% reduction package life compared to those aged at room temperature. In contrast, his analysis showed that the reliability performance of the eutectic tin-lead solder, Sn-37Pb, is much more stable and predictable over time and temperature than the lead-free solders. Zhang concluded that the primary failure mode caused by aging was associated with the growth of Cu_6Sn_5 intermetallic compounds, especially on the pad side of the

interconnects [16]. Another study conducted by Zijie Cai explored the possibility of reducing this aging-induced degradation of the material behavior of SAC solders through the use of various dopants such as Bismuth, Indium, Nickel, Zinc, and Titanium. They discovered that a SAC307 solder doped with 0.1% Bismuth showed reduced aging-induced degradations in thermal cycling performance for a wide range of aging temperatures between 25°C and 125°C. In addition, they found that after short durations of aging, the doped solder alloys had better stress-strain and creep mechanical properties than the control group and that their behaviors were more stable after long-term aging [17].

Objective of this Study

The above literature review explains the advantages of solder doping, especially in regards to extending vibration reliability and curbing the negative effects of aging on solder performance. The history of integrated circuits, printed circuit boards, and electronic packaging was discussed and the reasons for the industry-wide switch to lead-free alloys were covered. Various case studies were analyzed, and the effect of vibration intensity on lead-free BGA failure mechanisms was discussed. Next, the effect of aging on the thermal cycling performance of SAC105 and SAC305 BGA solder packages was studied. Finally, the effect of doping on the thermal cycling reliability performance of SAC solder alloys which had undergone isothermal aging was reviewed. In order to corroborate the data covered by the U.S. and China studies, it is necessary

for research to be performed involving doped solder BGAs that have undergone isothermal aging and have been subjected to vibrational loading. This requirement will be met through the completion of the proposed experiment. Twelve lead-free solder pastes and five lead-free solder ball alloys were selected for this current study. Tests were conducted using new boards and boards which had been aged for six months at 125°C to address how solder doping can reduce the effects of aging. The components used on the board consisted of a fairly standard type of BGA, QFN, and resistor in order to assure data analysis validity across a wide range of components. Tests were conducted on boards manufactured using two different stencil sizes; 4 mil and 6 mil to address the effect of solder paste volume. The test also included boards which had been produced at the manufacturer's recommended reflow temperature as well as some at a higher or lower reflow temperature in order to determine its effect on reliability of the doped solder joints. Finally, 75% of all components on the test board were reflowed using SAC305 solder balls while the remaining 25% used SAC105 solder balls in order to determine what effects solder doping would have on two of the most popular lead-free solder options currently available in the industry in order to improve their reliability under vibration and thermal-cycling. A wide range of data and numerous reliability performance factors were obtained for different lead-free doping mixtures and manufacturing variables that might be useful in determining the overall most reliable doping formula for a particular situation as well as revealing general trends that could serve to help predict the success of the addition of doped solder to existing electronic product designs.

Chapter 3

EXPERIMENTAL DESIGN OVERVIEW

The goal of the experiment was to observe the effects various formulations of doped lead-free solder used to electrically and mechanically connect BGA components to PCBs would have on their reliability performance under vibration for both new and artificially aged components and to be able to compare that to the current performance of the most successful lead-free alloys used in the electronics industry today.

In order to establish a starting point in the actual design of the experiment, it was imagined what the experiment would look like if the world was temporarily assumed to be “perfect” and “simple”. In a simple world, the straightforward approach to accomplish this goal would simply be to build hundreds of new and aged circuit boards with BGAs manufactured using many different doped lead-free solders and utilize an electric shaker table to vibrate the boards until all the BGA components failed an electrical test. This data could then be directly compared to a set of hundreds of new and aged boards manufactured using solely the control alloy, the absolute best lead-free alloy used in the industry currently, in order to establish the definitive positive or negative impacts the doping had on the components in comparison to the industry favorite. However, the world is not simple and thus the test could not be successfully performed in this manner for many glaring reasons. For one, there are many variables

that could be affecting the results of the failure data that are not addressed in this thought experiment, mainly the effects of the volume of doped solder used to bond the BGA components to the PCB, the temperature at which the components are reflowed during their production, the magnitude and frequency of the vibration, and the specific composition of the doped alloy contained in the solder paste and the solder spheres used for soldering the BGA components to the PCB. The second limitation of the thought experiment involves the usefulness of the data in regards to comparison to the performance of current alloys. There is no such thing as "the absolute best lead-free alloy" available in the electronics industry in which the data is intended to be compared. In fact, there are theoretically unlimited possible chemical combinations for lead-free solders and over 100 specific formulations commonly used in the industry today, each with its own unique advantages and disadvantages in terms of reliability, price, and manufacturability [18]. Not only that, but the experiment would have no way of proving that the data obtained from the lead-free BGAs was the direct result of doping the solder and not simply an inherent characteristic that would be experienced by all types of components under that particular vibration test environment. Thirdly, the experiment neglects to clarify the resistance threshold necessary that a component must reach to be considered to have electrically failed. The test also fails to mention whether the rate of failure and approximate time to initial failure, ATTIF, are important characteristics to take into consideration when determining the success of a certain test, in addition to the sheer number of failures that are recorded. The final flaw in the thought experiment involves the actual logistics of such a project. Although an

experiment that included the testing of hundreds of circuit boards for every possible combination of reflow temperature, doped and control solder alloy formulations, solder paste vs solder ball vs both, stencil size of solder paste, component type and location, vibration intensity and magnitude, and new vs. aged and recording their varying resistances in real-time would be ideal and certainly result in the most complete and reliable data, it would also most likely cost millions of dollars and take decades to complete. With all of this in mind, a modified version of the earlier thought experiment was designed that was believed to best address all the important issues it presented while still remaining fiscally, logistically, and temporally efficient.

To address the issues of data comparison to an industry standard, two of the most popular lead-free solders in use in the industry today were selected to serve as part of a control group. The two lead-free solder alloys chosen were SAC105 and SAC305, so named since they are alloys composing of various quantities of tin, silver, and copper whose chemical abbreviations are Sn, Ag, and Cu, respectively. SAC105 is composed of 5% copper and 1% silver with the remainder being tin. This alloy was selected to help serve as a form of control group because of its popularity in the industry and its remarkable reliability performance under high vibration and drop environments. SAC305, on the other hand, contains 2% more silver than SAC105 and is most popular in the electronics industry for its adept reliability performance in high thermal-shock environments. Despite performing well in extreme temperatures, SAC305 has relatively poor reliability performance during drop and vibration events, and so

finding a combination of manufacturing factors and solder chemistry that could improve its performance under vibration would be extremely beneficial.

In order to attempt to account for any effects on reliability performance of the doped alloys deriving from variations in paste volume, whether from differences in paste or solder ball alloy volume, it was decided to include samples that employed two different paste stencil sizes as well as standard and experimental alloy materials in the solder spheres. The first stencil size chosen was the 4 mil stencil, because it is the most common size used in the industry for the production of surface-mounted BGAs. Furthermore, since the primary object of the test was to view the effects due to the doped solder paste, it seemed logical that increasing the amount used for each sample by 100% would make any characteristic impacts it had even more apparent. Assuming that by having the solder spheres also be constructed using the experimental alloys would already increase the total experimental alloy volume by an estimated 50%, the remaining 50% alloy volume increase was accomplished through a 50% increase of the 4 mil stencil size to 6 mil. To incorporate any effects the reflow profile might have on reliability, the test samples were also decided to be manufactured using three varying temperature profiles. The first reflow profile, referred to as “best” in many cases, was the reflow profile recommended for that specific alloy by the manufacturer. The two other reflow profiles were variations on the “best” reflow profile, leaning towards either the high end or the low end of the acceptable profile temperature limits.

When determining what type of vibration to use to test the samples, it was determined that a single frequency and magnitude of vibration would be sufficient for

collecting reliability data for the test samples. In addition, the test vehicles were also designed to include resistors and QFNs mounted using standard lead-free solder for use as a point of reference for reliability performance during testing. In terms of number of lead-free alloy formulations, the experiment was able to obtain 12 lead-free pastes and 7 solder ball alloys from local electronics manufacturers. Finally, in order to address logistical and time concerns, it was decided to only vary the reflow profiles for the samples using a 6mil stencil and to only use the experimental solder ball alloys during the 6mil samples utilizing the best reflow profile. While not every possible combination of solder alloy, stencil size, or reflow profile were examined, this modified experimental design allowed for the maximum coverage of variables involving the doped lead-free solder alloys while minimalizing overall testing time and cost.

Experimental PCB Design

The test vehicle to be used as the physical substrate for all of the test samples was designed as a standard 4-layer PCB composed of copper vias and glass epoxy covered by a thin solder mask on both sides and an overlaid silkscreen on the front for labeling purposes, the exact specifications for which can be found in Figure 12. The test vehicle was designed to incorporate a total of 16 BGAs located at the #1 positions, 20 resistors distributed at the #2 positions, and 6 QFNs placed at the #3 positions. More detailed information regarding each specific component can be found in later sections of the report. Since the study involved the testing of aged and non-aged BGAs, the

testing procedure for the two types were slightly different. The first half of the study involved the testing of the no-aging boards. During this time, the test boards were shipped and fully tested within weeks of being manufactured. The second half of the study involving aged boards proceeded slightly differently. In order to most effectively simulate aging on the test vehicle, the PCBs were placed into an isothermal chamber machine that maintained a steady internal temperature of 125°C for 6 months before they were removed and then mounted onto the shaker table for testing.

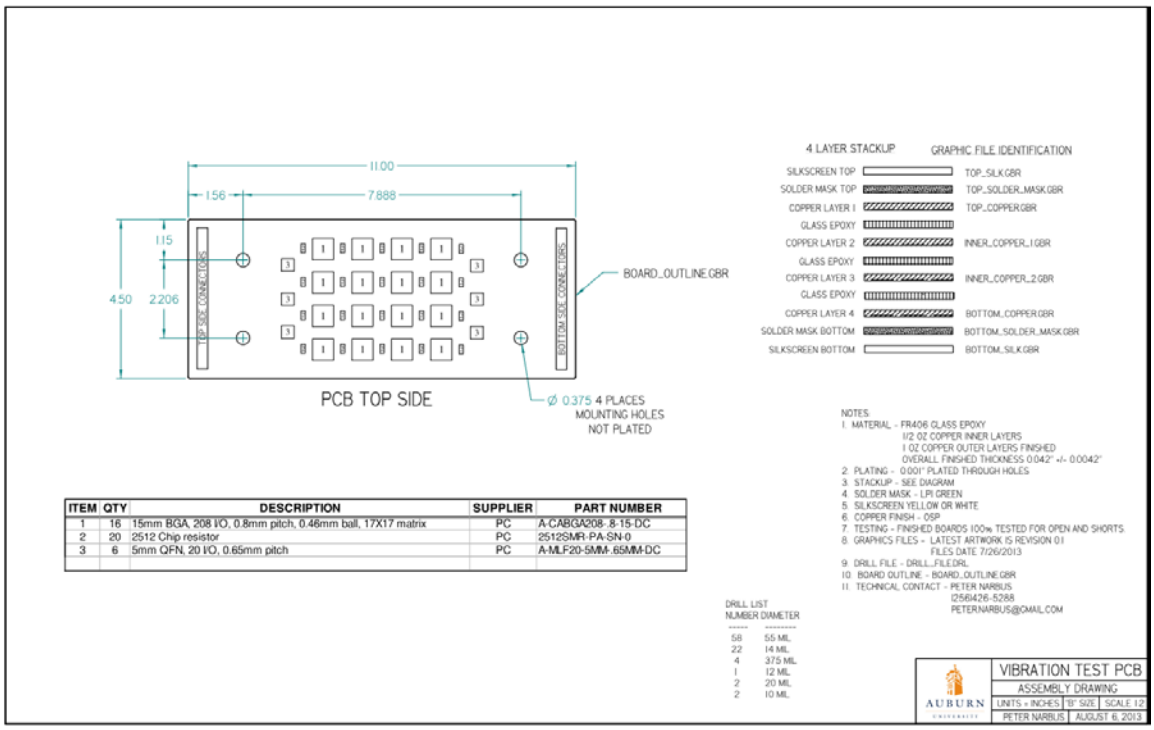

ITEM	QTY	DESCRIPTION	SUPPLIER	PART NUMBER
1	16	15mm BGA, 208 I/O, 0.8mm pitch, 0.46mm ball, 17X17 matrix	PC	A-CABGA208-.8-15-DC
2	20	2512 Chip resistor	PC	2512SMR-PA-SN-0
3	6	5mm QFN, 20 I/O, 0.65mm pitch	PC	A-MLF20-5MM-.65MM-DC

Figure 12: Test vehicle SolidEdge schematic [19]

BGA Component Design

Seeing as how the entire study is built around the evaluation of the performance of various solders used in BGA components, the actual design and type of BGA

component used in the study is understandably vital. The idea was to choose a design that was fairly representative of the BGAs currently being used most commonly in electronics. As such, the component that seemed to best accomplish that task was a 15mm^2 CABGA from Practical Components. This BGA was designed with 208 I/O while maintaining a 0.8mm lead pitch. The solder balls themselves were approximately 0.46mm in diameter and arranged in a standard 17x17 matrix as demonstrated in Figure 15 . The specific internal and external mechanical structures of the selected BGA component are illustrated in Figure 13 and Figure 14, respectively. Electrically, the BGA component employs a standard daisy chain wiring scheme in which all the test components are wired together in a linear sequence. The exact electrical configuration used for the component is demonstrated in Figure 16.

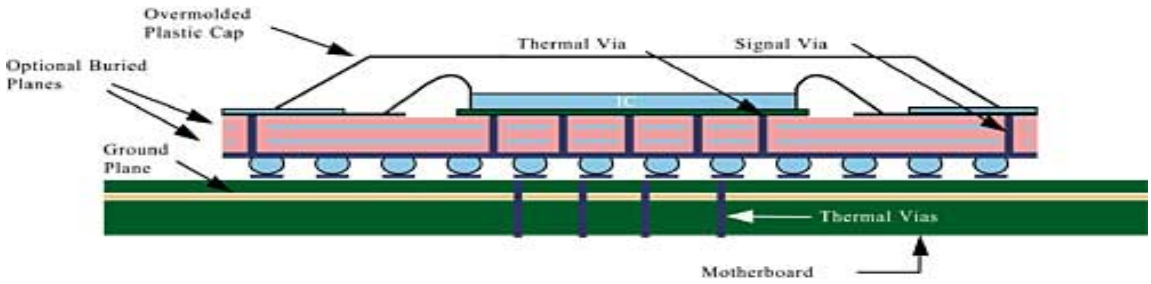

Figure 13: Internal structure of typical BGA [20]

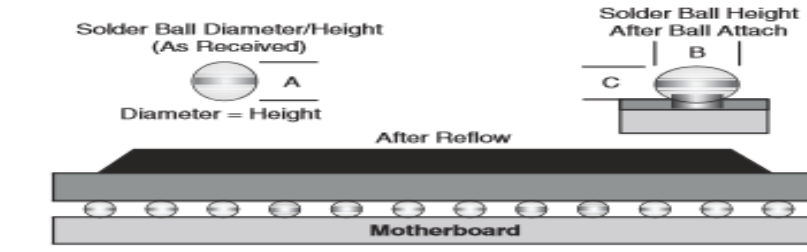

Package Pitch	A	B	C	D
1.00/0.80mm	0.46mm	0.48m (± 0.05mm)	0.36mm (± 0.05mm)	0.30mm (± 0.05mm)

Figure 14: Side view and measurements of BGA component design [21]

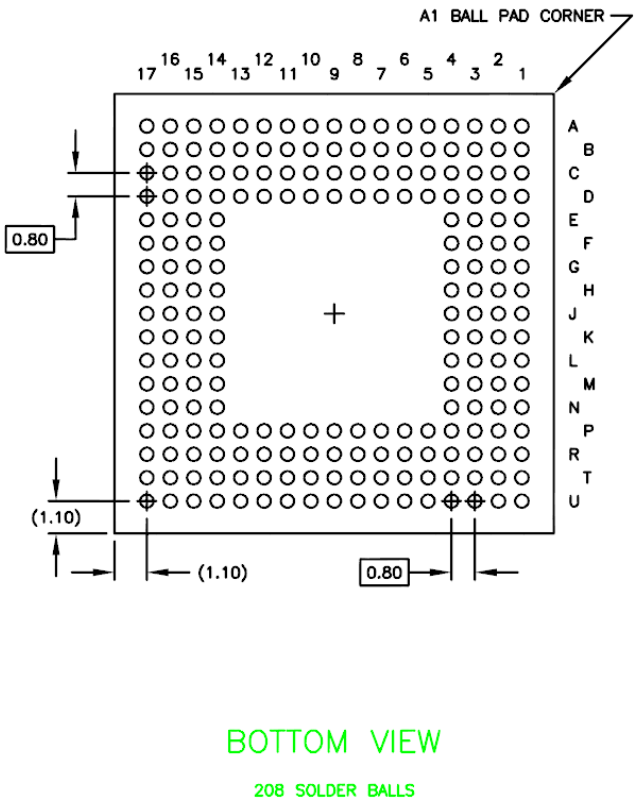

Figure 15: Bottom view of solder ball grid arrangement [22]

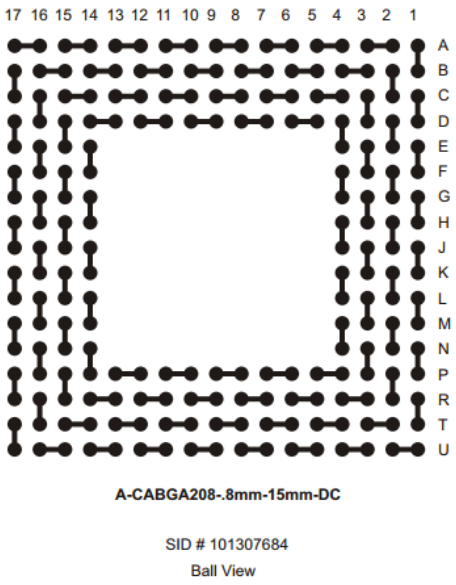

Figure 16: Electrical schematic of the daisy-chaned BGA design [22]

As was discussed previously, for the sake of maximizing testing data while controlling required testing time and cost, all of the BGA components were planned to be manufactured using either SAC105 or SAC305 as the solder ball alloy with the exception of the few cases where an experimental solder ball alloy was actually available. However, rather than producing essentially half of the components using SAC105 and the other half with SAC305, each individual BGA component was engineered to contain 75% SAC305 and 25% SAC105, and the reasoning for doing so is fairly simple. SAC105 is already known to, in general, perform better under drop/vibration circumstances but poorly under thermal cycling compared to SAC305. Since the test involved vibration and not a thermal cycling chamber, rather than finding a combination of parameters that improved the thermal cycling properties of an alloy shown to perform well under vibration (SAC105), the test hoped instead to find variable combinations which improved the vibration performance of an alloy already proven to perform well under thermal cycling. More precise data would be preferred for this alloy (SAC305), so a larger majority of the test balls would need to be constructed with it. But in order to still have a comparison of its performance to the standard SAC105 alloys already used in vibration environments in the industry, the remainder of the solder balls would need to be made with SAC105. The decision about which and how many components should be manufactured using each of the lead-free alloys was reached after considering which layout would allow for the most data being captured for SAC305 solder balls while still allowing for a fair comparison to the SAC105 components to be made without being tainted by location-based failures. Prior experiments conducted at

Auburn University revealed that the solder ball failures could typically be categorized into 4 different zones on the test vehicle, as shown in Figure 17.

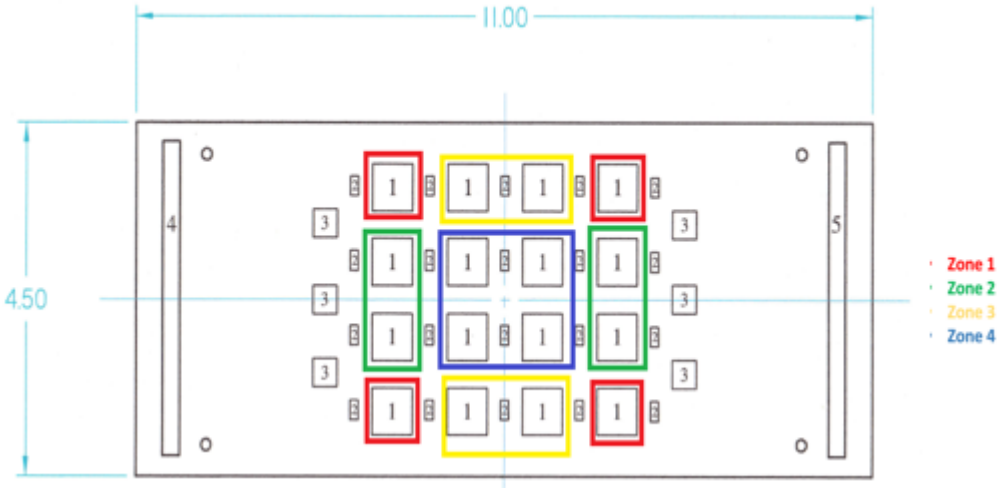

Figure 17: Test vehicle zone map

As such, even if a board was constructed entirely out of the same alloy, it would still theoretically experience different vibration forces which may cause entirely different failure rates and modes among components from different zones. To correct for this possibility and still satisfy the requirements for greater data precision for SAC305 and reliable comparison characteristics against SAC105, three out of the four components in each zone were constructed using SAC305 solder while the remaining components were made using SAC105. As a result, 75% of the BGA components are SAC305 while the last 25% are SAC105. The exact location of each component constructed using SAC105 and SAC305 is illustrated in Figure 18 with purple corresponding to the locations marked for SAC105 and gold corresponding to components using SAC305.

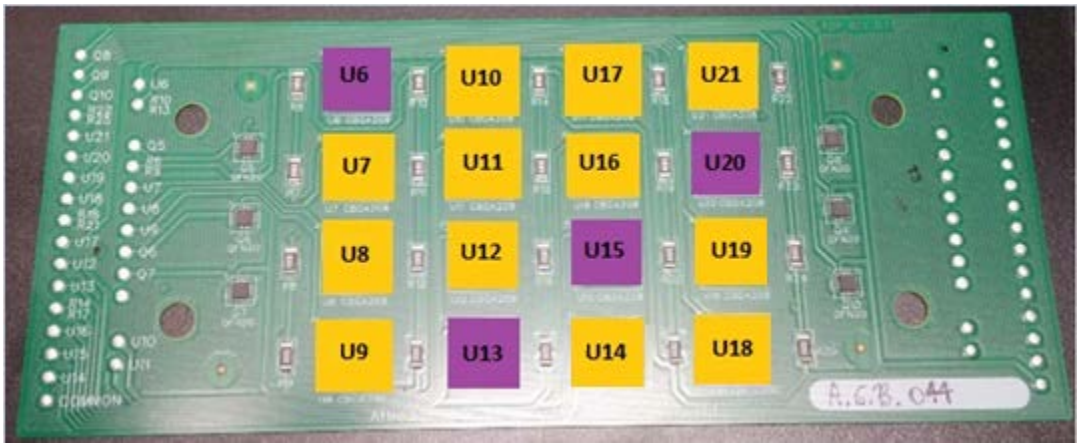

Figure 18: Test vehicle SAC105 and SAC305 BGA component locations

As was mentioned previously during the section covering the experimental design overview, the general design of the study was to follow the pattern illustrated below in Figure 19 where in phase I each test paste was used to create specimens using a 4 mil stencil, SAC105 & SAC305 solder balls, and the best reflow profile. Phases II and III would also use the test paste with a 6 mil stencil to create BGA samples using SAC105 & SAC305 solder balls but utilize a low and high reflow profile, respectively. The final phase would once again employ the test paste with a 6 mil stencil reflowed using the best profile, but the solder balls on the BGAs would be made up entirely of the same or "matched" alloy used for the test paste. This was the general outline for the entire study and it was repeated twice, once for the no-aging and once for the aged components. However, most of the electronics manufacturing companies that donated materials to be used as test specimens were not able to supply either a matching solder ball alloy or matching paste for their materials, while one company ended up providing two different

solder ball alloys to serve as the matching material the paste alloy they provided (J-Series). Furthermore, two of the test pastes (R & S-Series) were added so late into testing that only one set of test vehicles could be constructed with them, so they were manufactured using SAC105 and SAC305 solder balls with a 6 mil stencil using the best reflow profile.

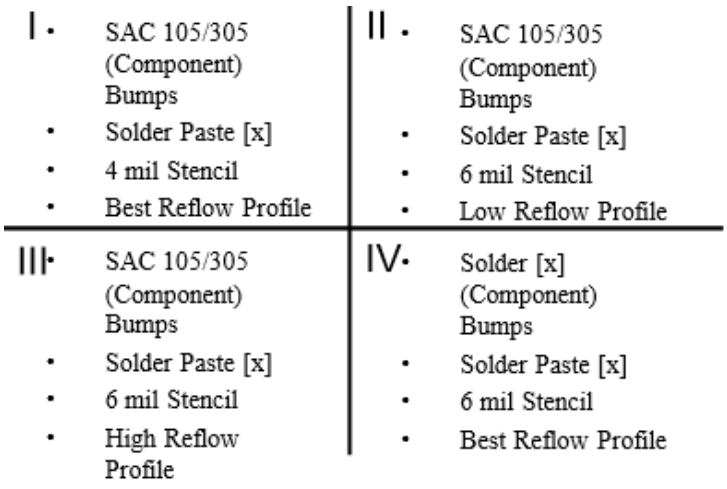

Figure 19: General overview of planned testing sequences

In order to give a better idea of which materials are actually tested during the study, the chart depicted in Figure 20 has been included for the reader's convenience. All test runs containing an "X" were performed as they were initially outlined in Figure 19. As part of the conditions in their agreement to participate in the study, most of the companies required that the exact names of the materials they provided be kept confidential. As such, each of the total 12 different lead-free pastes and 2 different solder ball-only alloys were assigned a series name to identify them during the test. Due to an initial labeling error made by a lab technician, the first four test runs involving varying stencil size, reflow temperature, and solder ball alloy for a single test paste were each given

four different labels. Since they all use the same paste, however, they will be analyzed together in the data analysis portion of the report and will be referred to as the BCDE-Series. Since SAC305 was used as the primary control solder ball alloy, CVP390, a special paste formulation using a SAC305 alloy, was also employed as the control solder paste for tests in which the manufacturers were able to supply a solder ball alloy without a corresponding paste version, namely the F and G-series. Due to the capacity limits of the shaker table used during the study and the approximately 20 hours of testing time required for 10 test vehicles, it was decided that in the interest of most effectively utilizing university resources to produce a total of 10 test vehicles manufactured following the construction variables prescribed to each portion of the experimental design; five for use as the no-aging group and five for use in the thermal chamber designed to simulate aging. This would allow a sufficient test pool size for each testing variable while enabling two sets of parameters to be tested during each 20 hour run.

Actual Tested Variables:		4 Mil BEST	6 Mil LOW	6 Mil HIGH	6 Mil BEST		Legend & Notes
BCDE-Series		X	X	X	X		X = Test performed as planned
H-Series		X	X	X	0		* = Substitution of material used for SB
I-Series		X	X	X	X	LF	~ = Substitution of material for Paste (Always CVP390)
J-Series		X	X	X	**	LF,LF	0 = Test was not performed
K-Series		X	X	X	0		LF or SAC = Substitution was made using Lead-free mixture or standard SAC mixture
L-Series		X	X	X	0		
M-Series		X	X	X	X	LF	
O-Series		X	X	X	0		
P-Series		X	X	X	0		
R-Series		0	0	0	*	SAC	Added late in testing
S-Series		0	0	0	*	SAC	Added late in testing
A-Series		0	0	0	*	SAC	
F-Series		0	0	0	~	LF	
G-Series		0	0	0	~	LF	

Figure 20: Summary of test pastes and solder ball alloys

Resistor Design

A few different factors were involved when considering the exact model of resistor to use for the experiment. The resistor should be a size that is commonly available for use by electronics manufacturers, and its failures should give the most relevant amount of data regarding the commonly used types of resistors in the industry as well as provide ample opportunities for cross-comparisons between the standard QFNs and BGAs also being tested. Since QFNs and BGAs are, by their very nature, surface mount components, the resistor used should also be a surface mount resistor so as to allow sound comparison between all three components. Once the resistor was determined to be surface-mounted, the next decision was the chip size to use. Chip resistors' body sizes usually range from 01005 to 2512 [23] with the most common resistor sizes used in industry today being 0402, 0603, 0805, and 1206 [24]. A list of the surface areas of some standard SMRs in metric and English units and their corresponding size codes used to identify them is included in Figure 21.

Size Code		Approximate Size	
Inch	Metric	Inch	Metric
0402	1005*	.04" x .02"	1.0 x 0.5mm
0504	1210*	.05" x .04"	1.2 x 1.0mm
0603	1508	.06" x .03"	1.5 x 0.8mm
0805	2012	.08" x .05"	2.0 x 1.2mm
1005*	2512	.10" x .05"	2.5 x 1.2mm
1206	3216	**.12" x .06"**	3.2 x 1.6mm
1210*	3225	.12" x .10"	3.2 x 2.5mm
1812	4532	.18" x .12"	4.5 x 3.2mm
2225	5664	.22" x .25"	5.6 x 6.4mm
2512	6432	.25" x .12"	6.4 x 3.2mm
* Caution: Overlapping size codes. Metric appears same as inches.			

Figure 21: English to metric conversion chart of resistor sizes [25]

Since it is known that larger components are more prone to failure from fatigue during vibration, it was decided that the largest size of resistor most commonly found in industry should be used for the experiment, a resistor more commonly known as a 2512. In this manner, any damage that occurred due to the test would be more readily exhibited as pronounced failures than would occur in smaller sizes of resistors. This allows the strong assumption to be made that if little to no failures occur in one of the largest commercially available resistor package sizes, then any resistors smaller in size should perform even better, i.e. experience less failures, under the same environment. After reviewing all the options, the exact resistor package chosen for use in the experiment was the 2512SMR-PA-SN-0 dummy resistor from Practical Components. The exact physical design and dimensions of the resistor can be found in Figure 22 and Figure 23. The resistor chosen covered an area of about 0.00005 in^2 and weighed approximately 0.055 grams. The chips were all manufactured using 100% Sn over Ni and delivered for manufacturing on a paper tape system. These are all common manufacturing standards for surface mount resistors and thus made this resistor the best candidate for use within the experiment.

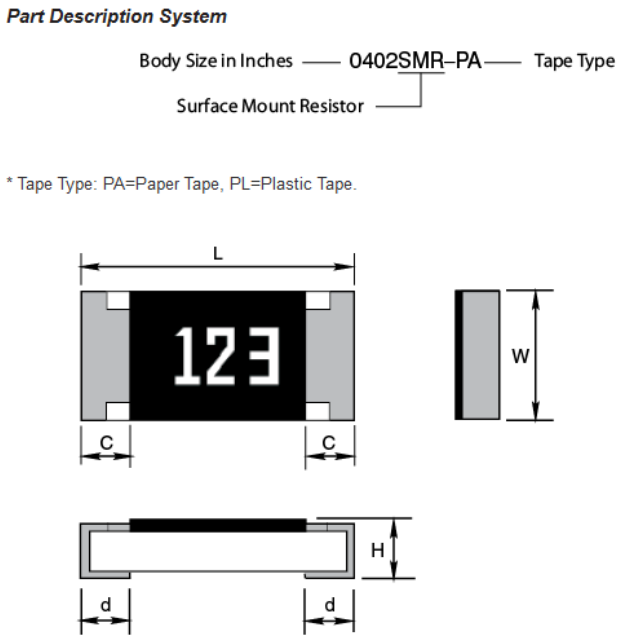

Figure 22: Profile of resistor design used in test vehicle [26]

Dimensions (mm) & Weight (g)							
	L	W	T	A	B	C	Wt.
1206	3.2±0.2	1.6±0.2	0.6±0.1	0.35±0.2	1.95 min	0.35±0.2	0.010
2010	5.1±0.2	2.5±0.2	0.7±0.1	0.45±0.2	3.70 min	0.4±0.25	0.035
2512	6.5±0.2	3.2±0.2	0.7±0.1	0.45±0.2	5.00 min	0.4±0.2	0.055

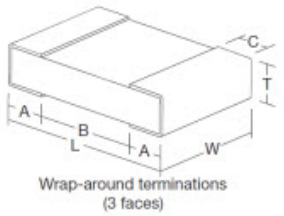

Figure 23: Dimension chart for resistor used in test vehicle [26]

QFN Design

Requirements for the QFN that was used on the test vehicle were very similar to those for the resistor in that the actual component should provide a general representation of the most commonly used versions of QFNs used in the electronics industry. After careful consideration, the exact package chosen for use in the study was

the A-MLF20-5mm-.65mm dummy QFN from Practical Components, similar in design to the one pictured in Figure 24. This package employed an Amkor® *Micro*LeadFrame® and contained 20 leads at a 0.65mm pitch with a total body size of 5mm. A cross-sectional view of the exact mechanical design used to construct the QFN is illustrated in Figure 25.

Figure 24: Picture of QFN similar in design to the QFN used on the test vehicle [27]

Part Description	Lead Count	Body Size	Pitch	Quantity Per Tube
A-MLF20-5mm-.65mm	20	5mm	.65mm	60

Notes

- Parts are packaged in tubes (standard).
- Parts are available in trays or on tape and reel upon special request.
- Solder plating finish available is 100% Matte Sn.
- Moisture sensitivity level is JEDEC 1.
- Two MLF® designs are available: Punch or Saw (see the cross-section drawing).
- Small size (50% space reduction as compared with TSSOP).
- MLF® package is a near CSP plastic encapsulated package with a copper leadframe substrate.
- MLF® is also known as QFN, MCC or MLP.
- 0.6mm to 1.5mm maximum height
- Body sizes ranging from 3 x 3mm to 12 x 12mm.
- Pin counts and body sizes change on an ongoing basis. Please call for updated listing of available packages.

Part Description System

Amkor — A-MLF12-3mm-.5mm-DC-Sn
MicroLeadFrame™ — Lead Count — Body Size — Pitch — Daisy Chain — (100% Matte Sn)

Cross-Sections MLF®

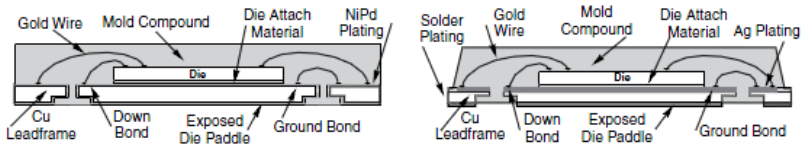

MAP Design "Saw" **Individual Unit Design "Punch"**

For kits see pages 93, 96, 98, 106 and 109.

Figure 25: Overall dimensions and internal structure of QFN design [28]

Vibration Fixture Design & Testing

In order to vibrate the test boards, a fixture system had to be designed that would be capable of holding the boards perpendicular to the electro-dynamic shaker table along the X and Y-axes while vibrating in the Z-direction. Due to sizing and attachment constraints of the pre-existing aluminum baseplate, a rectangular aluminum fixture was designed that could hold two PCB test vehicles (one on either side). Each board was affixed to one side of the aluminum fixture using a set of four screws, four washers, and either four large or small spacers**.** The fixture itself was then mounted vertically along its wide edge onto the pre-existing aluminum baseplate via two 5" long screws with two washers being placed in between the baseplate and the fixture. These screws were shown to shear off at the connection point between the baseplate and the test fixture if vibrated for 30 hours or more, so they were replaced at the end of every 20 hour test. Since the pre-existing baseplate only offered five suitable attachment locations for the designed aluminum fixture, a total of five of these substrates were manufactured. In order to ensure homogeneity between the fixtures, they were all machined and drilled from the same bar of material and by the same machinist. To further verify their characteristic uniformity, it was necessary to determine their natural frequencies. In order to accomplish this, a laser accelerometer connected to an oscilloscope was used to record the vibration-induced displacements experienced by the mounted test fixtures while the machine was operating using a 4.6 G_{rms} step stress random vibration profile. The results show that all the test fixtures experienced a similar vibration profile and had a natural frequency somewhere between 350 to 400 Hz, as

illustrated in Figure 26, Figure 27, Figure 28, Figure 29, and Figure 30. The initial oscilloscope results reported that Fixture 5 had a different natural frequency than the rest of the fixtures. However, after the fixture bolts had been tightened and the laser accelerometer was recalibrated, this variance in natural frequency was not present when the frequency test was re-run. Although the fixtures had very similar natural frequencies, in order to reduce unnecessary variability between tests, each aluminum fixture was marked to ensure it was always attached at the same location and orientation on the pre-existing baseplate for each test run. In this way, even if the slight variance in natural frequency of the fixtures had an effect on the test vehicles' failure performance, each specific test group would experience them equally and so would not skew the final results.

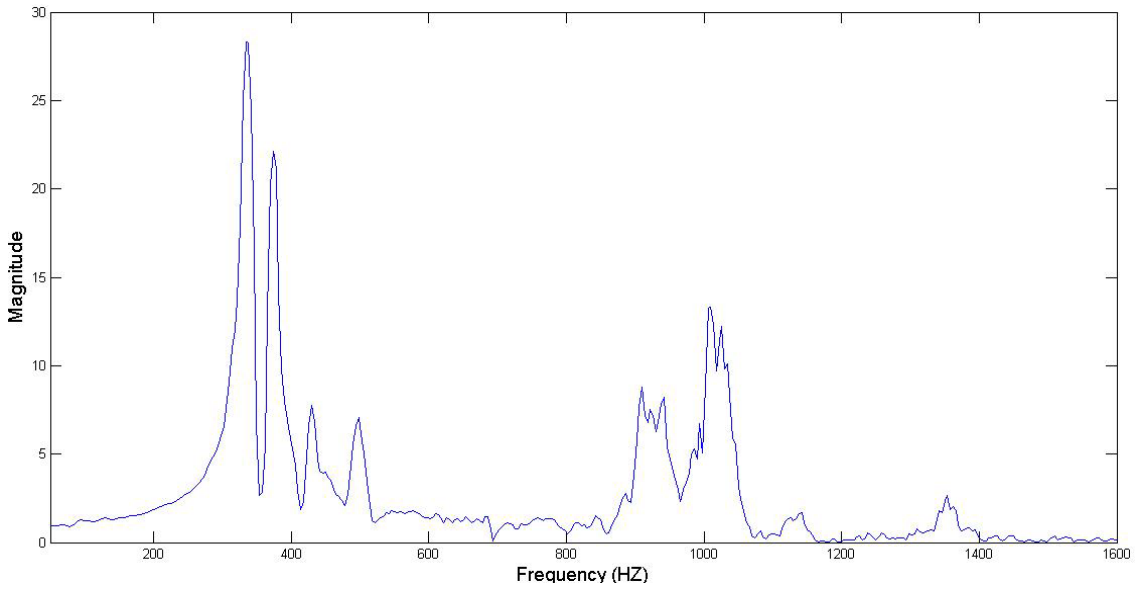

Figure 26: Natural frequency of Fixture 1

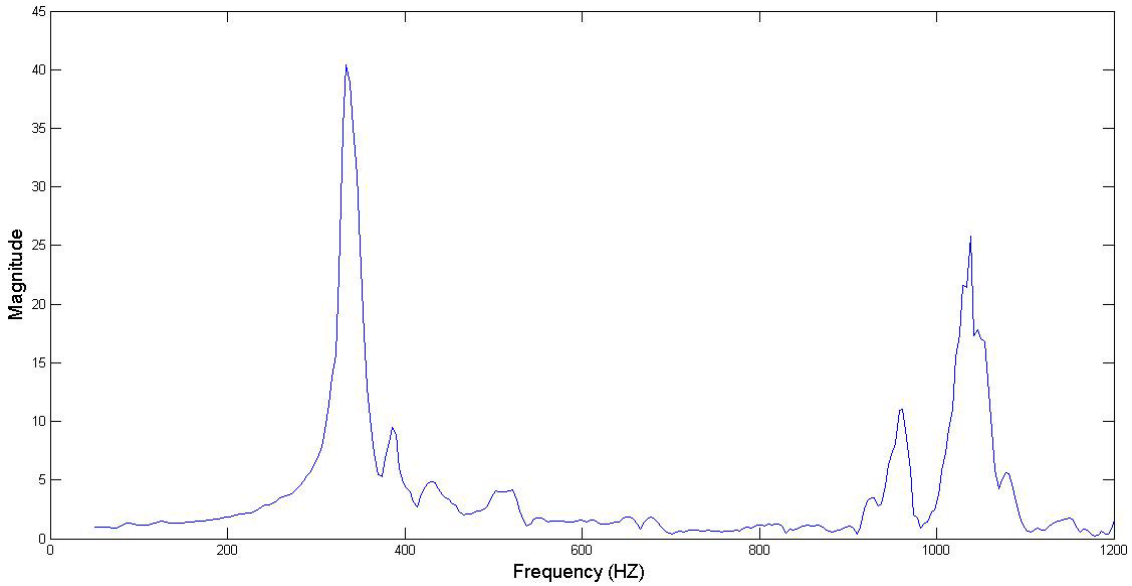

Figure 27: Natural frequency of Fixture 2

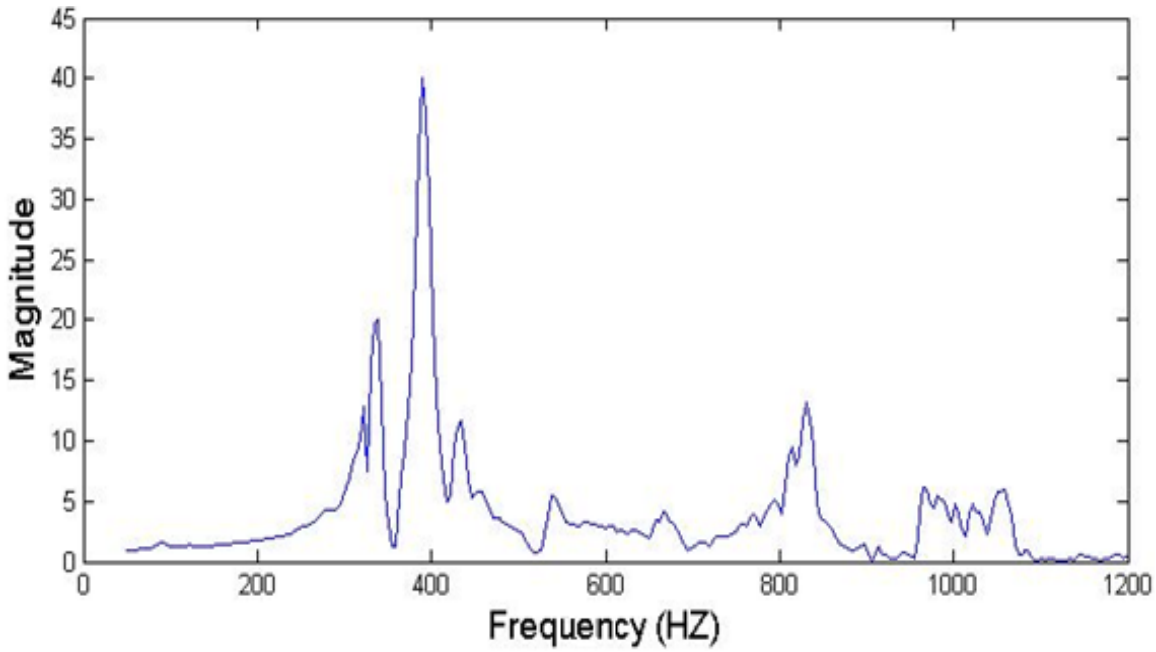

Figure 28: Natural frequency of Fixture 3

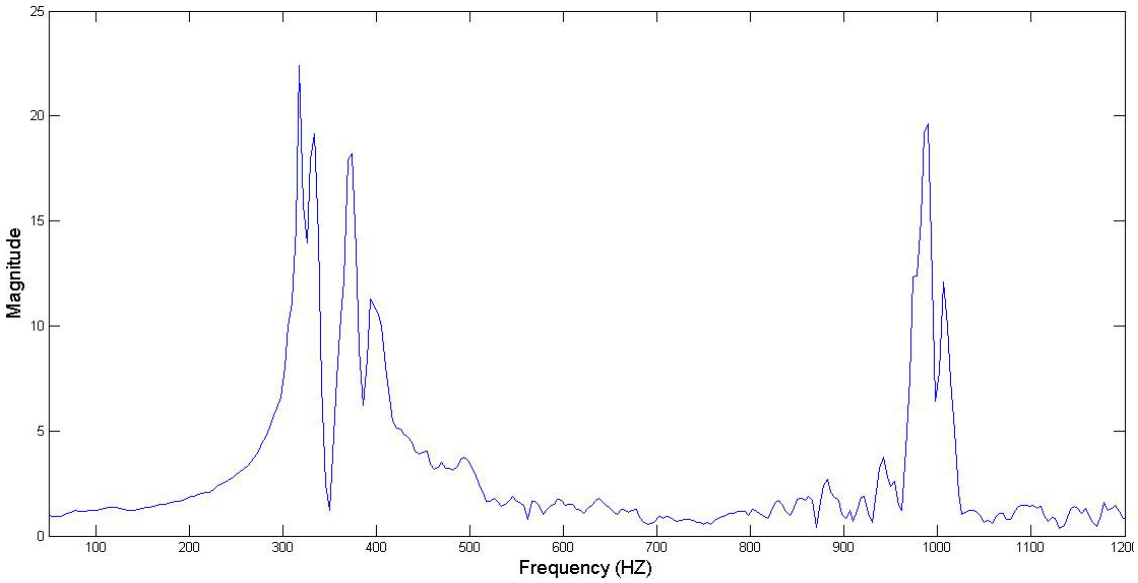

Figure 29: Natural frequency of Fixture 4

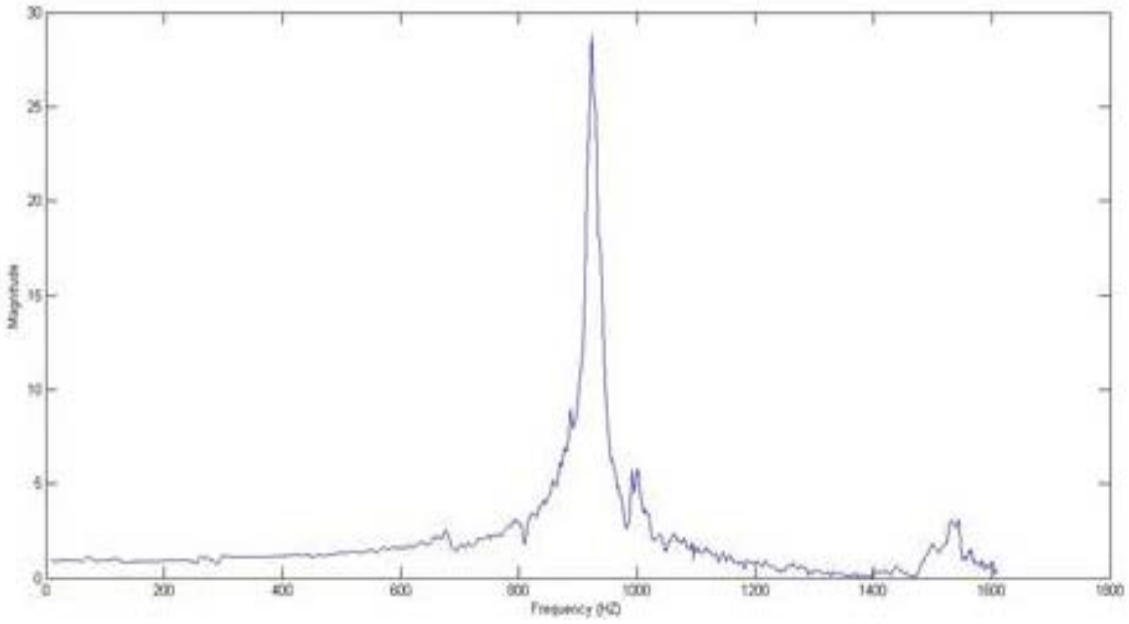

Figure 30: Natural frequency of Fixture 5

Despite the best efforts of the researchers to create the exact set of circumstances for every test during the experiment, there were several issues that could have affected the performance properties of the test fixtures. The torque applied to attach each test

vehicle to the fixture as well as the torque used to tighten the 5” vertical screws of the fixture against the baseplate were endeavored to be made the same for every test run, but no method of measuring this torque was used. In addition, over the course of a year of testing, it is possible that the threads of all the screws used within the test as well as the internal threads of the baseplate and the aluminum fixtures suffered wear sufficient to create torque differences between various areas of the test setup. This type of wear would be nearly impossible to quantify, and the mixing of the horizontal screws between different locations on the test vehicle would only make such quantification even more difficult. Finally, during very small portions of the study, the average room temperature and humidity levels might have fluctuated significantly during times when the laboratory door was left ajar by the repair technicians during their servicing of other machines in the lab. In an ideal test, these variations between tests would not exist. Luckily, however, their presence has most likely had a negligible effect on the results of the study.

Vibration Machine Testing Calibration

Once the method and apparatus for attaching the PCBs to the shaker table were created, the next step was to determine the most appropriate vibration profile to use during testing on the LDS LV217 electro-dynamic shaker machine shown in Figure 31.

Figure 31: LDS LV217 electro-dynamic shaker machine

As there was no international standard vibration testing profile that applied to this particular test setup, a slightly arbitrary vibration profile would have to be used instead. In order to keep the results of the tests within an acceptable range of resolution while still meeting the sponsor's specified deadlines for results, a set of boards would ideally begin to fail after one hour of testing and experience complete failure of all of its BGA components within 24-48 hours of vibrational stress testing. This type of failure schedule would allow for an estimated average and linear component failure rate of about one every half hour, meaning manual circuit probing could, in theory, be performed only once an hour without incurring a significant diminishment in data resolution. The best way of finding the vibration profile that would cause complete board failure in this relative timespan was through trial-and-error. As such, 15 test vehicles using half SAC105 BGAs and half SAC305 BGAs attached with the CVP390

control paste were constructed as test samples for use in these trials. The first vibration profile of 8 G_{rms} resulted in complete failure of all components except some resistors within three hours of testing. In the next test, a vibration profile of 6 G_{rms} was used which caused complete failure of all BGA components within four and a half hours. The third test at 4 G_{rms} caused all BGA components to electrically fail within 30 hours of testing. The final test run at 4.6 G_{rms} caused complete board failure within 23.5 hours of testing. Since this vibration profile seemed to yield fairly evenly-spaced component failures over the course of testing with complete failure of all BGA components occurring by the end of the 24th hour, a step stress random vibration profile of 4.6 G_{rms} along the Z-axis was chosen as the vibration profile for use within the LDS LV217 electro-dynamic shaker machine in the experiment. A sample of the typical distribution of vibrational forces experienced by the fixtures during testing in shown Figure 32.

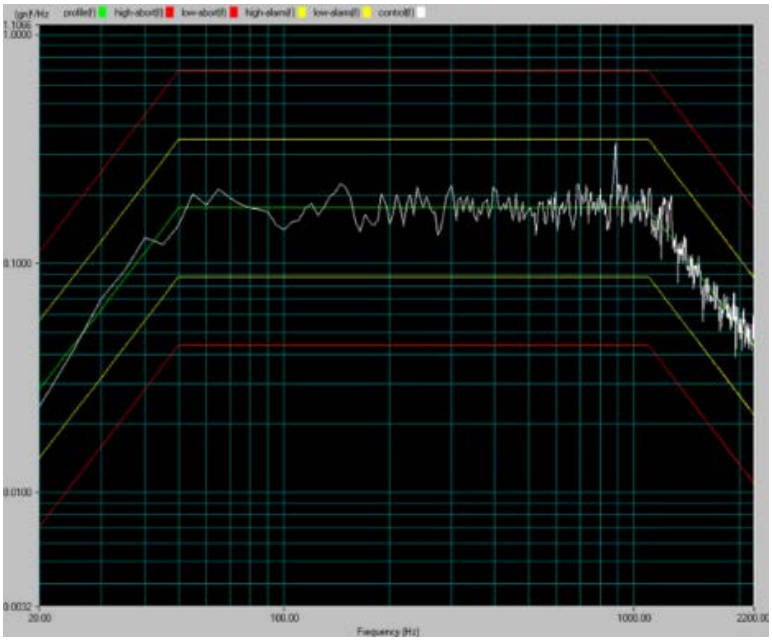

Figure 32: Frequency and magnitude distribution of typical vibration outputs

Method for Testing for Component Failure

Once the test boards had been manufactured and fitted onto the test substrates which were attached to the shaker table and a suitable vibration profile had been selected, the establishment of the classification of what constituted a component failure as well as the method by which it would be found was a critical step in the experimental process. During vibrational stress testing, there are four possible states that a specific component could be experiencing at the time data is being recorded. The first state is classified as the alpha state, where a component is still as electrically and mechanically robust as it was when it left the factory floor. Vibrated components in this state are, for all intents and purposes, indistinguishable from their non-vibrated counterparts. The second state the components could experience is referred to as the beta state. Beta-state components still pass electrical tests but small alterations in their mechanical structures due to the vibrational testing have increased the amount of resistance experienced within the component and have most likely weakened its overall mechanical support structure. The third state the electronic components could experience is referred to as the delta state. Components in a delta state are those whose mechanical and electrical structures have incurred enough damage to increase the resistance within their circuits just enough to cause them to fail an electrical test and be read as an open circuit. However, if the component continues to be vibrated after this, due to a phenomenon assumed to operate similarly to vibrational fretting that can occur during vibrational testing, it is possible for the mechanical structures within these components to slightly realign and repair themselves enough to reduce the

total resistance in the circuit down just enough past the measurement threshold to pass an electrical test later on in the future. Such an electrical test would no longer classify the component to be in a delta state, but rather a beta state since it now passes electrical testing but still has higher levels of resistance than would be found in alpha-state components. Components in a delta state can be very tricky to classify, as it is nearly impossible to predict whether a delta-state component will re-enter a beta state or enter the final type of component state, gamma. The mechanical support structure of gamma-state components have become so irreversibly damaged, that no amount of vibrational fretting is going to allow them to pass an electrical test in the future. The mechanical support structure has become so damaged that some gamma-state components may fly off the printed circuit board entirely. Therefore, due to the limitations of the testing abilities available to the tester, it was decided that delta- and gamma-state components both be considered failures. In addition, since the resistance of beta components could vary so widely that the disparities in resolution of different probing devices could lead to conflicting electrical results regarding the integrity of the circuit, it was decided that failure had occurred whenever the component was recorded to have an initial open event value of more than 300Ω.

Once the requirements for failure of a component had been established, it was necessary to determine the method by which to electrically verify each component. Electrical testing could either be done through automated sensors or by hand with a portable electrical probe. Automated sensors would have been able to record the exact moment during testing when a failure occurred and saved time from having to probe

them manually every hour, but it would also have required that every single test board have 27 wires hand-soldered to their electrical test pads. This means that each 20 hour test would have required 270 wires to be soldered before testing could have commenced. As was mentioned earlier, since the component failures of the initial profile calibration test were following a somewhat linear rate of failure, the gain in data resolution from having automated sensors instead of hourly probes would not be very significant. In addition, the time spent soldering the wires to the circuit boards would have most likely outweighed any time-saving benefit from not having to stop the test each hour and probe the boards manually. Finally, although the hand probing method may have resulted in lower data resolution, it most likely produced more reliable data as it was not subjected to any of the failure false positives that might have been recorded by the computer due to mechanical failures of the soldered wire joints required for automated probing during vibration testing. Due to these reasons, the experimental results were gathered through manual probing of the circuit boards once every hour.

Chapter 4

DATA ANALYSIS

The primary independent variables were solder paste alloy, solder ball alloy, stencil size, reflow profile, and component condition (aged v/s non-aged) during the experiment. Since the objective of the experiment was to discover the effects of solder doping on the reliability performance of BGA components, the failure data involving the QFNs and resistors has been excluded from the data analysis since preliminary examinations showed them to be significantly more structurally robust than most of the BGA test components. During the analysis, it was necessary to establish a set of criteria in order to accurately and fairly judge the reliability performance of the test specimens. The performance benchmarks that were analyzed were the magnitude of failure, ATTIF, MTTF, characteristic life, and failure rate. When evaluating the magnitude of failure that occurred for a sample, the total percent failure of the BGA components of that sample version on all five test boards was used as the primary indicator since it accounted for the difference in the sample sizes between the SAC105 and SAC305 groups. This percent failure was then evaluated for the subset of each sample test series and ranked from lowest to highest with a base margin of error of ±3%. This form of analysis is very limited in its usefulness but allowed for additional information to be provided for the few samples that were less-accurately characterized through Weibull analysis. The

Weibull++ software from Reliasoft was used to quickly create Weibull plots and chart data for all of the samples within a series using a standard two parameter Weibull analysis and to allow for greater ease in comparing samples from different series. In most cases, a two parameter Weibull distribution was found to accurately characterize the failure behavior of the test samples, resulting in a curve fit of 90% or higher. However, there were also many instances when the test samples possibly would have been more appropriately modeled using a three parameter Weibull distribution. This was most likely due to the presence of multiple modes of failure within certain test sets caused by variations in the microstructure of the solder alloys or defects created during the manufacturing process. However, any additional accuracy gained from modeling these specific test sets with a three parameter Weibull would likely have had a negligible impact on the study's overall results. All test data distribution models were confirmed to have a curve fit of 85% or higher, so the two parameter Weibull was deemed satisfactory. When ranking the reliability performance between samples, a heavy importance was placed on maximum ATTIF since it is a factor that essentially predicts the "warranty period" of guaranteed reliability for a sample. If two samples were relatively similar in ATTIF, the sample with the lowest failure rate and typically larger MTTF and characteristic life would be ranked higher. There are a few cases that do not follow these rules, such as when a sample with a larger rate was selected over a sample with a lower failure rate and higher ATTIF. This was done because the slight improvements in ATTIF gained from using a slow-failing sample did not outweigh the benefits of greater failure predictability gained by using a sample with a sharper failure

rate. Since only one test set using a 6mil stencil and the best reflow profile was performed for series A, F, G, R, and S, it was felt most appropriate to analyze them all together, as individually they offered no opportunities for cross-comparison between varying parameters like the other test series. Finally, the overall short-term and long-term failure analyses were conducted through the evaluation of the ranges of specific performance factors, rather than a comparison using a single value for each parameter. This is because these analyses included multiple sets of data from test runs involving varied SAC formulations and/or aging and no-aging effects, resulting in two to four different values for the same performance factor for a specific test set to be calculated. As there was no numerical method to convert these values into a single equivalent value for the performance factor in regards to their combinative testing conditions, the lowest and highest values recorded for each performance factor were used to create a general range to account for the representative effects of multiple testing conditions. The comparison of these ranges for specific performance factors between test sets was then conducted for both the short-term and the long-term analyses. The estimated values for the performance factors in the range-based analyses are less precise than their direct value counterparts, but the results they provide in terms of relative performance rankings between test sets are still highly reliable.

BCDE-Series Results

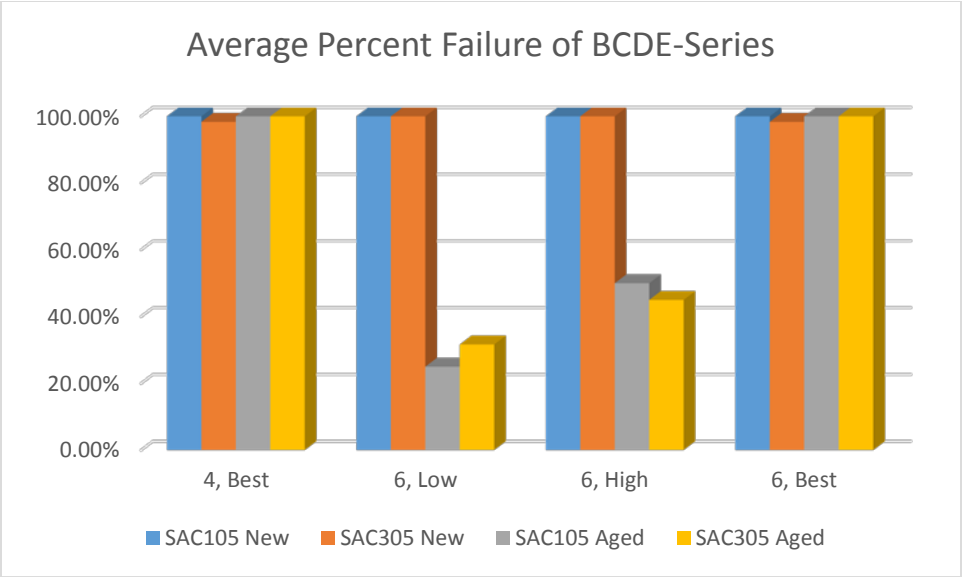

Figure 33: Average percent failure of BGA components in the BCDE-Series

Average Percent Failure ±3%	SAC105	<,>, or =	SAC305	Both
Lowest % Failures (No-Aging)	None	N/A	None	None
Lowest % Failures (Aged)	6, Low	performed better than	6, High	6, Low
Combo w/ Lowest % Failures (Total Life)	6, Low	performed better than	6, Low	6, Low

Table 1: Percent failure performance comparison for the BCDE-Series

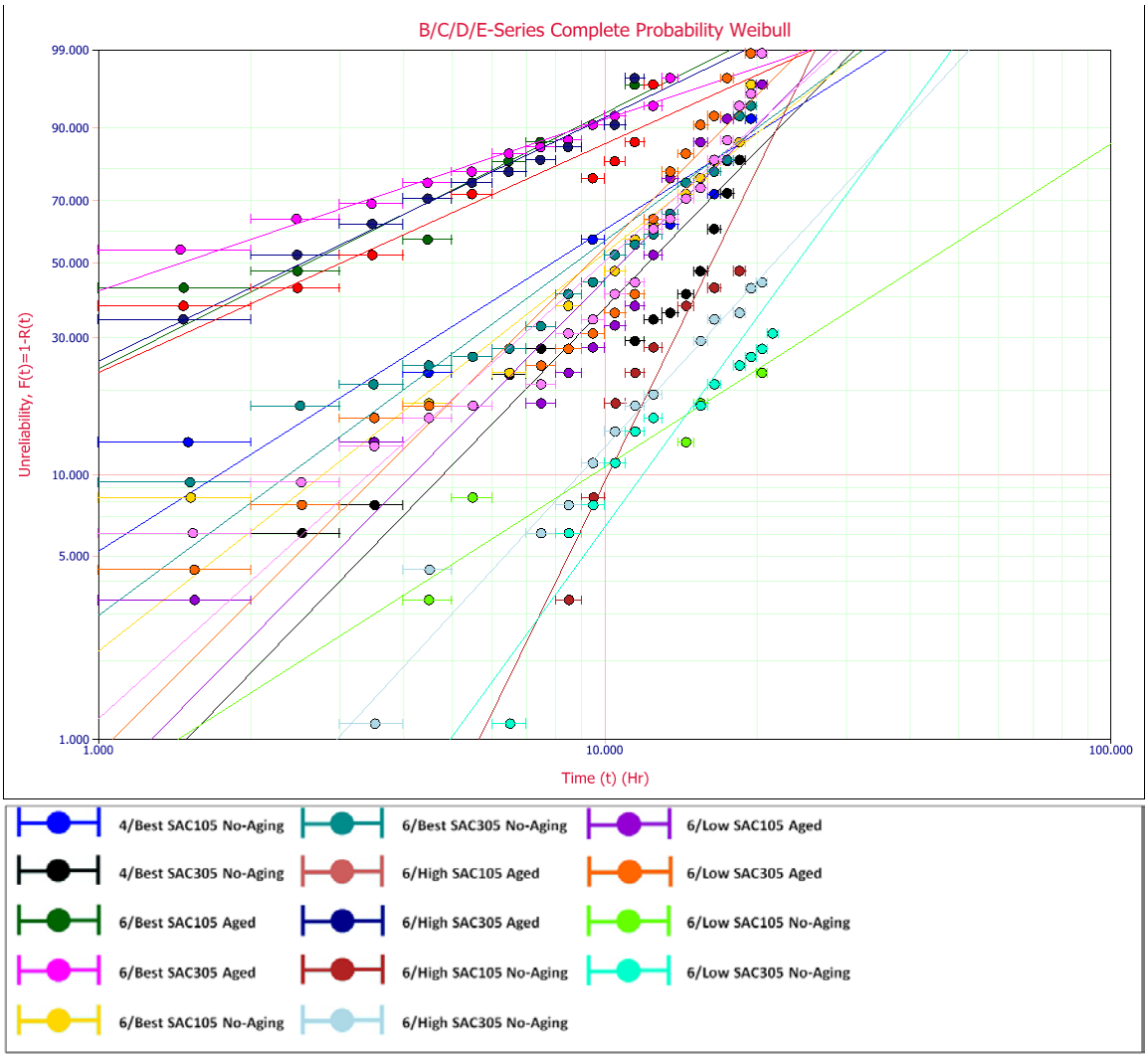

Figure 34: BCDE-Series complete probability Weibull plot

H-Series Results

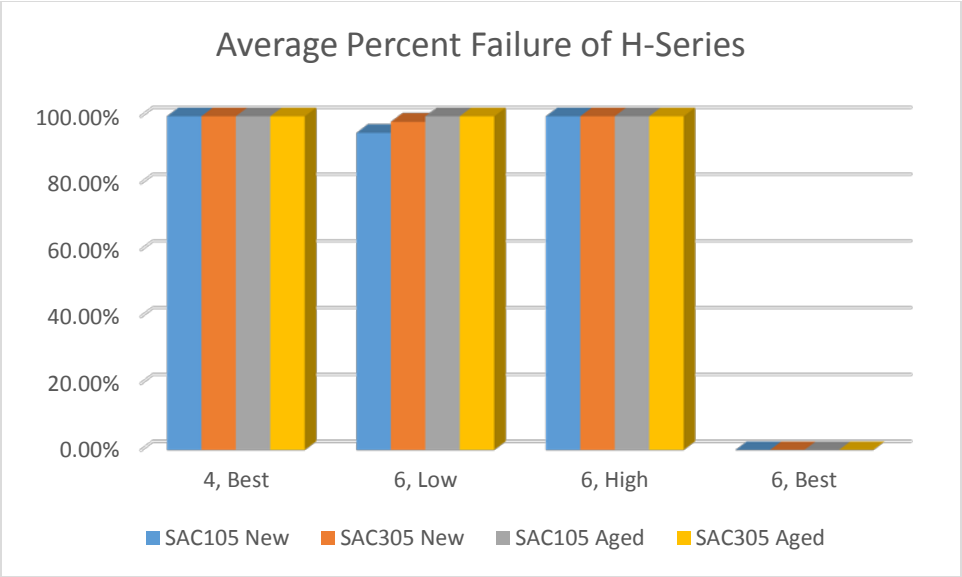

Figure 35: Average percent failure of BGA components in the H-Series

Average Percent Failure ±3%	SAC105	<,>, or =	SAC305	Both
Lowest % Failures (No-Aging)	6, Low	performed better than	6, Low	None
Lowest % Failures (Aged)	None	N/A	None	None
Combo w/ Lowest % Failures (Total Life)	6, Low	performed equally to	6, Low	6, Low

Table 2: Percent failure performance comparison for the H-Series

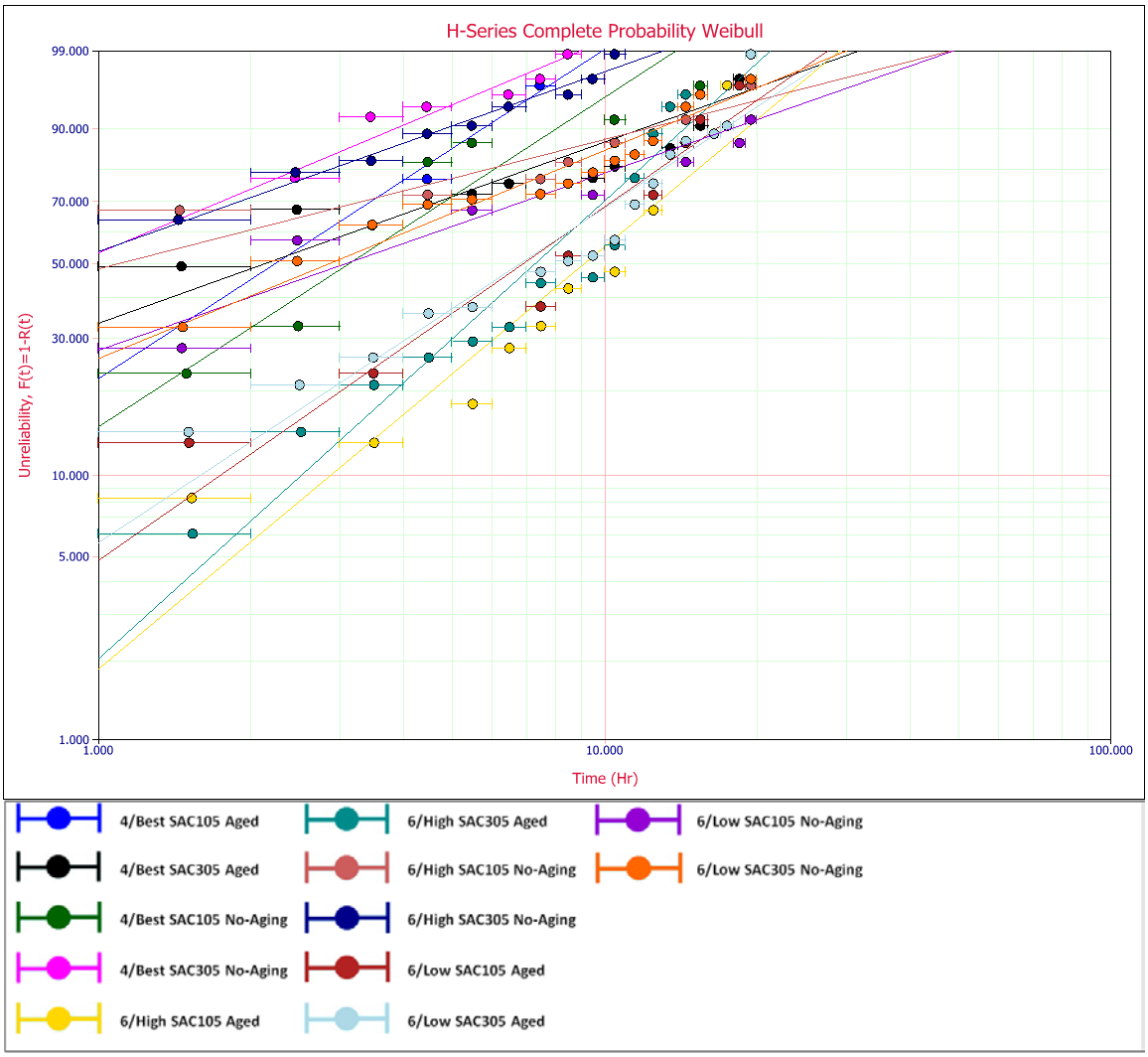

Figure 36: H-Series complete probability Weibull plot

I-Series Results

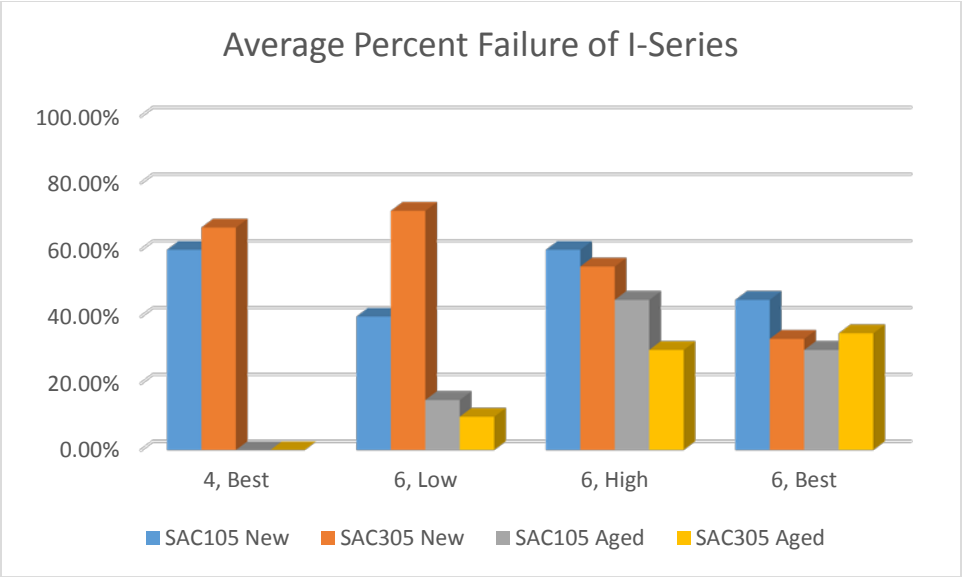

Figure 37: Average percent failure of BGA components in the I-Series

Average Percent Failure ±3%	SAC105	<,>, or =	SAC305	Both
Lowest % Failures (No-Aging)	6, Low	performed better than	6, Best	6, Best
Lowest % Failures (Aged)	6, Low	performed worse than	6, Low	6, Low
Combo w/ Lowest % Failures (Total Life)	6, Low	performed better than	6, Best	6, Low 6, Best

Table 3: Percent failure performance comparison for the I-Series

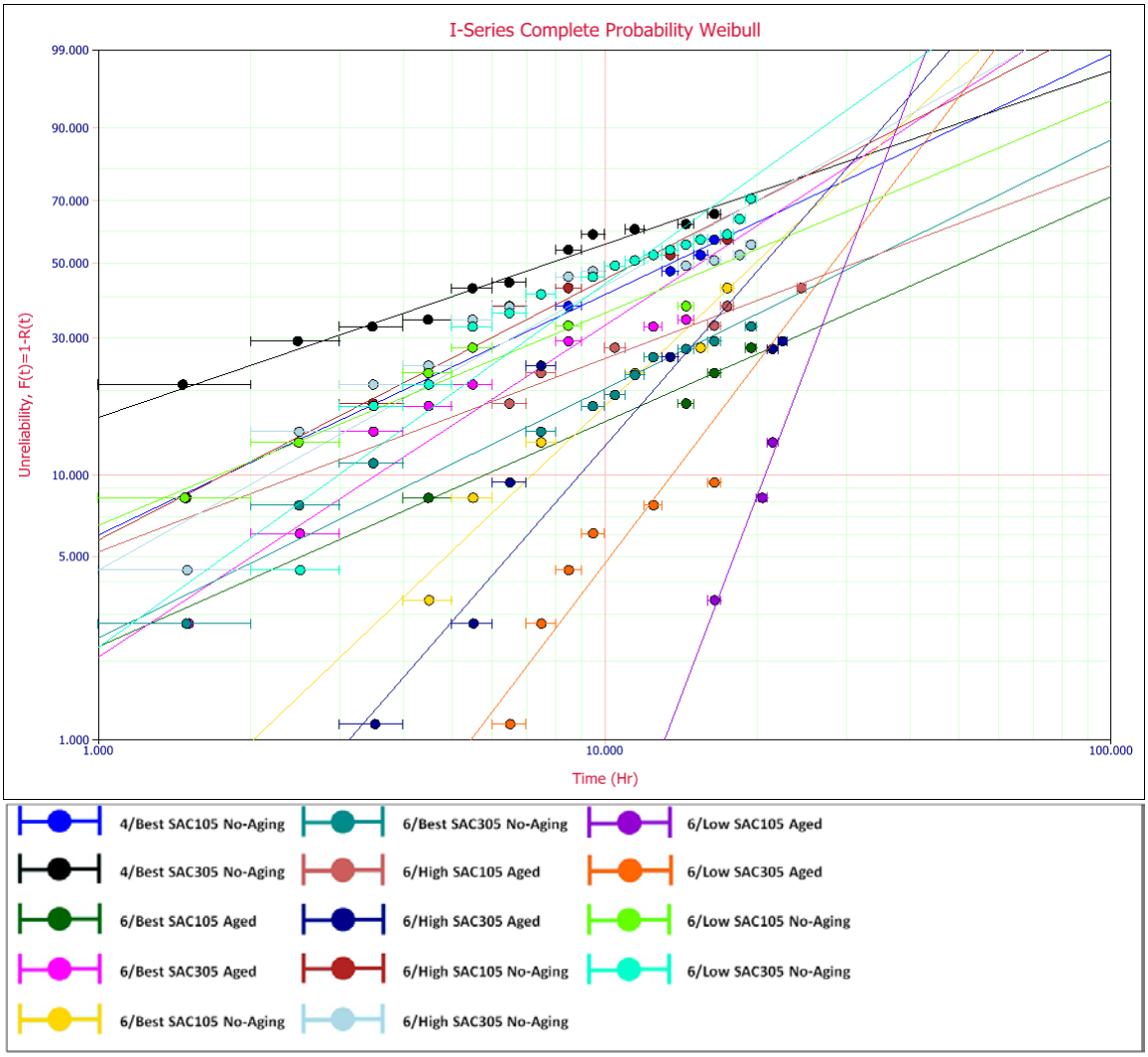

Figure 38: I-Series complete probability Weibull plot

J-Series Results

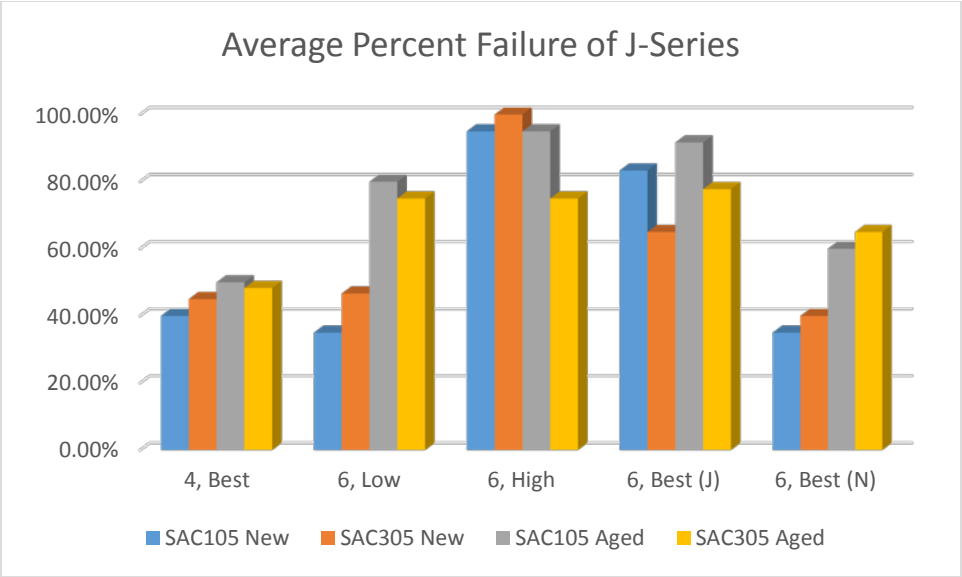

Figure 39: Average percent failure of BGA components in the J-Series

Average Percent Failure ±3%	SAC105	<,>, or =	SAC305	Both
Lowest % Failures (No-Aging)	6, Low 6, Best (N)	performed better than	6, Best (N)	6, Best (N)
Lowest % Failures (Aged)	4, Best	performed equally to	4, Best	4, Best
Combo w/ Lowest % Failures (Total Life)	4, Best	performed equally to	4, Best	4, Best

Table 4: Percent failure performance comparison for the J-Series

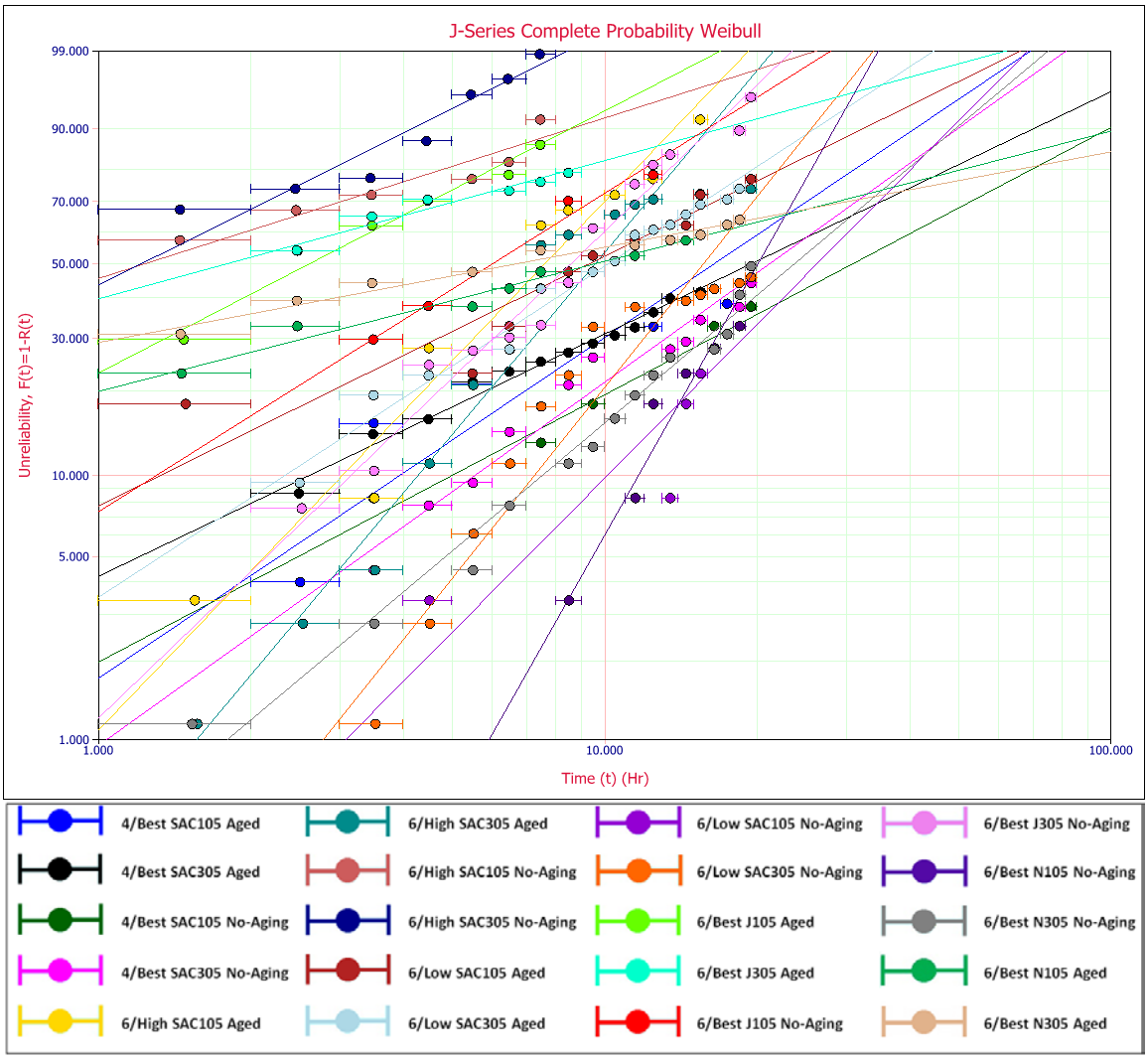

Figure 40: J-Series complete probability Weibull plot

K-Series Results

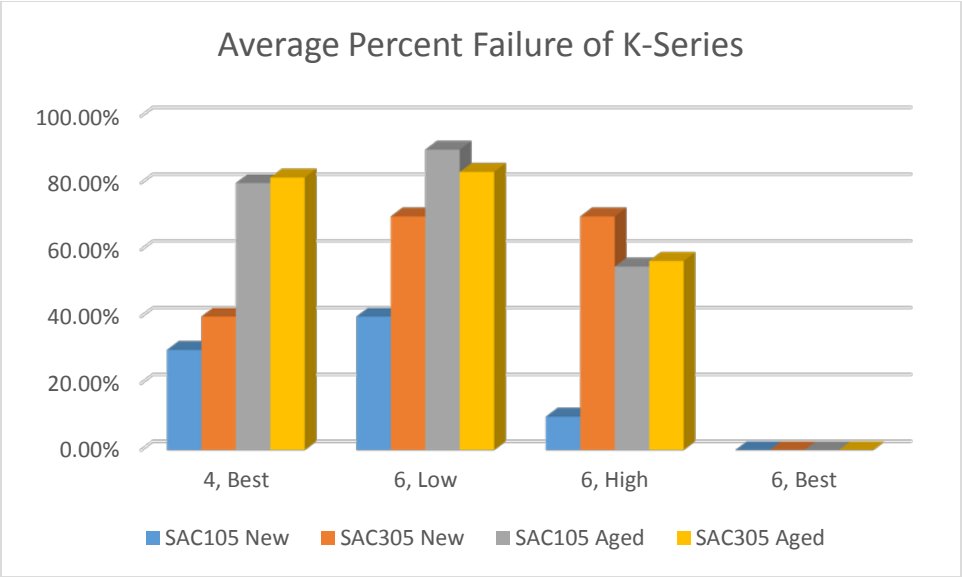

Figure 41: Average percent failure of BGA components in the K-Series

Average Percent Failure ±3%	SAC105	<,>, or =	SAC305	Both
Lowest % Failures (No-Aging)	6, High	performed better than	4, Best	Both
Lowest % Failures (Aged)	6, High	performed equally to	6, High	4, Best
Combo w/ Lowest % Failures (Total Life)	6, High	performed better than	4, Best 6, High	6, High

Table 5: Percent failure performance comparison for the K-Series

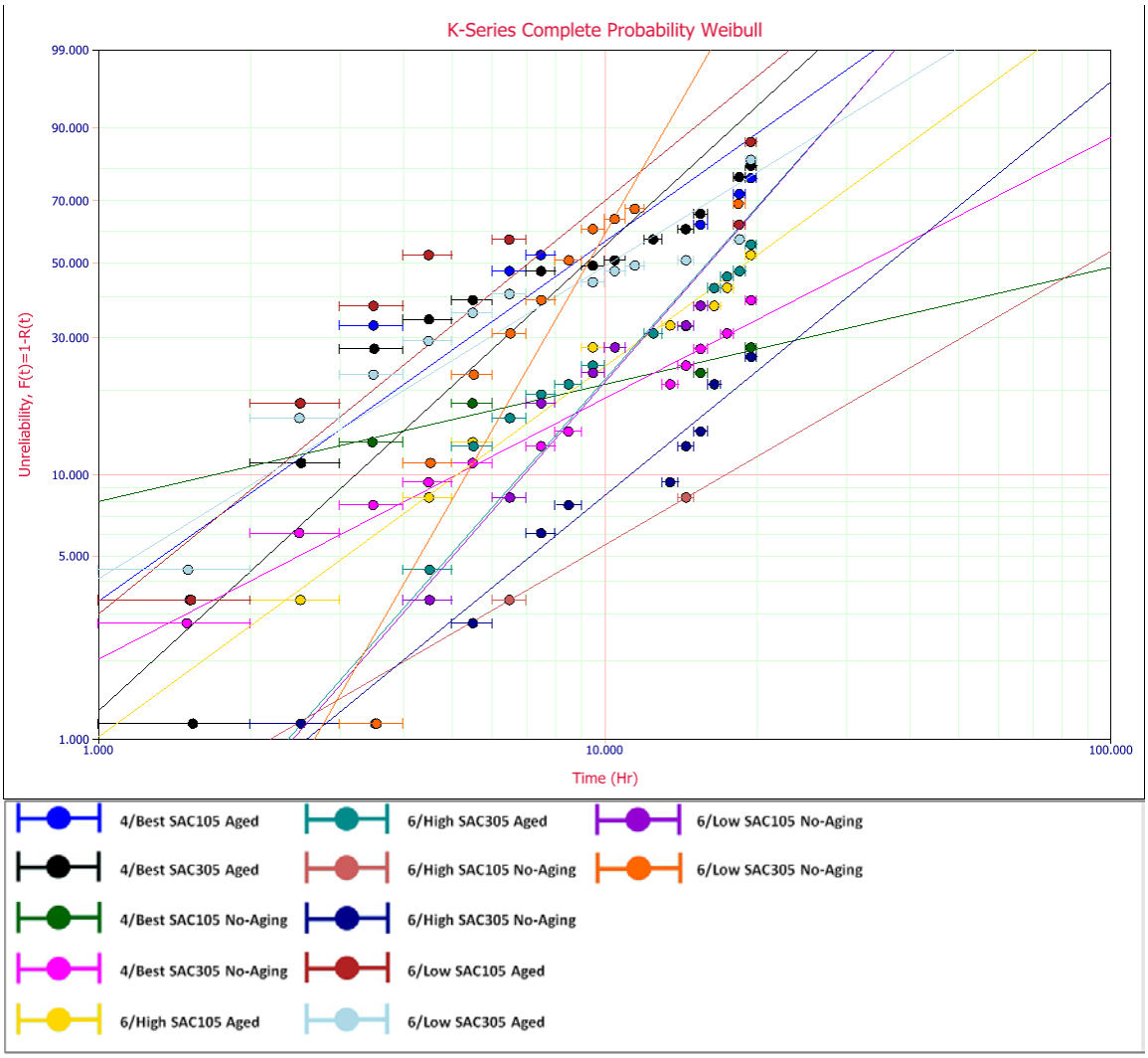

Figure 42: K-Series complete probability Weibull plot

L-Series Results

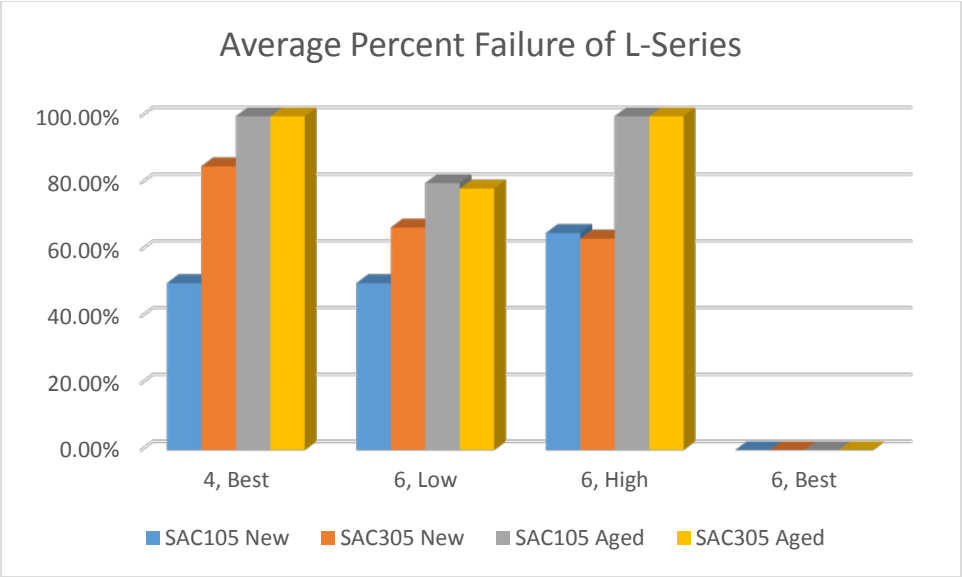

Figure 43: Average percent failure of BGA components in the L-Series

Average Percent Failure ±3%	SAC105	<,>, or =	SAC305	Both
Lowest % Failures (No-Aging)	4, Best 6, Low	performed better than	6, Low 6, High	6, Low
Lowest % Failures (Aged)	6, Low	performed equally to	6, Low	6, Low
Combo w/ Lowest % Failures (Total Life)	6, Low	performed better than	6, Low	6, Low

Table 6: Percent failure performance comparison for the L-Series

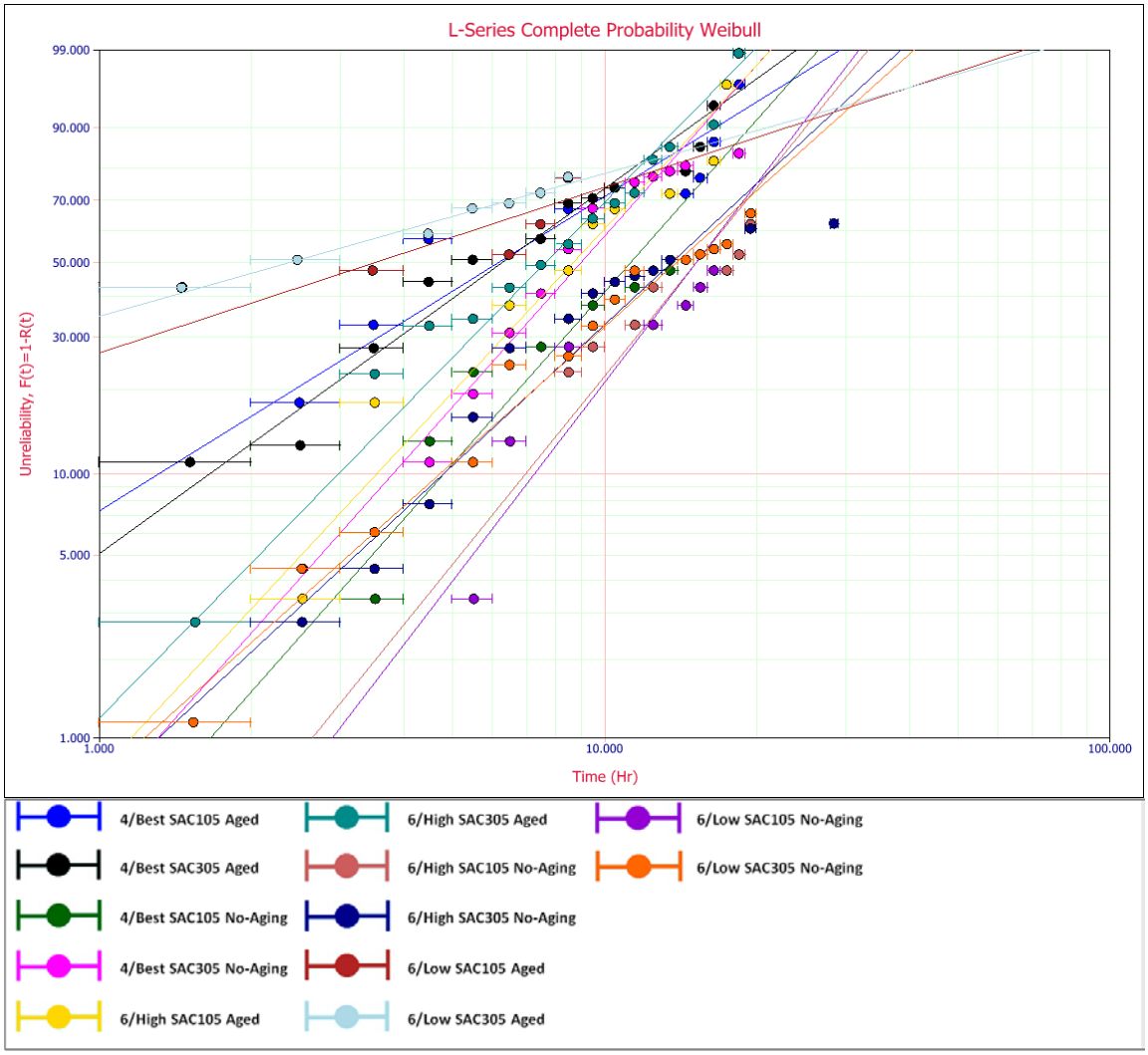

Figure 44: L-Series complete probability Weibull plot

M-Series Results

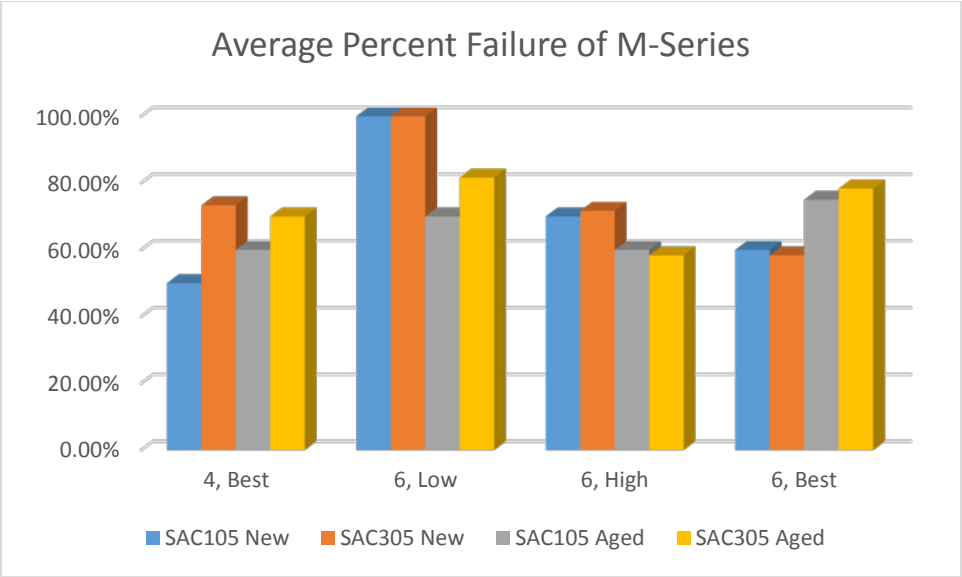

Figure 45: Average percent failure of BGA components in the M-Series

Average Percent Failure ±3%	SAC105	<,>, or =	SAC305	Both
Lowest % Failures (No-Aging)	4, Best	performed better than	6, Best	4, Best 6, High
Lowest % Failures (Aged)	4, Best 6, High	performed equally to	6, High	6, High
Combo w/ Lowest % Failures (Total Life)	4, Best	performed better than	6, High	4, Best

Table 7: Percent failure performance comparison for the M-Series

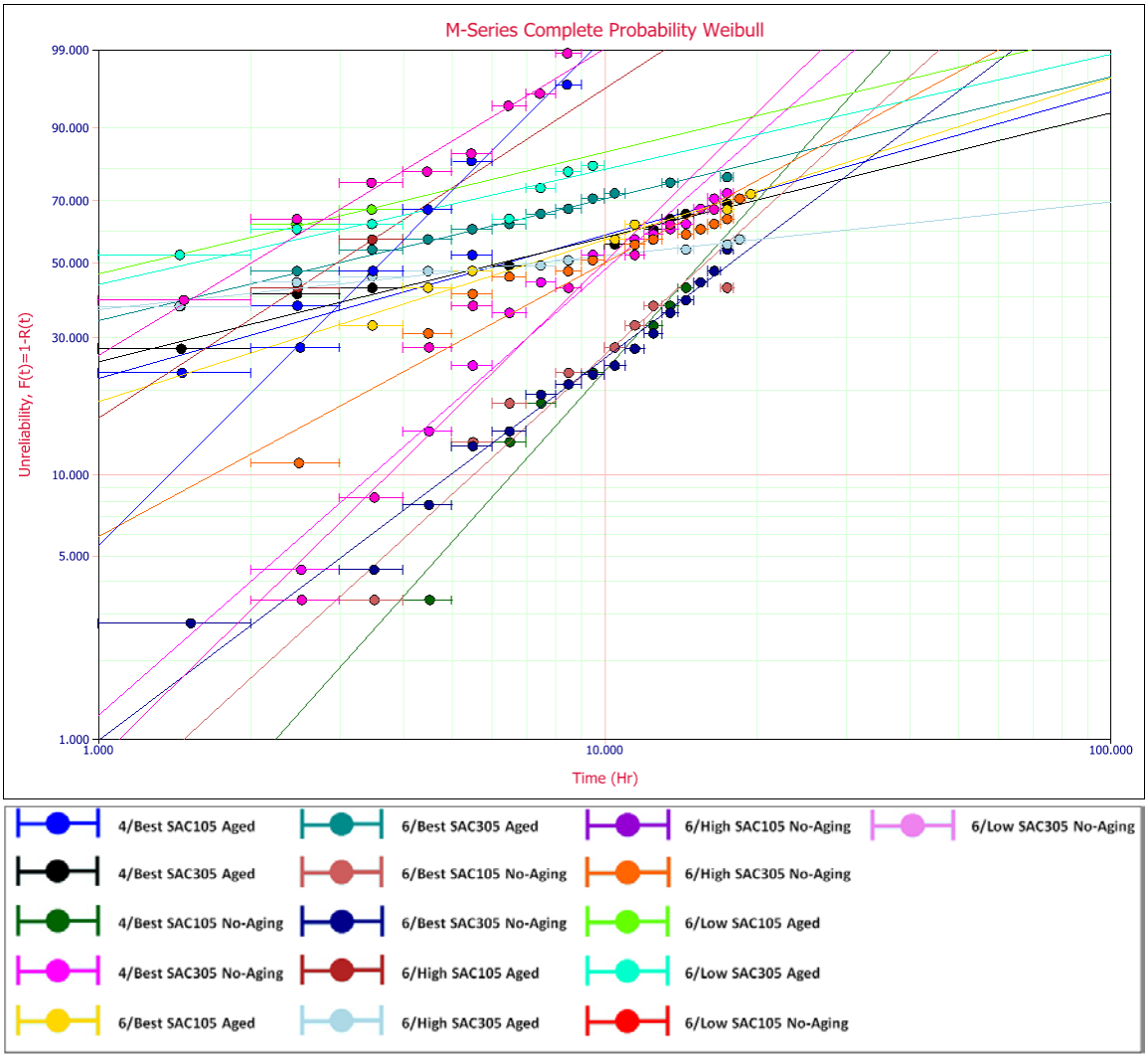

Figure 46: M-Series complete probability Weibull plot

O-Series Results

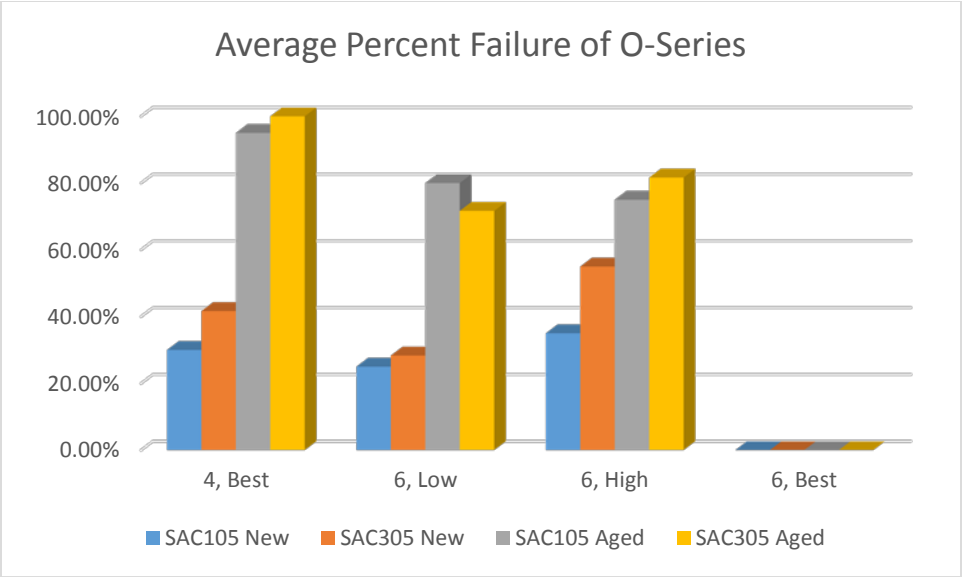

Figure 47: Average percent failure of BGA components in the O-Series

Average Percent Failure ±3%	SAC105	<,>, or =	SAC305	Both
Lowest % Failures (No-Aging)	6, Low	performed better than	6, Low	6, Low
Lowest % Failures (Aged)	6, High	performed worse than	6, Low	6, Low 6, High
Combo w/ Lowest % Failures (Total Life)	6, Low 6, High	performed worse than	6, Low	6, Low

Table 8: Percent failure performance comparison for the O-Series

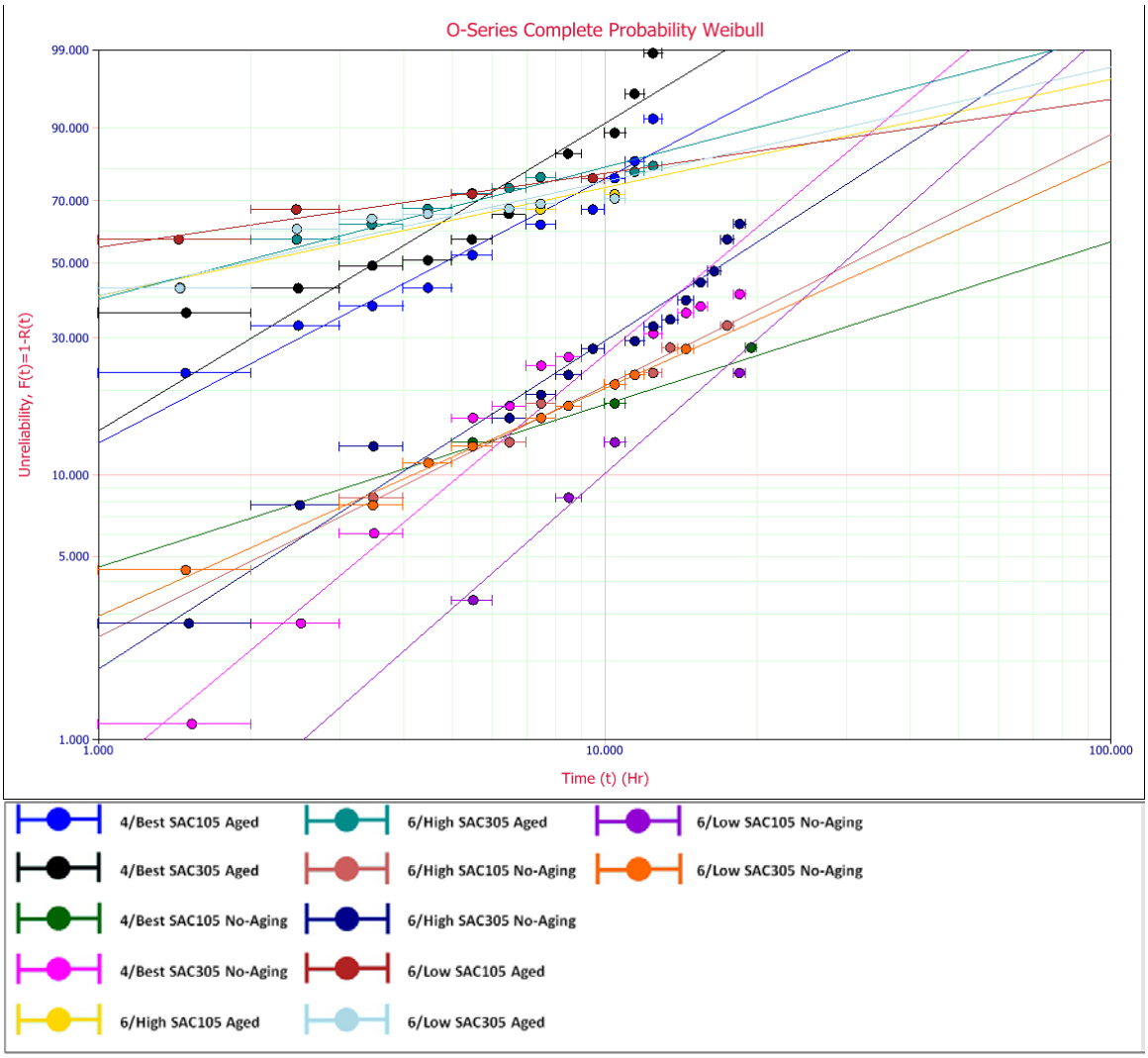

Figure 48: O-Series complete probability Weibull plot

P-Series Results

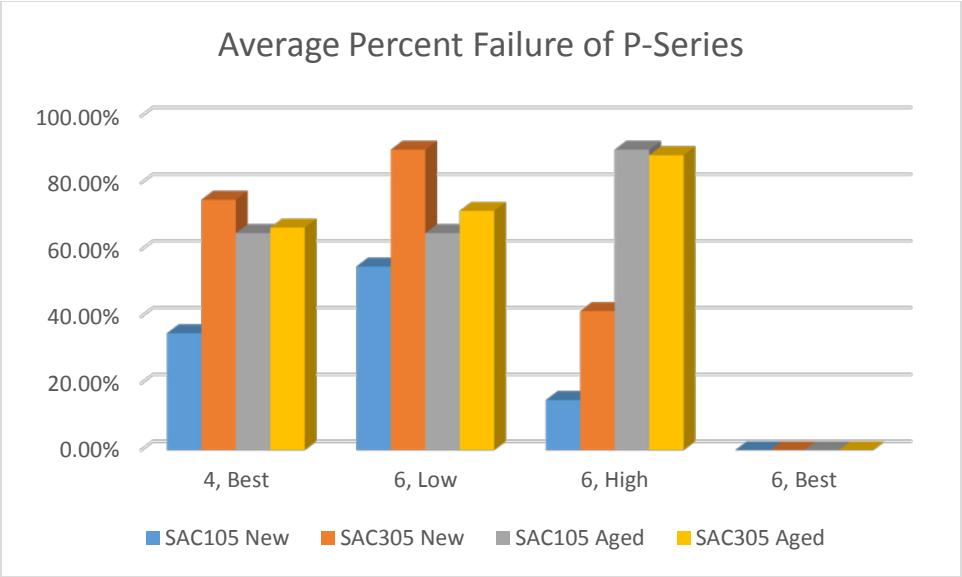

Figure 49: Average percent failure of BGA components in the P-Series

Average Percent Failure ±3%	SAC105	<,>, or =	SAC305	Both
Lowest % Failures (No-Aging)	6, High	performed better than	6, High	6, High
Lowest % Failures (Aged)	4, Best 6, Low	performed equally to	4, Best	4, Best 6, Low
Combo w/ Lowest % Failures (Total Life)	4, Best 6, High	performed equally to	6, High	6, High

Table 9: Percent failure performance comparison for the P-Series

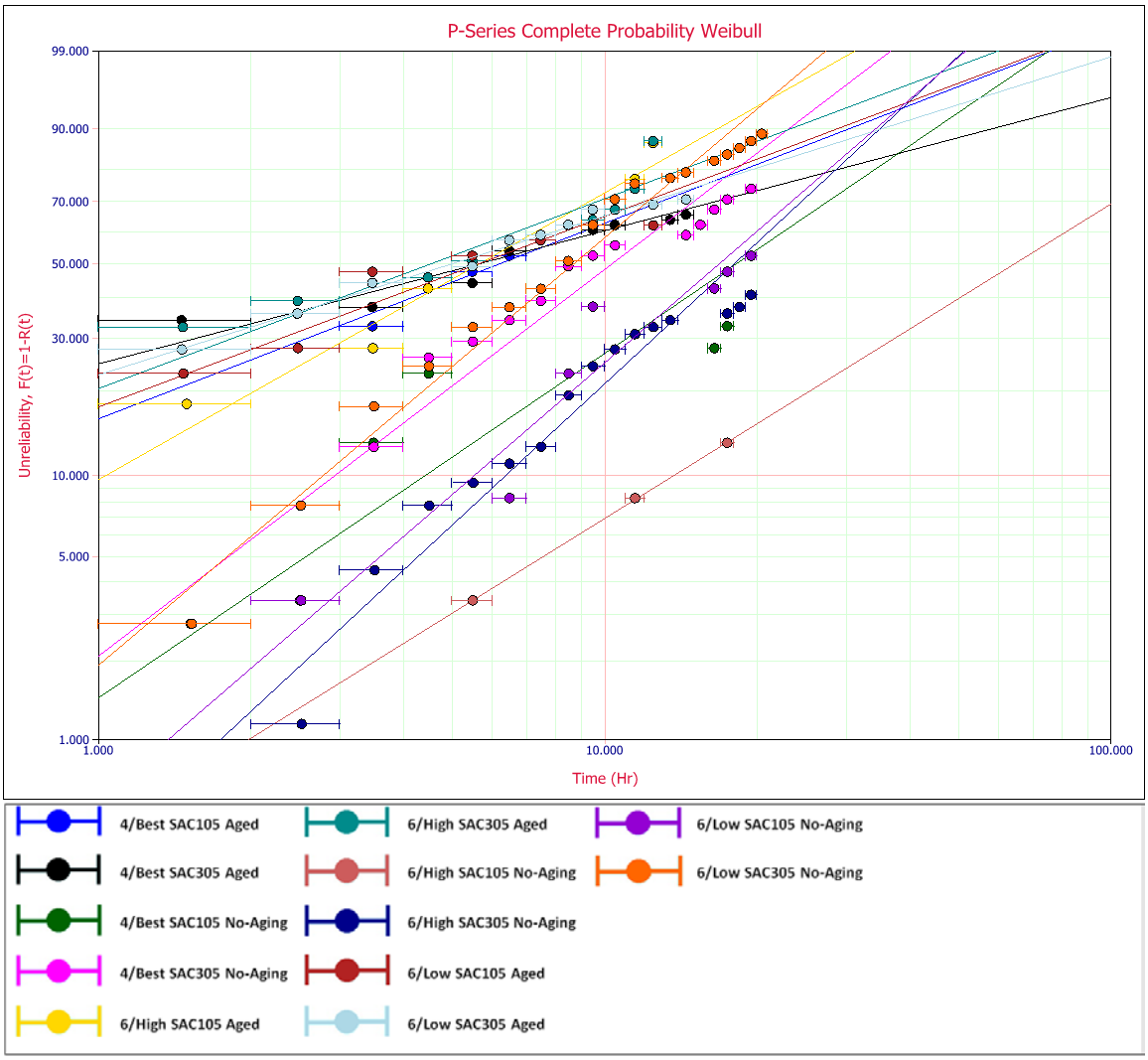

Figure 50: P-Series complete probability Weibull plot

A, F, G, R, & S-Series Results

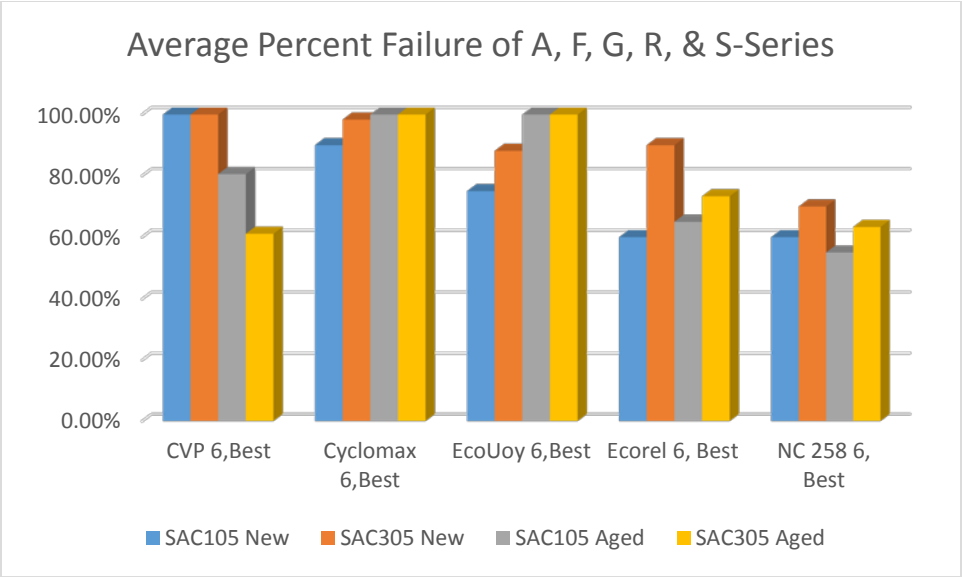

Figure 51: Average percent failure of BGA components in the A, F, G, R, & S-Series

Average Percent Failure ±3%	SAC105	<,>, or =	SAC305	Both
Lowest % Failures (No-Aging)	6, Best (R) 6, Best (S)	performed better than	6, Best (R)	6, Best (R)
Lowest % Failures (Aged)	6, Best (R)	performed better than	6, Best (A) 6, Best (R)	6, Best (R)
Combo w/ Lowest % Failures (Total Life)	6, Best (R)	performed better than	6, Best (R)	6, Best (R)

Table 10: Percent failure performance comparison for the A, F, G, R, & S-Series

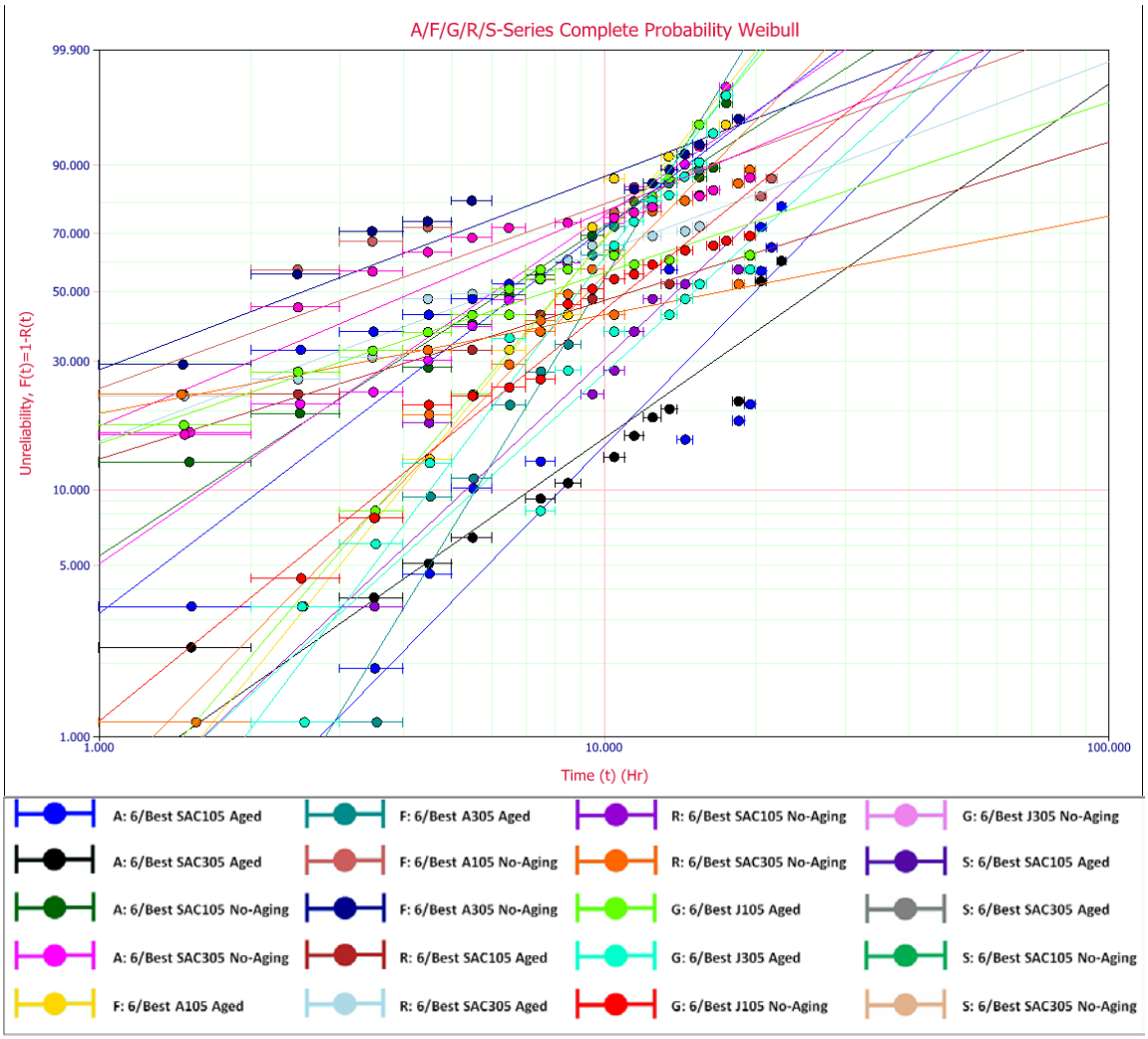

Figure 52: A, F ,G, R, and S-Series complete probability Weibull plot

No-Aging and Aging Top Performer Analysis

The 3-4 test samples that were calculated as having the greatest reliability for all of the no-aging and aged sample data, both individually and as a SAC pair, are listed in Table 11 and Table 12, respectively. Although interesting, this manner of organizing the data is rather unbeneficial and has been included as a matter of completeness. It is more useful to examine the performance of a single sample over the entire course of its lifecycle. As such, the top performing test formulations for SAC105, SAC305, or both for the no-aging and aging portions of the experiment are outlined in Table 13 and Table 14. The results are listed in a somewhat relative order of decreasing overall reliability performance that was determined by placing primary importance on maximizing ATTIF while maintaining a secondary goal of minimizing beta and evaluating each formulation's net achievement in the optimization of these two critical values. The rankings in many cases are not absolute and should only be taken as a literal guide under situations that share the same goals for ATTIF and MTTF that were used during its compilation.

Overall Top Performers (No-Aging)	ATTIF (hours)		Beta		Characteristic Life (hours)		MTTF (hours)	
J-Series: 6, Best N105	**5.9**		**3.5**		**22.3**		**20.1**	
J-Series: 6, Low SAC105	**3.1**		**2.0**		**31.6**		**28.0**	
L-Series: 6, Low SAC105	**2.9**		**2.6**		**17.5**		**15.6**	
Overall Top Combination Performers								
J-Series: 6, Low 2nd in SAC105 2nd in SAC305	**3.1 SAC105**	**2.8 SAC305**	**2.0 SAC105**	**2.4 SAC305**	**31.6 SAC105**	**18.2 SAC305**	**28.0 SAC105**	**16.1 SAC305**

Table 11: Summary of overall top performers (no-aging)

Overall Top Performers (Aged)	ATTIF (hours)		Beta		Characteristic Life (hours)		MTTF (hours)	
I-Series: 6, Low SAC105	**13.1**		**5.1**		**32.1**		**29.5**	
I-Series: 6, Low SAC305	**5.4**		**2.6**		**32.5**		**28.9**	
E-Series: 6,High SAC105	**5.6**		**4.0**		**17.8**		**16.1**	
E-Series: 6,Low SAC305	**5.0**		**2.7**		**27.4**		**24.4**	
Overall Top Combination Performers								
I-Series: 6, Low 1st in SAC105 & 1st in SAC305	**13.1 SAC105**	**5.4 SAC305**	**5.1 SAC105**	**2.6 SAC305**	**32.1 SAC105**	**32.5 SAC305**	**29.5 SAC105**	**28.9 SAC305**

Table 12: Summary of overall top performers (aging)

Top Performers (SAC105)		ATTIF (hours)		Beta		Characteristic Life (hours)		MTTF (hours)	
No-Aging									
1st	**J-Series: 6, Best (N)**	**5.9**		**3.5**		**22.3**		**20.1**	
2nd	**J-Series: 6, Low**	**3.1**		**2.0**		**31.6**		**28.0**	
3rd	**O-Series: 6, Low**	**2.5**		**1.72**		**36.6**		**32.7**	
4th	**L-Series: 6, Low**	**2.9**		**2.5**		**17.5**		**15.6**	
5th	**K-Series: 6, High**	**2.2**		**1.1**		**125.9**		**120.3**	
6th	**K-Series: 6, Low**	**2.4**		**2.2**		**18.9**		**16.8**	
7th	**L-Series: 6, High**	**2.6**		**2.4**		**17.7**		**15.7**	
8th	**P-Series: 6, High**	**2.0**		**1.2**		**87.25**		**81.8**	
9th	**I-Series: 6, Best**	**2.0**		**1.9**		**24.2**		**21.5**	
10th	**M-Series: 4, Best**	**1.4**		**2.2**		**18.3**		**12.4**	
11th	**L-Series: 4, Best**	**1.7**		**2.2**		**13.3**		**11.8**	
12th	**R-Series: 6, Best**	**1.6**		**1.96**		**16.8**		**14.9**	
Aged									
1st	**I-Series: 6, Low**	**13.1**		**5.1**		**32.1**		**29.5**	
2nd	**BCDE-Series: 6, High**	**5.6**		**4.0**		**17.8**		**16.1**	
3rd	**A-Series: 6, Best**	**2.7**		**2.1**		**23.6**		**20.9**	
4th	**BCDE-Series: 6, Low**	**1.4**		**1.2**		**57.4**		**53.4**	
5th	**F-Series: 6, Best**	**1.6**		**2.6**		**9.5**		**8.4**	
6th	**G-Series: 6, Best**	**1.5**		**2.5**		**9.5**		**8.4**	
7th	**K-Series: 6, High**	**1.0**		**1.4**		**24.6**		**22.4**	
8th	**L-Series: 6, High**	**1.2**		**2.1**		**10.3**		**9.1**	
9th	**J-Series: 6, High**	**1.0**		**2.0**		**9.1**		**8.1**	
Full Life									
1st	**K-Series: 6, High**	**2.2**	**1.0**	**1.1**	**1.4**	**125.9**	**24.6**	**120.3**	**22.4**
2nd	**L-Series: 6, High**	**2.6**	**1.2**	**2.4**	**2.1**	**17.7**	**10.3**	**15.7**	**9.1**

Table 13: Summary of overall top performers (SAC105)

Top Performers (SAC305)		ATTIF (hours)		Beta		Characteristic Life (hours)		MTTF (hours)	
No-Aging									
1st	**K-Series: 6, High**	**2.6**		**1.6**		**45.9**		**41.2**	
2nd	**J-Series: 6, Low**	**2.8**		**2.4**		**18.1**		**16.1**	
3rd	**K-Series: 6, Low**	**2.7**		**3.4**		**10.3**		**9.3**	
4th	**J-Series: 6, Best (N)**	**1.8**		**1.6**		**29.6**		**26.5**	
5th	**P-Series: 6, High**	**1.7**		**1.8**		**22.0**		**19.6**	
Aged									
1st	**I-Series: 6, Low**	**5.4**		**2.6**		**32.5**		**28.9**	
2nd	**BCDE-Series: 6, Low**	**5.0**		**2.7**		**27.4**		**24.4**	
3rd	**I-Series: 6, High**	**3.1**		**2.2**		**24.3**		**21.5**	
4th	**BCDE-Series: 6, High**	**3.0**		**2.1**		**25.6**		**22.7**	
5th	**F-Series: 6, Best**	**2.8**		**3.4**		**10.7**		**9.6**	
6th	**K-Series: 6, High**	**2.4**		**2.2**		**18.8**		**16.7**	
7th	**G-Series: 6, Best**	**1.9**		**2.8**		**10.1**		**9.0**	
8th	**A-Series: 6, Best**	**1.4**		**1.5**		**33.2**		**30.1**	
9th	**BCDE-Series: 4, Best**	**1.5**		**2.0**		**14.6**		**13.0**	
10th	**J-Series: 6, High**	**1.6**		**2.3**		**11.2**		**9.9**	
Full Life									
1st	**K-Series: 6, High**	**2.6**	**2.4**	**1.6**	**2.2**	**45.9**	**18.8**	**41.2**	**16.7**

Table 14: Summary of overall top performers (SAC305)

Short-Term and Long-Term Analysis

Due to the substantial amount of data collected as well as the wide variety of industry needs and possible applications of the lead-free solder formulations being tested, it was decided to organize the data analysis into two different categories, short-term and long-term, in order to maximize its usefulness. The phrase “short-term reliability” is used to indicate that the analysis being performed contains data exclusively from the no-aging category of the experiment and thus can only be used to predict the initial behavior of the test formulations and not their performance after aging or over long-periods of time. This was done to account for the possibility of the

existence of formulations whose exceptional performance early on would be overshadowed by their lackluster performance after aging when performing an analysis on simply the overall performance of the test parameters. This type of analysis is also relevant to certain producers in the electronics industry that are only concerned with initial reliability instead of long-term performance. The phrase "long-term reliability," on the other hand, is used to indicate that the analysis being executed includes data from both the aged and no-aging groups and exists as a guide for the predicted long-term performance of the formulations being discussed. The short-term reliability performance analysis is conducted first, followed by the analysis for the long-term reliability performance.

A brief summary of the performance characteristics of the top candidates in regards to short-term reliability can be found in Table 15 and Figure 53 along with the equivalent factors from the control group for use as benchmarks for overall performance.

Short-Term Reliability Summary					
Doped Group	**Best Performing Alloy**	**ATTIF (hours)**	**Beta**	**Characteristic Life (hours)**	**MTTF (hours)**
SAC105	**J-Series: 6, Best N**	**5.9**	**3.5**	**22.3**	**20.1**
SAC305	**K-Series: 6, High**	**2.6**	**1.6**	**45.9**	**41.2**
Both	**J-Series: 6, Low**	**2.8⇔3.1**	**2.0⇔2.5**	**18.2⇔31.6**	**16.1⇔28.0**
Control Group					
SAC105	**A-Series: 6, Best**	**0.3**	**1.4**	**8.3**	**7.6**
SAC305	**A-Series: 6, Best**	**0.3**	**1.4**	**7.8**	**7.1**
Both	**A-Series: 6, Best**	**0.3**	**1.4**	**7.8⇔8.3**	**7.1⇔7.6**

Table 15: Short-term reliability analysis summary

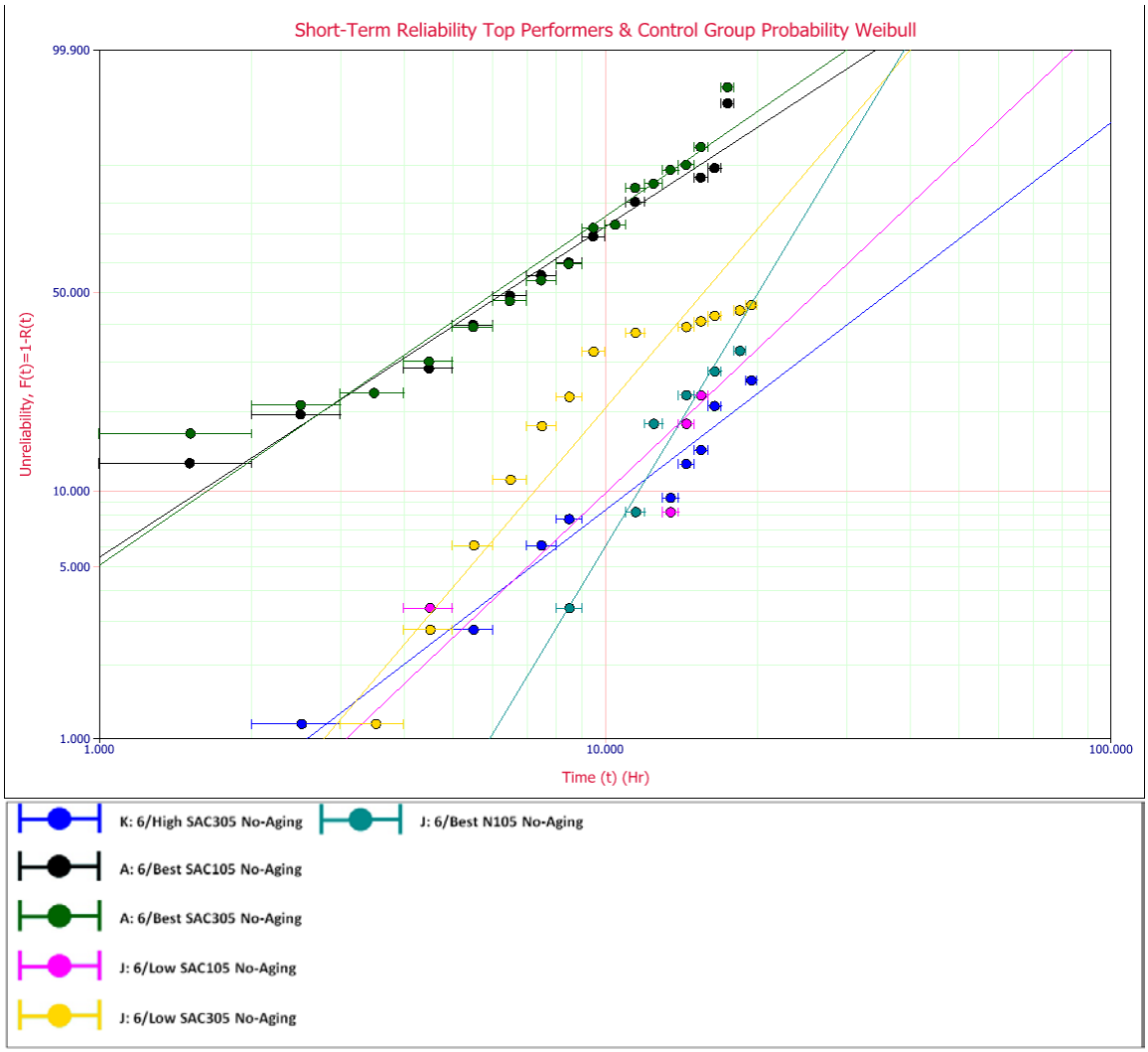

Figure 53: Short-term reliability analysis Weibull plot

The best reliability performance for non-aged BGAs at SAC105 solder ball locations was actually obtained using a combination of 6mils of J-series paste with a matching solder ball formulation known as “N” that was reflowed at the manufacturer’s recommended temperature profile. The test group achieved the highest ATTIF of any other non-aged combination tested during the experiment and the second highest ATTIF overall. At nearly six hours, the test run’s ATTIF represents more than a 1900% improvement over the corresponding test run for the A-Series control group. Although

the group's failure curve was approximately twice that of the A-Series reference test, the components' failure intensity was actually much lower than the control group, as illustrated in Figure 53. This explains why the J6BN's MTTF was still found to be almost three times more than what was experienced in the control group, even though the test group was documented as having a greater failure rate. This formulation would be most beneficial for use together as an A-series paste substitute and SAC105 solder ball replacement by manufacturers seeking to obtain the longest complete short-term reliability possible for their SAC105 BGA components with no concern for the adverse effects on short-term failure rate or long-term reliability performance.

The best reliability performance for non-aged BGAs using SAC305 solder balls resulted from the K-series permutation utilizing a 6mil stencil and a reflow profile on the high end of the manufacturer-recommended temperature range. These specimens were recorded as having an ATTIF of 2.6 hours, more than an 800% improvement over the control group but still a little less than half of the ATTIF achieved by the best-performing non-aged SAC105 test group. However, although it does begin to fail earlier than the aforementioned SAC105 test group, the K6H test components' failure rate is so much lower that their overall failure intensity is quickly eclipsed by the BPAFN for SAC105 at around 10 hours of vibration testing. As such, the MTTF derived for the K6H test group, 41.2 hours, is actually more than double the MTTF of the J6BN test boards and an impressive 580% increase over the corresponding control paste test group. This test formulation would ideally be for use as a drop-in paste replacement by companies seeking to obtain the longest, guaranteed short-term reliability possible for their BGA

components but who are unwilling or unable to make the switch from SAC305 solder balls to SAC105 and have concern for the adverse effects it may have on short-term failure rate or long-term reliability performance.

In order to mathematically determine the single test paste and reflow temperature combination that produced the best reliability performance for non-aged BGAs using both SAC105 and SAC305 solder balls, the numerical values for the ATTIF and MTTF of each non-aged test series were first paired with their corresponding SAC105 and SAC305 counterpart values from the same series to create a performance range for each alloy before comparing those ranges to the ATTIF and MTTF of the no-aging control test series. The testing parameter formulation that produced the greatest optimization of performance over the control group for both ranges of SAC105 and SAC305 was then selected to serve as the overall best performing combination for no-aging. This selection process yielded the J6L test group as the overall leader in terms of short-term reliability for a mixed SAC component. The J6L no-aging test group was constructed using a 6mil stencil to print J-series paste onto the solder pads of the PCB before placing BGA components utilizing either SAC105 or SAC305 solder balls onto the paste and reflowing the entire assembly at a lower than recommended reflow temperature profile. Depending on the specific proportions of SAC105 and SAC305 solder balls being used, components in the J-series test group could have an ATTIF of somewhere between 2.8 and 3.1 hours, which represents an average 980% increase from the performance of components manufactured using 6mils of the control paste at the manufacturer's recommended reflow temperature profile. In addition, the J6L test

specimens were also calculated to have an MTTF of anywhere between 16.1 and 28.0 hours, a range that is 2-4x that obtained by the control group. Although J6L did not outperform the J6BN or K6L series in terms of its SAC105 or SAC305 short-term reliability performance, respectively, this test arrangement provides manufacturers with the ability to only need to employ a single A-series paste substitute in order to dramatically increase the short-term reliability performance of the products constructed in their mixed-SAC production facility without concern for the adverse impacts on long-term reliability.

In conclusion, the J6BN, K6H, and J6L test formulations all offer distinct advantages over the short-term performance of the industry-standard A-series, especially in regards to ATTIF. Utilizing the J6BN formulation in place of existing SAC105 BGAs has the possibility of granting the user the absolute maximum short-term ATTIF possible out of all the other available options presented during the experiment. Employing K6H as manufacturing parameters will likewise offer users with the maximum short-term ATTIF performance of any SAC305-based BGA and one of the top ATTIF performances that can be achieved by use of any other formulation in the study while still hopefully retaining the thermal-shock advantages inherent to the SAC305 alloy. Finally, use of the materials and production procedures employed by J6L permutation would result in the maximum short-term ATTIF performance possible for mixed SAC105 and SAC305 BGA components out of all the options covered during the investigation. Since all of these formulations, except K6H, perform relatively poorly after aging, they should only be of significant interest to manufacturers of mission-critical electronic

devices intended for single-use before being replaced or discarded, where it is necessary to have guaranteed and complete reliability of BGA components but only for a short timeframe.

The performance analysis regarding the long-term reliability of the alloy formulations will now be discussed. A short summary of the performance characteristics of the frontrunner formulation in regards to long-term reliability can be found in Table 16 and Figure 54 along with the equivalent factors from the A-series control group for use against as comparisons for overall improvements in performance.

Long-Term Reliability Summary					
Doped Group	**Best Performing Alloy**	**ATTIF (hours)**	**Beta**	**Characteristic Life (hours)**	**MTTF (hours)**
SAC105	**K-Series: 6, High**	**1.0⇔2.2**	**1.1⇔1.4**	**24.6⇔125.9**	**22.4⇔120.3**
SAC305	**K-Series: 6, High**	**2.4⇔2.6**	**1.6⇔2.2**	**18.8⇔45.9**	**16.7⇔41.2**
Both	**K-Series: 6, High**	**1.0⇔2.6**	**1.1⇔2.2**	**18.8⇔125.9**	**16.7⇔120.3**
Control Group					
SAC105	**A-Series: 6, Best**	**0.3⇔2.7**	**1.4⇔2.1**	**8.3⇔23.6**	**7.6⇔20.9**
SAC305	**A-Series: 6, Best**	**0.3⇔1.4**	**1.4⇔1.5**	**7.8⇔33.3**	**7.1⇔30.1**
Both	**A-Series: 6, Best**	**0.3⇔2.7**	**1.4⇔2.1**	**7.8⇔33.3**	**7.1⇔30.1**

Table 16: Long-term reliability analysis summary

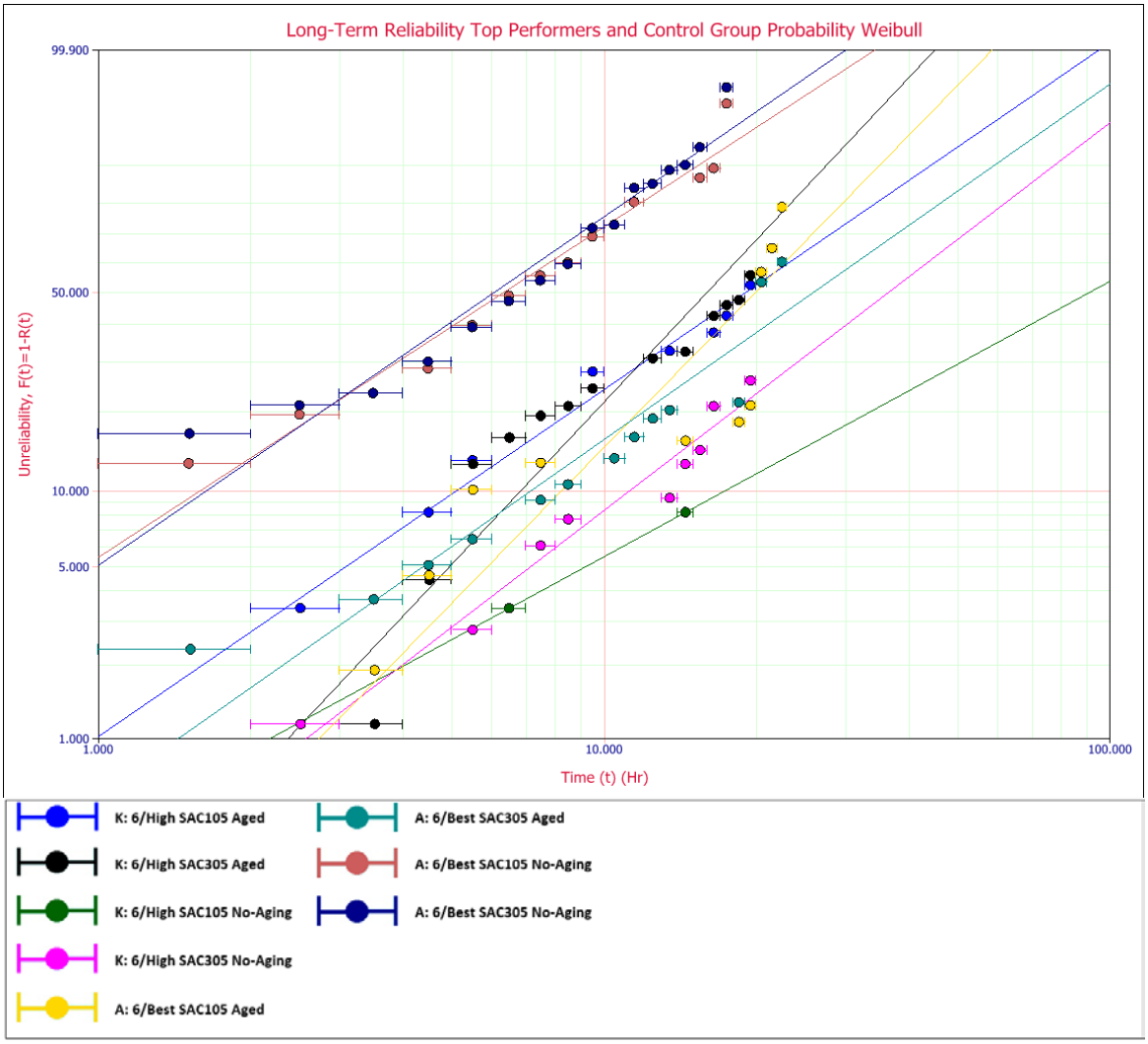

Figure 54: Long-term reliability analysis Weibull plot

In order to quantitatively determine the single test paste and reflow temperature combination that produced the best cross-reliability performance between non-aged and aged BGAs using SAC105 solder balls, the numerical values for the ATTIF and MTTF of each non-aged SAC105 test series were first paired with their corresponding aged SAC105 counterpart values from the same series to create a performance range for each formulation before comparing those ranges to the paired aging and no-aging ranges of ATTIF and MTTF of the control test series. The testing

parameter formulation that produced the greatest optimization of SAC105 performance over the control group for both ranges of aged and no-aging was then selected to serve as the best long-term reliability performance combination. This selection process yielded the K6H test group as the frontrunner in terms of long-term reliability performance for SAC105 BGA components. The BGAs in this specific test group were manufactured using a 6mil stencil, K-Series paste, and SAC105 solder balls that were reflowed onto the test substrate using a higher-than-recommended reflow temperature. This construction method should allow the BGA components to maintain a minimum ATTIF of at least 1 hour under extreme vibration but with their actual performance more likely to be closer to 2.2 hours, approximately seven times greater than the non-aged ATTIF performance of the control group. In addition, these components are expected to have a MTTF of anywhere between 22.4 hours and 120.3 hours during the course of their product lifecycle if subjected to continuous, intense vibration as was done in the experiment. Such a performance would constitute somewhere between a minimum of 7% to 720% increase in performance compared to the A-series group.

The same method used to mathematically determine the formulation with the best cross-reliability performance between non-aged and aged BGAs using SAC105 solder balls was employed to find the formulation that fit all the same requirements but used SAC305 instead of SAC105 solder balls. Interestingly enough, however, the result was the same paste series and reflow profile as before, but with SAC305 solder balls instead of SAC105 solder balls, of course. These test samples were measured to have an

ATTIF of about two and a half hours under extreme vibration, even after being artificially aged for six months. Not only is this around two to eight times the ATTIF of the control group, it is also an estimated 20% improvement over the K-series employing SAC105 solder alloy, which has been dominating use as one of the most popular lead-free solder alternatives in the industry largely due to its performance advantages over SAC305 in highly vibrated environments. And while the test group's MTTF is still lower than when using SAC105 BGAs, it is still around 60% more than the current A-series paste.

Discovering the test formulation that most optimized the long-term performance of both SAC105 and SAC305 BGAs was done similarly as was done before during the short-term reliability performance analysis, but of course included all data from aged and no-aging and both SAC options. This process was fairly simple to complete as the K6H-series was the only formulation to place within the top six performers for each category from both aged and no-aging data. The K6H-series was the testing parameter formulation that produced the greatest optimization of performance over the control group for both ranges of SAC105 and SAC305 by an extensive margin. Depending on the specific proportions of SAC105 and SAC305 solder balls being used, BGA components in this test group are estimated to have an ATTIF of somewhere between 1 and 2.6 hours, which represents an average 20% increase from the long-term performance of mixed-SAC BGA components manufactured using 6mils of the control paste at the manufacturer's recommended reflow temperature profile. In addition, the K6H test specimens were also calculated to have an MTTF of anywhere between 16.7 and 120.3

hours, a value that is approximately 1x to 17x that obtained by the control group at any given point during its life cycle.

Some of the test samples from the K6H-series were carved out of the test vehicle to be viewed through a SEM, or scanning electron microscope, in hopes of gaining greater insight into the exact cause of failure for this test series. A 300x magnification image of the U12 BGA joint with SAC305 captured by the SEM during the no-aging testing is detailed in Figure 55. In addition, a 100x magnification examining the U15 BGA failure with SAC105 was also performed, as shown in Figure 56. The initial SEM analysis revealed that most of the samples that were viewed had clear failure signs caused by separation between the BGA and the solder ball material, a situation commonly referred to as adhesion failure. Unfortunately, since this and all other samples viewed under the SEM were not removed from the test vehicle immediately once they failed an electrical test, it is unclear whether this adhesion failure between the solder balls and the BGA pads was the primary failure mechanism at work within these samples or if there was another failure mechanism causing the initial electrical failures with the adhesion failure occurring at some point afterward.

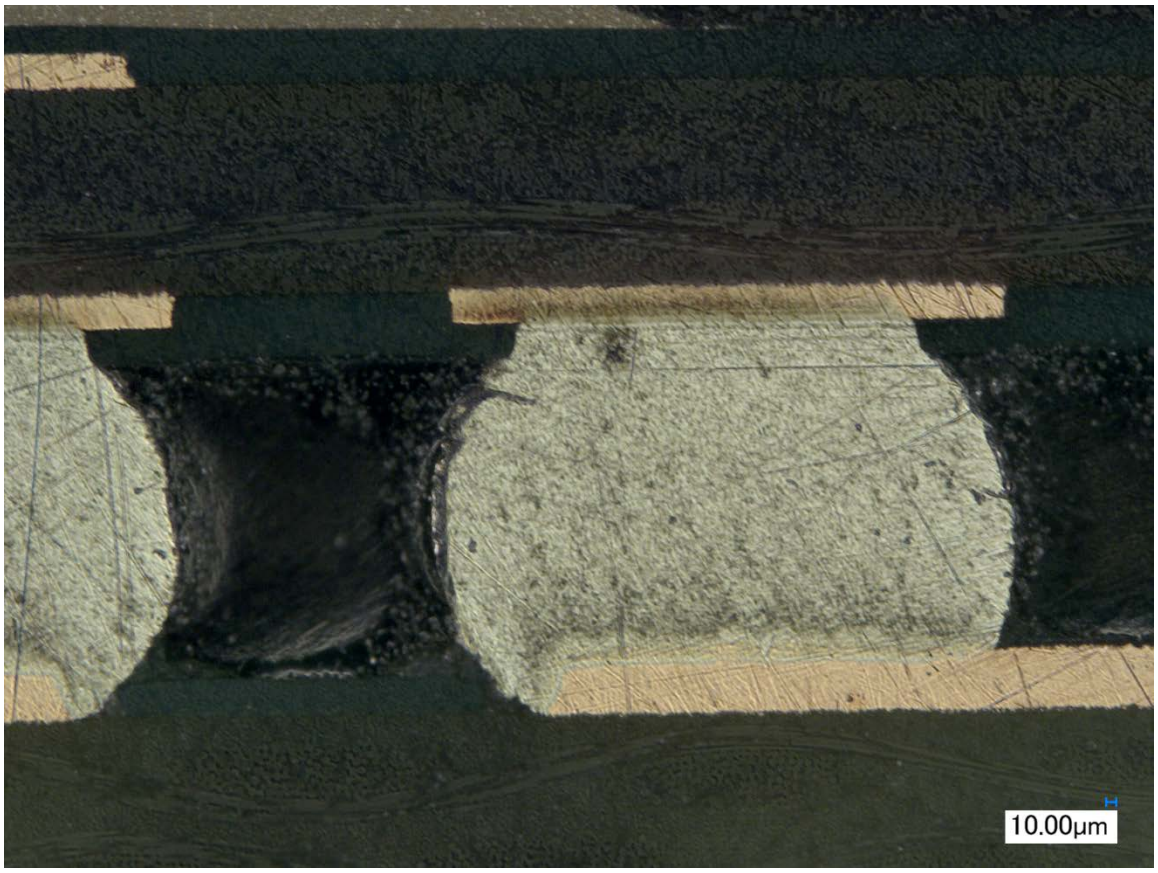

Figure 55: K6H-series SEM solder ball image (300X)

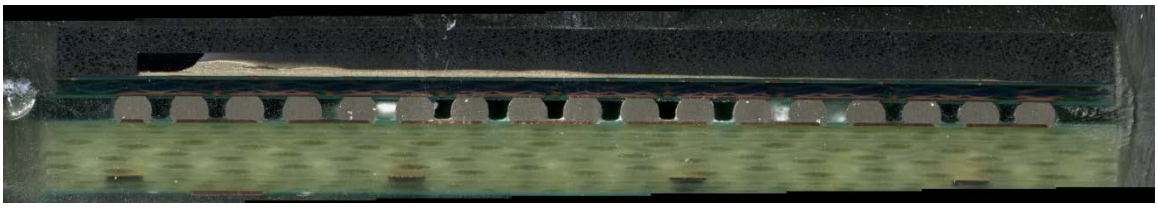

Figure 56: K6H-series SEM solder ball image (100X)

In conclusion, although it is still generally outperformed by the J6BN and J6L series in terms of initial ATTIF performance, the K6H test group utterly surpasses them in every other regard, especially when considering long-term reliability performance. This formulation provides manufacturers with the ability to only need to employ a single A-series paste substitute and a slightly higher reflow temperature in order to

dramatically increase the long-term reliability performance of the products constructed in their single or mixed-SAC BGA production facility as well as the initial reliability performance for all of their SAC305 BGA components, and when used as such, would be most appropriate for use in less reliability-critical applications like consumer mobile electronics. This formulation would be most effective, however, when applied for use in situations that require SAC305 BGAs to have very high initial-use reliability in terms of ATTIF, fairly low failure rate and failure intensity over the course of product life, perform just as well or better than an equivalent SAC105 BGA, and still maintain the advantageous thermal-shock properties inherent to SAC305 solder alloys.

Recommendations for Future Research

An attempt was made in this current work to study the reliability performance of various doped solder formulations used in BGA components. Great improvements in short-term ATTIF were made using J-series and K-series pastes using a 6 mil stencil, using varying profiles and solder ball alloys. In addition, the long-term reliability performance of in terms of ATTIF and MTTF was successfully improved through the implementation of the K-series paste using a 6 mil stencil, high reflow temperature profile, and both SAC105 and SAC305 solder balls. Additional research investigating the thermal shock performance of these specific formulations with using a larger sample size would provide useful information regarding the overall success of these testing parameters and truly confirm if the implementation of 6 mils of K-series paste using

SAC305 solder balls reflowed at a high temperature profile would create a hybrid lead-free alloy capable of performing as or more reliably under vibration and thermal shock environments than either standard SAC105 or SAC305, respectively. In addition, this future research could employ an automated electrical failure monitoring system so that the samples could be removed from the stress test immediately after failing. The examination of these samples with an SEM would then be able to provide greater insight into the primary mechanism of failure occurring within these samples.

References

[1] Soclof, Sidney. "How Circuits Work." 21 January 2008. *HowStuffWorks.com.* <http://science.howstuffworks.com/environmental/energy/circuit5.htm>.

[2] Jojo. "Integrated Circuits (IC) - Concept, Classification, and Advantages." 21st May 2014. *Circuits Today.* <http://www.circuitstoday.com/integrated-circuits>.

[3] Brown, James. "The History of Printed Circuit Boards." 3rd January 2013. *Rapid PCB.* <http://www.rapidpcb.com/history-of-printed-circuit-boards.html>.

[4] Sanders, Thomas. *Electronics Manufacturing - Chapter 10: Solder & Solder Paste*. Auburn University, 2015. Powerpoint.

[5] "Making a PCB - PCB Manufacture Step by Step." 2015. *EuroCircuits.* <http://www.eurocircuits.com/pcb-prototype-and-small-batch-services/making-a-pcb-pcb-manufacture-step-by-step>.

[6] Fjelstad, Joseph. "Materials and Methods for IC Package Assemblies." 2015. *Solid State Technology: Insights for Electronics Manufacturing.* <http://electroiq.com/blog/2005/08/materials-and-methods-for-ic-package-assemblies/>.

[7] Jimbo. "Integrated Circuits." 2015. *Sparkfun.* <https://learn.sparkfun.com/tutorials/integrated-circuits>.

[8] "Brazing vs. Soldering." 2011-2012. *Lucas Milhaupt.* <http://www.lucasmilhaupt.com/en-US/brazingfundamentals/brazingvssoldering/>.

[9] Koskulics, Jeff. "Soldering vs. Brazing vs. Welding." 2014. <http://www.howcast.com/videos/504744-Soldering-vs-Brazing-vs-Welding-Soldering>.

[10] "Wetting." 2015. *Wikipedia.* <http://en.wikipedia.org/wiki/Wetting>.

[11] LeProvost, and Hunt. "Getting the Lead Out - Soldering with Lead-free Solders." 2007. *Johnson MFG.* Proceedings of the RCI 22nd International Convention. <http://www.johnsonmfg.com/temp/Papers/leadout.pdf>.

[12] Knott, Dr. Laurence. "Lead Poisoning." 19th August 2011. <http://www.patient.co.uk/doctor/Lead-Poisoning.htm>.

[13] "SAC396 Pb-free Solder Spheres." 2015. *Caplinq.* <http://www.caplinq.com/sac396.html>.

[14] Briggs, Ed. "Stencil Printing for SMT Assembly Success Part 2: Print Metrics." 7th July 2014. *Indium Corporation.* <http://blogs.indium.com/blog/tombstoning>.

[15] Liu, Fang and Guang Meng. "Random Vibration Reliability of BGA Lead-Free Solder Joint." *Microelectronics Reliability* 54.1 (2014): 226-232. <http://www.sciencedirect.com/science/article/pii/S0026271413003314>.

[16] Zhang, Jiawei. "The Effects of Aging on the Reliability of Lead Free Fine-Pitch Electronics Packaging." Dissertation. Auburn University, 2012.

[17] Cai, Zijie. "Mitigation of Lead Free Solder Aging Effects Using Doped SAC-X Alloys." *Thermal and Thermomechanical Phenomena in Electronic Systems (ITHERM)*. San Diego, 2012. 896-909.

[18] Lau, John H. and Katrina Liu. "Global Trends in Lead-free Soldering." 2015. *Solid State Technology:Insights for Electronics Manufacturing.* <http://electroiq.com/blog/2004/01/global-trends-in-lead-free-soldering/>.

[19] Narbus, Peter. *Vibration Test PCB: Assembly Drawing*. Auburn University, 4th August 2013.

[20] Guenin, Bruce. "The Many Flavors of Ball Grid Array Packages." 1st February 2002. *Electronics Cooling.* <http://www.electronics-cooling.com/2002/02/the-many-flavors-of-ball-grid-array-packages/>.

[21] "CABGA." 2015. *Sibalco.* <http://www.sibalco.ch/images/stories/docs/practical/PC-Kat-04-S16-23.pdf>.

[22] "CABGA - ChipArray Ball Grid Array." 2015. *Practical Components.* <http://www.practicalcomponents.com/Dummy-Components/product.cfm?ChipArray-Ball-Grid-Array-%28CABGA%29-Dummy-Component-4AB79E6FD4C2471C>.

[23] "Surface Mount Resistors Size Chart." 2015. *West Florida Components.* <https://www.westfloridacomponents.com/surface-mount-resistor-sizes.html>.

[24] "Common Surface Mount Packages." 2010. *MicroBuilder.eu.* <http://www.microbuilder.eu/Tutorials/Fundamentals/SMDPackages.aspx>.

[25] Bowling, Bruce and Al Grippo and Lance Gardiner. "MegaSquirt." 18th July 2013. <http://www.megasquirt.info/UMS.htm>.

[26] "SMR Lead-Free Surface Mount Resistors." 2015. <http://www.practicalcomponents.com/Dummy-Components/product.cfm?Lead-Free-Surface-Mount-Resistors-%28SMR%29-B85A7606ED496168>.

[27] "Amkor MicroLeadFrame Package." 2015. *Practical Components.* <http://www.practicalcomponents.com/media/packages/photos/9482.png>.

[28] "MLF Data Sheet." 2015. *Practical Components.* < <http://www.practicalcomponents.com/assets/cfc/Attachments.cfc?method=Download&AttachmentID=877>.

[29] "Reliability Basics: Characteristics of the Weibull Distribution." *Reliability HotWire: The eMagazine for the Reliability Professional* 14 (2002). <http://www.weibull.com/hotwire/issue14/relbasics14.htm>.

Appendix

Weibull Distribution and Mechanics

Applying a Weibull distribution is a widely accepted method for generating common reliability metrics when analyzing lifecycle data. Like all other distributions, the Weibull distribution is mathematically defined by its probability density function, which is composed of a three-parameter expression in its most general form and is of the form:

$$f(T) = \frac{\beta}{\eta}\left(\frac{T-\gamma}{\eta}\right)^{\beta-1} e^{-\left(\frac{T-\gamma}{\eta}\right)^{\beta}}$$

$$f(T) \geq 0,\ T \geq 0 \text{ or } \gamma,\ \beta > 0,\ \eta > 0,\ -\infty < \gamma < \infty$$

Figure 57: Probability density function for 3-parameter Weibull distribution

Where

- β is the shape parameter, also known as the Weibull slope
- η is the scale parameter, also known as the characteristic life
- γ is the location parameter
- T is time or number of testing cycles

For the analysis performed during the study, the location parameter was not used and therefore its value was set equal to zero. Doing so results in a standard two-parameter of the form shown below [29]:

$$f(T) = \frac{\beta}{\eta}\left(\frac{T}{\eta}\right)^{\beta-1} e^{-(\frac{T}{\eta})^{\beta}}$$

Figure 58: Probability density function for 2-parameter Weibull distribution

From this equation, the reliability function R(T) and the unreliability function Q(T) are defined as:

$$R(T) = e^{-(\frac{T}{\eta})^{\beta}}$$

$$Q(T) = 1 - R(T) = 1 - e^{-\left(\frac{T}{\eta}\right)^{\beta}}$$

Figure 59: Definition of the reliability and unreliability functions

The unreliability function predicts what percentage of the total components for a test set will have failed at various points in time during testing. To aid in the analysis of the failure data, the point in time at which unreliability reached 1%, or rather when reliability fell to 99%, was arbitrarily chosen to represent the most probable time it would take for a given test set to experience its first failure. This time was deemed the approximate time to initial failure, or ATTIF, and was used as a primary performance parameter for the study. The mean time to failure, or MTTF, is a value representing the

average time taken for a test group to fail and was used as a secondary performance factor. The other secondary performance factor that was calculated for the study was the characteristic life parameter, or η, which represents the time at which 63.2% of the total components will have failed.

To generate the desired plots of component unreliability used during the failure analysis, it was necessary to linearize the unreliability function into the general slope-intercept form for a straight line, shown in Figure 60, by following the mathematical steps outlined in Figure 61. The logarithmic plot that results is shown in Figure 62.

$$Y = mx + b$$

Figure 60: Slope-intercept form for a straight line

$$\begin{aligned}
Q(T) &= 1 - e^{-\left(\frac{T}{\eta}\right)^{\beta}} \\
\ln(1 - Q(T)) &= \ln\left(e^{-\left(\frac{T}{\eta}\right)^{\beta}}\right) \\
\ln(1 - Q(T)) &= -\left(\frac{T}{\eta}\right)^{\beta} \\
\ln\left(-\ln(1 - Q(T))\right) &= \beta \ln\left(\frac{T}{\eta}\right) \\
\ln\left(\ln\left(\frac{1}{1 - Q(T)}\right)\right) &= \beta \ln(T) - \beta \ln(\eta)
\end{aligned}$$

$$y = \beta x - \beta \ln(\eta)$$

$$y = \ln\left(\ln\left(\frac{1}{1 - Q(T)}\right)\right) \qquad x = \ln(T)$$

Figure 61: Solving for the x and y functions for the unreliability Weibull plot

From the resulting equations, it is obvious to see why β is often referred to as the Weibull slope parameter since it directly correlates to the slope of the unreliability plot. This was also used as a primary performance factor during the study, since it succinctly describes the failure rate of each test set. This slope value along with the ATTIF, a factor that most closely correlates to the x-intercept on a plot of unreliability versus time, allowed for very complex analyses to be conducted just from quick visual comparisons of the unreliability Weibull plots for different test runs.

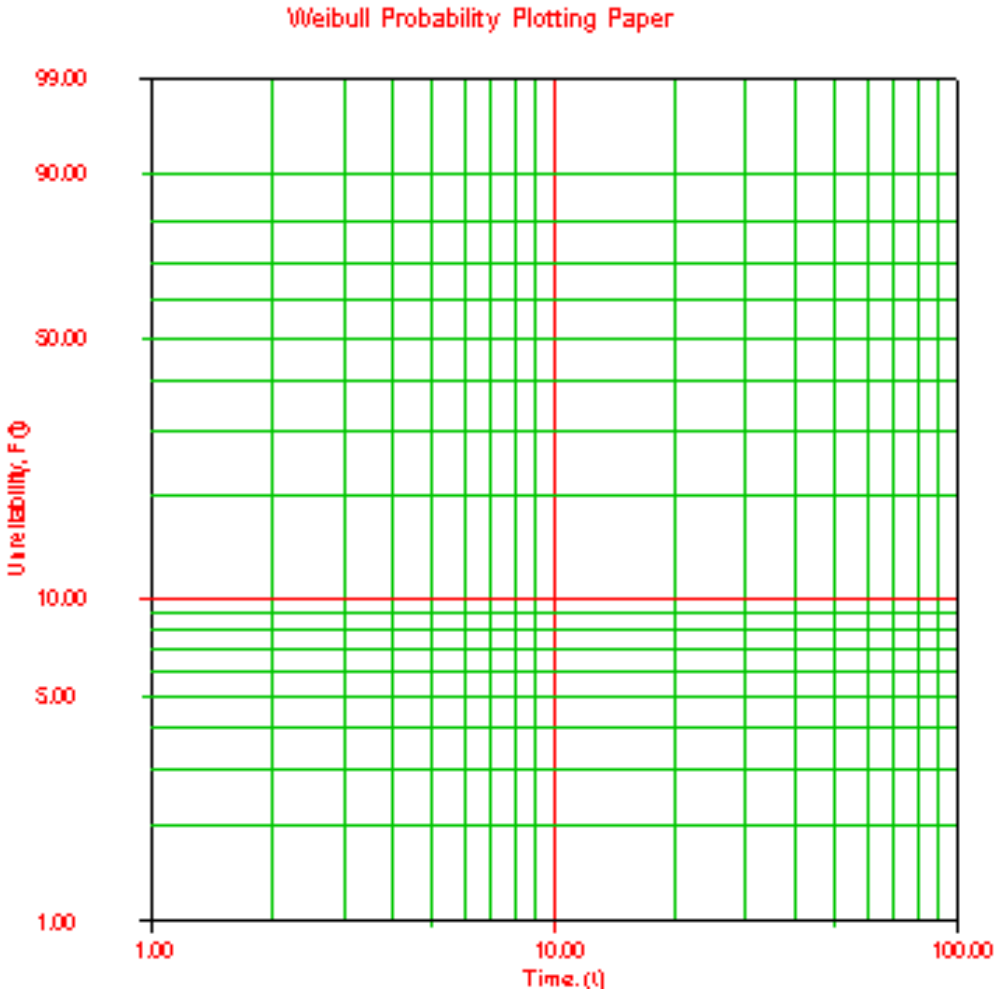

Figure 62: Typical Weibull logarithmic plot of unreliability versus time [29]

Complete Vibration Failure Data

Test Set (No-Aging)	U 6	U 7	U 8	U 9	U 10	U 11	U 12	U 13	U 14	U 15	U 16	U 17	U 18	U 19	U 20	U 21
A-Series 6/Best 50-50																
A6B24	6	10	12	8	10	7	8	16	6	8	10	18	6	10	12	16
A6B26	3	12	16	14	1	3	15	18	10	7	9	12	13	14	9	12
A6B28	5	7	9	11	8	13	10	18	5	7	9	12	16	1	8	6
A6B30	3	3	1	3	5	7	10	17	2	2	2	12	12	1	6	6
A6B32	5	7	7	12	7	7	13	18	12	7	4	15	4	1	2	2
A6B34	10	10	8	8	10	12	16	18	9	5	6	12	12	1	6	4
A6B36	10	9	9	10	5	9	6	10	9	7	12	8	16	8	12	14
A6B38	5	5	1	5	7	2	18	10	5	3	3	5	6	1	1	6
A6B40	2	1	1	2	2	2	6	12	2	2	2	3	1	1	1	3
A6B42	9	8	8	12	7	9	18	16	7	6	6	12	16	18	12	16
A6B44	6	7	10	12	10	9	18	12	12	8	12	16	14	18	16	12
BCDE-Series 4/Best																
B4B002	6	5	1	7	5	3	6	6	3	3	1	2	1	1	1	4
B4B006	8	3	1	5	3	7	7	5	4	6	3	5	1	1	2	4
B4B010	5	2	1	2	2	2	1	2	1	2	1	1	2	1	1	1
B4B014	1	1	1	1	1	1	1	1	1	1	2	1	1	1	1	1
B4B018	12	14	14	6	10	13	11	12	8	7		10	1	3	7	9
BCDE-Series 6/Best																
C6B002	2	3	4	3	1	5	4	6	5	2	5	3	1	1	3	2
C6B006	11	6	1	5	12	7	7	12	5	6	3	9	2	2	2	9
C6B010	13	8	1	4	12	11		10	3	4	8	11	4	1	4	12
C6B014	1	3	1	1	2	1	2	6	4	2	3	3	1	1	1	2
C6B018	2	3	1	2	2	6	3	13	12	6	6	4	3	1	1	11
BCDE-Series 6/Low																
D6L002	11	6	1	11	20	11	17	11	11	11	16	19	9	18	13	18
D6L006	17	19	13	18	15	9	9	5	13	15	21	11	2	12	5	19
D6L010	12	14	1	9	13	2	5	4	4	5	3	4	13	3	3	13
D6L014	13	13	8	12	15	13	13	13	9	9	14	13	17	10	6	13
D6L018	18	5	15	17	15	17	10	13	16	11	8	21	17	9	5	19

BCDE-Series 6/High																
E6H002	14	16	14	16	9	4	11	12	13	13	11	18	13	2	8	9
E6H006	14	14	13	12	13	13	17	9	13	16	10	18	10	13	2	5
E6H010	14	13	13	14	4	15	14	21	3	16	13	20	14	3	14	4
E6H014	14	15	14	14	14	13	16	11	14	13	8	11	13	2	13	13
E6H018	18	8	12	15	8	2	12	10	18	4	13	16	4	8	4	4
F-Series 6/Best																
F6B002		19	6	5		16	19	22	4	21	15	14	4	4	2	15
F6B006	4	2	2	2	3	3	3	3	3	3	3	12	3	2	1	2
F6B010	3	2	1	3	4	3	3	3	3	2	2	4	3	2	3	3
F6B014	11	1	1	3	14	2	6		3	4	13	6	2	1	2	2
F6B018	5	4	4	2	5	4	3	3	12	3	6	4	2	1	2	3
G-Series 6/Best																
G6B004	21	6	3	12	3	3	9		17	6	4	3	13	2	4	7
G6B008		4	2		4	7	16	21	5	3	5	11	2	1	3	
G6B012			3		6	3	20		20	14	16		3	3	21	3
G6B016	3	3	3	3	6	3	NA		2	3	3	4	2	1	2	2
G6B020	5	2	4	4		5	3	3	3	7	5	4	3	2	3	
H-Series 4/Best																
H4B002	4	1	1	3	4	4	3	4	2	5	5	4	1	2	3	4
H4B006	1	1	1	1	1	1	1	6	1	4	4	2	1	1	1	1
H4B010	5	1	1	1	1	1	2	11	1	1	1	2	1	1	1	4
H4B014	4	1	2	2	4	2	1	5	3	4	4	2	2	1	3	2
H4B018	16	8	1	3	3	7	3	5	2	4	1	9	3	3	2	4
H-Series 6/Low																
H6L002	15	4	4	3	10	15	4	3	4	20	15	15	1	4	15	15
H6L006	4	5	1	5	4	5	3	6	3	2	2	2	1	3	2	2
H6L010	3	2	2	2	2	1	1	3	2	1	2	3	1	1	1	1
H6L014		11	2	3	8	16	13	10	3	3	11	20	12	2	3	5
H6L018	2	9	3	3	3	6	9	19	4	3	10		13	3	2	2
H-Series 6/High																
H6H002	11	3	2	1	2	1	9	2	5	8	3	5	1	2	2	3
H6H006	1	1	1	1	3	1	5	1	3	1	11	1	1	1	1	1
H6H010	1	1	1	1	1	1	2	5	3	2	2	1	1	1	1	1

H6H014	2	2	1	2	1	1	5	20	2	2	3	2	4	1	1	1
H6H018	9	10	6	7	3	7	3	15	1	2	1	4	2	1	2	2
I-Series 4/Best																
I4B002										14		6				
I4B006	6	1	1	2	2	2	4	4	3	16	3	3	2	2	1	2
I4B010	17		9		9		10		17				3	2	9	
I4B014			2	9	6	15	10				12	9		4	2	5
I4B018	9	17	6	9	10	6	9	4	3	14	2	6	2	2	6	7
I-Series 6/Low																
I6L002	15	5	4	4		6	6		3	9	10		8	4	5	19
I6L006			10	4	4	4			20	2	20			4	1	8
I6L010		10	7	6	8	18			11				15	5	6	
I6L014		6	14	6	19	4			7					3	3	
I6L018		19	12	20	6	11			16		13		20	3	5	6
I-Series 6/High																
I6H002																
I6H006		5	6	2	19	6	2	5	5	2	4		3	2	4	9
I6H010				7	9					10				6	7	
I6H014	4		3	6	4	4		7	3	6		17	10	3	1	
I6H018		20	6	9	6	9	20	18	4	14	9	3	7	3	9	15
I-Series 6/Best																
I6B002									20		17				5	
I6B006	16	11	12						4				12			13
I6B010			3				10		3	12	8		20	2		
I6B014	18				15	13	8	18	10	8				4		
I6B018	6		2		3			12							18	
J-Series 4/Best																
J4B002														5		16
J4B006	8	7	4	9	7	4	10	15	5	4	7	16	8	4	4	8
J4B010					10					17	14				20	
J4B014					19				15				19			
J4B018		16	20		10	20			20	17		20		6	10	9
J-Series 6/Low																
J6L002					7				10	15						
J6L006	16	9	7	8	10	10	9	19	10	14	9	10	10	12	5	8

J6L010			17		20				8		15		12	6		
J6L014			8	5	4	12				15			6	7	17	16
J6L018						19										
J-Series 6/High																
J6H002	8	6	6	5	6	5	6	8	2	7	5	8	5	5	4	7
J6H006	2	1	1	1	1	2	6	6	2		1	1	1	1	1	1
J6H010	3	3	2	2	2	2	2	3	3	2	2	4	2	2	2	3
J6H014	1	1	1	1	1	1	1	2	1	1	4	1	1	1	1	1
J6H018	1	1	1	1	1	1	1	2	5	1	1	3	1	1	1	1
J-Series 6/Best																
J6B002	NA	NA	NA	NA	NA	NA	NA	NA	NA	NA	NA	NA	NA	NA	NA	NA
J6B006	NA	NA	NA	NA	NA	NA	NA	NA	NA	NA	NA	NA	NA	NA	NA	NA
J6B010		6	19	12	12	7	5	4	3	9	10	9	12	8	5	10
J6B014	13		5	13	10	13	19	9	3	9	12	10	10	5		10
J6B018	4	20	NA	20	5	4	9	9	5	4	9	9	12	1	4	14
J-Series 6/Best (N)																
N6B002			19		20											
N6B006			7	9	20				11	12	20		2	14	9	
N6B010			4	20	20	12	9	15	12		11	13		10		
N6B014		19				19	19		18		19			6	13	18
N6B018	17		14		19					19		13		17	13	7
K-Series 4/Best																
K4B002	6	3			3										20	
K4B006							20							9		
K4B010			20	15	4	6	5	4	2	4	14	8	14	1	1	14
K4B014					16					16						
K4B018		18	15		20	20			20		18		16	14		
K-Series 6/Low																
K6L002			12		5				5							
K6L006		5	5	6	6	9	10		6	11	8	8	10	6	5	
K6L010		11	10	7	7	5	8		10	8	4		5	9	10	9
K6L014					7	7	19		8					6	7	
K6L018		9	9	10	12	11	9	16	8	15	6	10	7	6	8	9

K-Series 6/High																
K6H002																
K6H006			17			16	9				3	17				
K6H010																
K6H014					17				15			20				
K6H018		20	15		20		8		14	15	17			8	7	6
L-Series 4/Best																
L4B002									9					10		12
L4B006	14	9	12	9	7	5	8		9		3	15	13	8	5	6
L4B010	10	10	6	8	9	10	7	12	11	10	14	10	10	3	4	7
L4B014		19	6	7	12	6	10		12	6	8	8	8	6	5	10
L4B018		9	7	9	19	5	7		7	8	3	5	10	9	6	5
L-Series 6/Low																
L6L002							10		12							12
L6L006			10	12	10	20				13	15					9
L6L010		7	6		15	11	12	9	6	6		11		20	7	16
L6L014		10	7	20	7	12			3	17	7	20	7	4	7	17
L6L018	16		20	18	20	7	7	9	3	15	6	11	11	2	9	7
L-Series 6/High																
L6H002			20		7									5	20	20
L6H006			10	6		6	20		10	20				9	19	7
L6H010	7	10	7	9	9	6	3	10	4	9		10	3	6	7	
L6H014		7	7	20	13		16		5	9	11		6	9	18	14
L6H018	13		20		7	29	12	12	11	13			7	14	6	
M-Series 4/Best																
M4B002			6	6	7	5	9	13	9	8	13	6	5	8	10	9
M4B006		5	5	8	5	8	3		12	7	17	3	3	5	13	10
M4B010			12		16		16		12	14	7		16	6	17	14
M4B014					8				7	5	6			15		
M4B018				7	7	9			17	15	6	7	7	8	7	18
M-Series 6/Low																
M6L002	9	7	6	7	3	7	7	9	7	9	9	9	4	3	4	8
M6L006	6	1	1	3	4	7	2	4	2	5	3	3	1	1	4	5
M6L010	3	3	3	2	2	3	3	4	3	6	3	4	3	1	3	3
M6L014	1	1	1	1	2	1	1	6	3	5	6	6	1	1	1	2

M6L018	1	1	1	4	4	1	3	5	4	5	4	5	1	1	1	1
M-Series 6/High																
M6H002				17	13	15	7	4	9	12			16	7	9	12
M6H006		7	5	5	6	5	6	5	3	5	5	5	5	5	5	5
M6H010	13			10	19	18	19		6	14	12			12	17	19
M6H014					3				10	12	19					
M6H018	6	6	6	3	3	3	5	6	3	5	5	6	5	3	3	5
M-Series 6/Best																
M6B002					15	12	18	18		19	19			19		
M6B006	13		2	15					4	19	10	13		17	4	
M6B010					14	12			11	11	14	16	18	13		
M6B014					7	8	8	19	6	12			6	17	6	16
M6B018		18	8	6	5	14		7	9	6	16	5	18	2	9	
O-Series 4/Best																
O4B002		19	19		4				13					9		
O4B006					15					11						
O4B010	6	15	8	8	16		6	6	4	20				2	6	6
O4B014			8						6		10		15	6		7
O4B018			6		13	6			8	19			3			
O-Series 6/Low																
O6L002	11				12				9							
O6L006			5		6											
O6L010		11	2	8	4	5				19					6	15
O6L014			15	2					4		8		2	15	9	
O6L018					11										19	
O-Series 6/High																
O6H002					15	12	18				16			19		
O6H006			17			17	13		13	14	16		19	18	13	
O6H010						16			15				18	19	8	15
O6H014			18	8	4	7			10	4	10	18	18	3	18	14
O6H018		7	4	2	3	3			9	7	8	10	9	1	4	4
P-Series 4/Best																
P4B002		7	5	20	9	5	8		10	4	15		18	4	5	
P4B006		5	5	8	5	3			9	17	2		5	17	5	3
P4B010		11	15	17	6	10	16		7				5	1	3	9

P4B014					16	11			20		3			5	4	
P4B018			7	18	6	8	4		9	18		17	4	9		9
P-Series 6/Low																
P6L002			11	3	10	11	11	18	20	3	17	18	10	11		21
P6L006		5	1	9	6	7	3	9	8	17	5	4	4	3	10	4
P6L010			6	9	7	9			4	9	5	6	10	5	7	10
P6L014		17	19	11	9	12	15		12	9	10	12	10		10	8
P6L018		9	14	4	10	8			7	20	6		6	2	10	4
P-Series 6/High																
P6H002			12			20			10					10		
P6H006			6	9	5	12	11		3	18			9			5
P6H010					9		13		8	12				11		
P6H014				19		4	18		20				9	7	6	4
P6H018					14								10			
R-Series 6/Best																
R6B002	10	8	13	5	7	9			8		19		7	12	4	16
R6B006	11	12	5	5	12	7	11		2	12	12	10	8	4	5	10
R6B010			4	7	11	5	20		7		4	7	9	8		10
R6B014	5	12	9	5	12	10	15	12	9	13	4	5	11	13	13	11
R6B018	15	19	9		8	15	20	19	10				8	5	5	8
R-Series 6/Best																
S6B002			12	11			13		8						15	
S6B006	20		18	15	20			14	15		10	9	5	5	8	
S6B010		9	6	15	13	17				11			5	5	9	
S6B014	9	9	9	9	9	11	10	11	9	9	9	9	9	3	9	5
S6B018	16	7	5	5	5	9	10		4			9	3	4	3	3

Table 17: Raw no-aging failure data

Test Set (Aged)	U 6	U 7	U 8	U 9	U 10	U 11	U 12	U 13	U 14	U 15	U 16	U 17	U 18	U 19	U 20	U 21
A-Series 6/Best 50-50																
A6B027	15	23	20	23	21		21	22		21	23		21	8	21	
A6B051	23		6		11					23			16	13	5	
A6B055	21	21	21	21		21	21	21	21	21	23	21	21	11	19	21
A6B031	21	21	21	21	21	21	21	21	21	21	21	22	21	21	21	21
A6B035	21	4	3	13	8	4	21	21		21	21	21	16	2	6	12
A6B039	6	5	7	9	14	11	21	20	21	8	21	21	5	2	4	6
A6B059			21			23		22				23	23	21	21	
A6B043		23												19	23	
A6B063	23		21		12	23	21			22				21	23	
NA	NA	NA	NA	NA	NA	NA	NA	NA	NA	NA	NA	NA	NA	NA	NA	NA
NA	NA	NA	NA	NA	NA	NA	NA	NA	NA	NA	NA	NA	NA	NA	NA	NA
BCDE-Series 4/Best																
B4B003	2	8	1	21	17	6	20	10	12	10	17	15	18	21	21	17
B4B007	10	7	19	8	20	17	18	17	20	17	18	15	17	19	18	7
B4B011	10	4	13	13	8	6	19	14	19	18	14	20	3	1	2	13
B4B015	5	16	16	6	19	18	20	2	7	10	15	6	19	17	5	20
B4B019	10	16	20	18	1	17	18	19	6	10	20	6	17	16	20	18
BCDE-Series 6/Best																
C6B003	16	21	8	3	9	3	19	20	15	2	19	2	9	20	20	19
C6B007	12	18	17	21	2	9	11	5	3	11	5	14	7	19	15	11
C6B011	11	2	5	11	15	15	14	15	2	13	13	13	3	1	9	14
C6B015	19	12	8	15	9	12	14	4	19	7	6	21	17	18	12	4
C6B019	9	8	19	11	10	1	4	9	3	1	15	11	15	10	17	9
BCDE-Series 6/Low																
D6L003									13	5	21		10			
D6L007									19					16	16	
D6L011			22		17		9		11	6	12			9		
D6L015					9		7		11		12					
D6L019	21		22	19				15			20		17			

BCDE-Series 6/High																
E6H003	15					19	16			11		16				12
E6H007		17		16	10	20	11								11	21
E6H011	12	20	5	17	11					15			9	5	10	
E6H015					20	16	10			9	4			16		
E6H019	13		13		12		16		8	17			20	17	19	
F-Series 6/Best																
F6B001	11	4	11	5	11	10	7	7	16	6	18	18	11	10	10	10
F6B005	9	14	7	11	10	13	18	14	5	5	8	7	10	6	6	9
F6B009	10	15	9	8	18	10	8	11	10	10	10	9	5	10	10	18
F6B013	8	13	11	14	13	18	5	7	13	10	9	8	11	10	10	14
F6B017	4	10	7	7	10	5	10	18	10	11	14	7	10	10	4	10
G-Series 6/Best																
G6B003	4	11	6	7	17	3	16	12	5	7	7	8	7	11	14	7
G6B007	7	15	12	8	12	6	11	8	6	13	7	12	13	8	8	8
G6B011	12	6	4	11	11	15	17	16	13	12	5	5	8	7	16	17
G6B015	7	14	5	8	6	12	11	3	6	8	4	12	16	8	7	8
G6B019	6	13	13	7	15	11	8	6	18	11	7	18	8	4	6	8
H-Series 4/Best																
H4B001	3	14	1	19	16	3	3	3	3	5	20	11	14	19	1	3
H4B005	3	2	1	1	3	3	3	3	16	8	2	2	5	2	5	2
H4B009	1	3	10	1	7	1	1	1	1	8	1	1	2	3	5	3
H4B013	1	1	1	6	11	2	2	3	2	1	2	2	2	3	1	1
H4B017	8	1	6	19	16	1	1	1	1	8	1	19	1	7	5	14
H-Series 6/Low																
H6L001	16	8	3	12	12	13	1	2	12	19	4	1	8	8	9	9
H6L005	15	14	1	15	12	12	14	4	13	8	12	20	14	17	1	1
H6L009	15	8	8	18	5	5	8	15	15	13	20	11	11	2	4	10
H6L013	9	2	2	3	3	4	9	8	5	8	11	6	1	1	2	4
H6L017	13	12	20	5	14	20	5	13	5	9	14	13	13	3	13	20
H-Series 6/High																
H6H001	18	12	8	11	11	7	13	18	5	13	8	13	12	2	7	11
H6H005	18	12	8	13	12	8	8	18	4	9	4	12	14	3	4	12
H6H009	8	3	2	10	11	20	8	7	4	13	8	3	5	1	2	3
H6H013	18	6	4	12	11	14	12	6	12	18	15	3	6	2	1	5
H6H017	11	12	13	12	13	20	13	9	7	13	12	12	14	13	13	11

I-Series 4/Best																
I4B001	NA	NA	NA	NA	NA	NA	NA	NA	NA	NA	NA	NA	NA	NA	NA	NA
I4B005	NA	NA	NA	NA	NA	NA	NA	NA	NA	NA	NA	NA	NA	NA	NA	NA
I4B009	NA	NA	NA	NA	NA	NA	NA	NA	NA	NA	NA	NA	NA	NA	NA	NA
I4B013	NA	NA	NA	NA	NA	NA	NA	NA	NA	NA	NA	NA	NA	NA	NA	NA
I4B017	NA	NA	NA	NA	NA	NA	NA	NA	NA	NA	NA	NA	NA	NA	NA	NA
I-Series 6/Low																
I6L001									17							
I6L005	21													10		9
I6L009										17						
I6L013	22								13		7					
I6L017									8							
I-Series 6/High																
I6H001	25														17	
I6H005								18							11	
I6H009		7		7			8		22		23			6	7	
I6H013					8		8							7		
I6H017	8		14		4		8	7	8	7	8	8	8	7	7	8
I-Series 6/Best																
I6B001	17	13	9		2	3	3		9		5		15		5	
I6B005	15	8	4								4				5	
I6B009			6										1			
I6B013									6		5					9
I6B017	8			8	4	13								4	20	4
J-Series 4/Best																
J4B001	2		1	4	3		11	13	1	3	7		14	2	2	
J4B005					12					4	14					
J4B009									6	6						
J4B013			16		1	6	9	18	1	4	8	13	10	5		6
J4B017	2	13	2	3	3				4	13			4	3		3
J-Series 6/Low																

J6L001	8	16	14	16	8	12		6	8	15		8	15	8	2	5
J6L005		8	8		10	13		20	11	9	19			8	10	12
J6L009		12	11	15	8								12	10	16	
J6L013	7	4	1	4	1	3	4	2	4	1	3	4	1	1	1	4
J6L017	8		7	7	12	18	19	12	8	16		9	7	5	7	
J-Series 6/High																
J6H001	5	8	4	12	9	9		16	11		12			6	9	
J6H005	13				13	20		16	8	5			8	7	11	8
J6H009	8	5	5	6	6	8	3	8	7	8	5	7	8	2	2	8
J6H013	5		11	11	7	6		7	11	5	6		16		16	
J6H017	8	8	8	8	8	6	8	8	5	4	8	8	8	8	8	8
J-Series 6/Best																
J6B001	NA	NA	NA	NA	NA	NA	NA	NA	NA	NA	NA	NA	NA	NA	NA	NA
J6B005	NA	NA	NA	NA	NA	NA	NA	NA	NA	NA	NA	NA	NA	NA	NA	NA
J6B009	3	9	3	5			4	4			3	1	3	1	3	4
J6B013	8	8	4	3				5	7	7	5		3	1	1	4
J6B017	2	1	1	1	1	1	1	3	1	1	1	1	1	1	1	3
J-Series 6/Best (N)																
N6B001			16													8
N6B005		18		4	3		4	15		2			12	14	3	3
N6B009			1	8		18	2	12	6	6	19	2	6	2	2	2
N6B013	3	2	2	2	3	8			2				2	2	1	3
N6B017	2	2	1	1	3	2		8	2	7	2	8	1	1	1	4
K-Series 4/Best																
K4B001			20		6		16		3	7	15	19	13	6	16	13
K4B005			20			11		19		7			8	5		8
K4B009	3	3	4	4	4	4	4	7	5	3	3	4	2	3	2	3
K4B013	20	19	19	19	13	8	19	19	4	16	19	8	4	3	4	7
K4B017	8	16	4		5	5	19	4	13	3	15	6	16	10	4	4
K-Series 6/Low																
K6L001	5		5	12	3	19	20			4	19	10	6	3	4	20
K6L005	20		20	20	20			20	11	3	20			5	20	
K6L009	3	3	3	2	4	4	2	4	4	4	5	4	3	3	3	2
K6L013	20	20	19	20	3	20	20	20	20	5	20	20	20	6	2	11

K6L017	19	20	15	7	6	5	6			5	10	19	7	7	7	
K-Series 6/High																
K6H001					17	20						18		17	17	6
K6H005										20	8	15			10	10
K6H009		20	18		6		7	3	13	5		6		20	20	
K6H013	10	17	13	17	7				20			20	17	19	14	17
K6H017	18	13	4	5	6	13	8		6	10			9	10	6	5
L-Series 4/Best																
L4B001	4	5	2	5	9	16	17	3	5	4	9	15	11	9	5	2
L4B005	3	2	5	13	6	4	4	5	17	5	6	5	17	8	15	4
L4B009	17	9	16	13	5	6	4	19	4	3	10	17	4	8	9	19
L4B013	5	2	8	4	8	4	16	16	6	17	2	3	11	19	5	9
L4B017	9	5	5	9	2	16	19	19	9	3	2	5	5	4	4	17
L-Series 6/Low																
L6L001			6													
L6L005	8		3	6	7		5	9	9	9	5	9	5	2	8	8
L6L009	1	1	1	1	1	1	1	1	1	1	1	3	1	1	1	1
L6L013	1	1	1	1	6	8	9	4	2	7	5	5	1	1	1	6
L6L017	1	1	1	1	1	1	3	9	3	2	3	6	1	1	1	1
L-Series 6/High																
L6H001	9	8	7	7	4	13	17	18	11	10	4	14	2	13	17	19
L6H005	7	8	14	19	9	7	12	7	12	10	3	5	19	4	4	10
L6H009	18	4	13	13	17	9	10	11	19	9	13	17	10	10	4	7
L6H013	7	6	8	4	5	11	13	14	10	10	2	4	8	4	4	4
L6H017	17	4	7	9	4	11	5	3	5	18	4	19	5	9	7	5
M-Series 4/Best																
M4B001									11							
M4B005			15	13			5		16				13			
M4B009	3	1	1	2	2	3	12	19	3	6	14	2	1	1	1	3
M4B013	2	2	1	2	1	3	3	5	3	3	5	9	1	1	1	3
M4B017	1	2	1	1	18	11	5	3	14	4	11	3	4	1	1	7
M-Series 6/Low																
M6L001			10													
M6L005		9	3	4	8	9	9	4	8		8	8	7	3	3	8
M6L009	1	1	1	1	1	3	3	3	1	1	8	3	1	1	1	1

M6L013	1	1	1	1	1	1	1	2	2	1	2	2	1	1	1	1
M6L017	1	1	1	1	1	1	1	2	1	1	1	2	1	1	1	1
M-Series 6/High																
M6H001										3						
M6H005			12						8				19		4	15
M6H009	1	1	1	1	1	5	3	1	3	4	2	3	1	1	1	2
M6H013	1	3	1	1	2				9					1	1	2
M6H017	1	1	1	1	2	4	1	4	1	1	18	2	1	1	1	1
M-Series 6/Best																
M6B001						6			2	5	4			2	11	
M6B005		10	6	2	3	7	8		5			18	14	1	1	
M6B009	18	2	2	4	4	4	11	20	10	12	14		2	2	4	9
M6B013	11	1	1	3	2	3	1	6	3	5			2	2	1	3
M6B017	1	1	1	1	3	2	5	4	1	4	8	2	1	1	1	1
O-Series 4/Best																
O4B001	2	2	1	2	2	2	2	6	2	2	8	7	2	2	1	2
O4B005	13	6	3	7	5	11	4	11	2		13	12	4	4	5	7
O4B009	4	7	1	7	8	9	11	13	9	3	12	8	13	4	3	3
O4B013	8	3	1	3	2	1	8	11	2	12	6	6	2	2	1	6
O4B017	8	2	1	11	9	8	8	6	8	10	12	12	2	1	2	9
O-Series 6/Low																
O6L001															10	
O6L005	3	4	1	3	3	3			3	6				3	2	3
O6L009	2	1	2	1	2	1	3	2		1	3	4	7	1	1	3
O6L013	1	1	1	1	1	1	3	2	1	1	1	1	1	1	1	1
O6L017	1	1	1	1	8	3	1	1	1	3	5	11	1	1	1	2
O-Series 6/High																
O6H001		3	3	2	3									8	8	
O6H005	11	13	1	5	3	6			5				3	1	1	5
O6H009	3	2	1	6	4	2	4	2	2	3	1		4	1	1	2
O6H013	1	1	1	1	1	1	3	1	1	1	2	3	1	1	1	1
O6H017	3	3	1	1	1	7	6	2	8	4	2	12	1	1	1	3
P-Series 4/Best																
P4B001	11				8						6		11	7		
P4B005			15						14		7		7		7	

P4B009	1	1	1	1	3	2	2	4	1	6	6	6	1	1	1	2
P4B013	2	2	1	1		8	7		8	8	10		1	1	2	4
P4B017	6	1	1	2	2	7	6	6		3		7	1	1	1	2
P-Series 6/Low																
P6L001		4	9	4	2	7	4	4	3	4	13		2	2	2	
P6L005				15	9								10			
P6L009	8	1	1	2	6	3	3	6	6	2	2	3	1	1	1	1
P6L013	3	1	1	7	7	10		4	7	13			2	1	1	4
P6L017	4	3	1	8	4		10		6				1	1	2	7
P-Series 6/High																
P6H001	8	1	1	2	2	4	8	9	3	5	9	9	6	2	1	2
P6H005	8		8	3	4	11	8	12	2	5		12	10	2	2	
P6H017	12	12	5	13	13	8						4	11	3	5	
P6H013	2	2	1	2	2	2	3	4	2	12	12	8	2	1	2	2
P6H009	8	2	2	6	12	13	13	13	13	13	13	13	6	1	4	13
R-Series 6/Best																
R6B001					5				5	10						
R6B005	6	13	6	5	5	5	13		7	14	10		9	2	3	9
R6B009	6	16	1	5	3	5			5		10	9	5	1	1	9
R6B013	20	7	1		2	5		20	4				4	15	8	3
R6B017	1	1	1	1	2	4	2	8	2	1	10	9	1	1	1	1
NC 6/Best																
S6B001														5		
S6B005			2	9	8	7	2		3	5				3	2	
S6B009	19	6	1	3	4	14	6	5	7	8		7	4	1	1	5
S6B013		20	3	5	8	7	12		9				3	3	1	4
S6B017	1	1	1	1	7	2		19	6	11			1	1	1	2

Table 18: Raw aged failure data